

11-34  
126507  
p. 67

# Turbulent Fluid Motion IV-Averages, Reynolds Decomposition, and the Closure Problem

Robert G. Deissler  
*Lewis Research Center*  
*Cleveland, Ohio*

September 1992

(NASA-TM-105-822) TURBULENT FLUID  
MOTION IV-AVERAGES, REYNOLDS  
DECOMPOSITION, AND THE CLOSURE  
PROBLEM (NASA) 67 6

105-822  
000175

**NASA**

U15-21

105-822



# TURBULENT FLUID MOTION IV—

## Averages, Reynolds Decomposition, and the Closure Problem

Robert G. Deissler  
National Aeronautics and Space Administration  
Lewis Research Center  
Cleveland, Ohio 44135

### SUMMARY

Ensemble, time, and space averages as applied to turbulent quantities are discussed, and pertinent properties of the averages are obtained. Those properties, together with Reynolds decomposition, are used to derive the averaged equations of motion and the one- and two-point moment or correlation equations. The terms in the various equations are interpreted. The closure problem of the averaged equations is discussed, and possible closure schemes are considered. Those schemes usually require an input of supplemental information unless the averaged equations are closed by calculating their terms by a numerical solution of the original unaveraged equations. The law of the wall for velocities and temperatures, the velocity- and temperature-defect laws, and the logarithmic laws for velocities and temperatures are derived. Various notions of randomness and their relation to turbulence are considered in the light of ergodic theory.

### INTRODUCTION

Although the unaveraged equations of the last chapter can, in principle, be applied directly to turbulence, the historical tendency has been to average out the fluctuations so as to obtain simply varying functions. The idea is that simply varying nonrandom values are easier to deal with than the haphazard motion characteristic of turbulent flow. Physically relevant equations are obtained in this way, but the price to be paid as far as obtaining solutions is concerned (the closure problem) is considerable, as will be seen later in this chapter. First we will consider various averages of the turbulent quantities.

#### 4.1 AVERAGE VALUES AND THEIR PROPERTIES

For the most general turbulent flows an ensemble average over a large number of macroscopically (but not microscopically) identical flows is appropriate. In all of those flows, the macroscopic determining parameters (e.g., mean velocity, scales, etc.), but not fluctuating quantities, are the same. The ensemble average of a quantity, say the velocity, at a point  $x_k$  and time  $t$  is the arithmetic average of that quantity for all the flows. For instance, for a velocity component  $u_i$  at point  $x_k$  and time  $t$ ,

$$\overline{u_i(x_k, t)}_n = \lim_{n \rightarrow \infty} \sum_{n=1}^N u_i(n, x_k, t) / N, \quad (4-1)$$

where  $n$  indicates the  $n$ th flow,  $N$  is the total number of flows over which the average is taken, and the overbar with the subscript  $n$  designates the ensemble average (the average over  $n$ ). Needless to say, this type of average, although often used in theoretical work, would be hard to implement experimentally, because a large number of macroscopically identical flows would not likely be available.

Fortunately, in most cases statistical uniformity or stationarity with respect to one or more coordinates and/or with respect to time obtains. Then the average is taken with respect to the one or more coordinates and/or with respect to time. For instance, if the turbulence is statistically stationary with respect to time (if the ensemble average does not vary with time  $t$ ), the time average of  $u_i$  at a point  $x_k$  is

$$\overline{u_i(x_k)}_t = \lim_{T \rightarrow \infty} \int_0^T u_i(x_k, t) dt / T, \quad (4-2)$$

where the time average is designated by the overbar and the subscript  $t$ .

If the turbulence is statistically stationary with respect to one or more variable coordinates  $x_j$  (if the ensemble average does not vary with the one or more coordinates  $x_j$ ), then the space average with respect to  $x_j$  at a time  $t$  and at fixed coordinate(s)  $x_k$ , where  $j \neq k$ , is

$$\overline{u_i(x_k, t)}_{x_j} = \lim_{X_j \rightarrow \infty} \int_{-X_j}^{X_j} u_i(x_k, t, x_j) dx_j / (2X_j), \quad (4-3)$$

where the space average is designated by the overbar and the subscript  $x_j$ , and the integration is over the one or more coordinates  $x_j$  for which statistical uniformity obtains. (Note that if  $j$  can have the values 1, 2, and 3,  $x_k$  will be absent from equation (4-3), since  $k \neq j$ .)

A space average also makes sense for periodic boundary conditions, even if the turbulence is not statistically uniform over one or more coordinates. In that case as in the preceding case, the space-averaged quantities (averaged over a period) do not vary with position, since it makes no difference where the period starts ( $\partial \overline{u_i(x_k, t)}_{x_j} / \partial x_j = 0$ ,  $k \neq j$ ). Then

$$\overline{u_i(x_k, t)}_{x_j} = \int_{-X_j}^{X_j} u_i(x_k, t, x_j) dx_j / (2X_j), \quad (4-4)$$

where  $2X_j$  is one spatial period.

Finally, it might be useful to take the average over both time and one or more coordinates, when the turbulence is statically stationary with respect to both. Then the average with respect to  $t$  and  $x_j$  is

$$\overline{u_i(x_k)}_{t, x_j} = \lim_{X_j, T \rightarrow \infty} \int_{-X_j}^{X_j} \int_0^T u_i(x_k, t, x_j) dt dx_j / (2X_j T). \quad (4-5)$$

Of course, if the boundary conditions in equation (4-5) are periodic in some of the directions  $x_j$ , the average in those directions need be taken only over one period, as in equation (4-4).

The averaging processes considered in this section have been illustrated by taking average values of a velocity component  $u_i$ . The same processes can, of course, be applied to the mechanical pressure  $\sigma$  (eq. (3-14)) and to functions of velocities and of pressures such as  $u_i u_j$ ,  $u_i u_j u_k$ ,  $u_i u'_j u''_k$ , and  $\sigma u'_k$ , where the unprimed, primed, and double-primed quantities refer to values at different spatial points. The  $u_i$  in equations (4-1) to (4-5) need only be replaced by  $\sigma$ ,  $u_i u_j$ , etc. It might be mentioned that the simplest

average which is descriptive of turbulence is not that of  $u_i$ , which describes the overall flow rather than the turbulence, but that of the second-order tensor  $u_i u_j$ .

#### 4.1.1 Ergodic Theory and the Randomness of Turbulence

Turbulence is generally taken to be ergodic, in which case the ensemble, time, and space averages of a turbulent quantity (say  $u_i u_j$ ) should all have the same value, assuming that those averages exist. An ergodic system embodies the weakest notion of randomness in a hierarchy of systems (refs. 1 and 2). The so-called mixing systems (those whose variables become uncorrelated as their temporal separation  $\Delta t \rightarrow \infty$ ) have a stronger notion of randomness than do those that are only ergodic, and systems that exhibit sensitive dependence on initial conditions, or chaoticity, have a stronger notion of randomness than do those that are only ergodic or only ergodic and mixing. Mixing implies ergodicity, and chaoticity implies both ergodicity and mixing, but the converse is not true. At the top of the hierarchy are the most random systems; those that, though deterministic, may appear in a certain sense to behave as randomly as the numbers produced by a roulette wheel (ref. 1)

So in order for a flow to be identified as being random (or apparently random) in some sense, and thus as turbulent, it must be at least ergodic. As mentioned in chapter I, turbulent systems appear to be at least as random as chaotic systems. In chapter VI it is argued that they are likely more random.

Because of the ergodicity of turbulence a distinction among the various kinds of averages will not usually be made, and they will be written simply as  $\overline{u_i}$ ,  $\overline{u_i u_j}$ ,  $\overline{u_i \sigma'}$ , etc., the subscripts  $n$ ,  $t$  and  $x_j$  in equations (4-1) to (4-5) being omitted. It will always be assumed, of course, that the averages taken are of an appropriate type, in line with equations (4-1) to (4-5).

#### 4.1.2 Remarks

The averaging considered here, which is known as Reynolds averaging, is the type which will be used in this book. There are, of course, other types of averaging, which have specific uses. For instance conditional averaging, in which averages are taken under some specified condition, such as the condition that only velocities greater than some value be used in the average, is sometimes useful. However none of the methods of averaging circumvents the closure problem (considered in section 4.3) which occurs when the nonlinear continuum equations are averaged.

#### 4.1.3 Properties of Averaged Values

Finally, we will consider some properties of averaged values which will be useful in obtaining the averaged equations of fluid motion. We note first that the derivative of an average equals the average of the derivative. Thus, for example,  $\partial \overline{u_i u_j} / \partial x_k = \overline{\partial u_i u_j / \partial x_k}$ . This equation can be obtained from equation (4-2) (with  $u_i$  replaced by  $u_i u_j$ ) if the average is taken over time. Thus

$$\begin{aligned}
\frac{\partial \overline{u_i u_j}}{\partial x_k} &= \left( \frac{\partial}{\partial x_k} \right) \left[ \lim_{T \rightarrow \infty} \int_0^T (u_i u_j) dt / T \right] \\
&= \lim_{T \rightarrow \infty} \int_0^T \left[ \frac{\partial (u_i u_j)}{\partial x_k} \right] dt / T = \overline{\frac{\partial (u_i u_j)}{\partial x_k}}.
\end{aligned}
\tag{4-6}$$

The same result is obtained if the average is other than that over time. Also, it is easy to show that the sum of averages equals the average of the sum. Thus, again using equation (4-2),

$$\begin{aligned}
\overline{u_i u_j'} + \overline{u_i' u_j} &= \lim_{T \rightarrow \infty} \int_0^T (u_i u_j') dt / T + \lim_{T \rightarrow \infty} \int_0^T (u_i' u_j) dt / T \\
&= \lim_{T \rightarrow \infty} \int_0^T (u_i u_j' + u_i' u_j) dt / T = \overline{u_i u_j' + u_i' u_j}.
\end{aligned}
\tag{4-7}$$

Moreover, taking an average of an average (designated by a double bar) does not change its value, since, for example,

$$\overline{\overline{u_i u_j}} = \lim_{T \rightarrow \infty} \int_0^T \overline{(u_i u_j)} dt / T = \overline{u_i u_j} \lim_{T \rightarrow \infty} \int_0^T dt / T = \overline{u_i u_j}.
\tag{4-8}$$

Finally, the average of the product of an averaged and an unaveraged quantity is the product of the first (averaged) quantity by the second quantity averaged. For example,

$$\begin{aligned}
\overline{\overline{u_i} (u_j u_k)} &= \lim_{T \rightarrow \infty} \int_0^T \overline{u_i} (u_j u_k) dt / T = \overline{u_i} \lim_{T \rightarrow \infty} \int_0^T (u_j u_k) dt / T \\
&= \overline{u_i} \overline{u_j u_k}.
\end{aligned}
\tag{4-9}$$

As an example of a relation for averages which does not hold, we note that

$$\overline{u_i u_j} \neq \overline{u_i} \overline{u_j},$$

since

$$\lim_{T \rightarrow \infty} \int_0^T (u_i u_j) dt / T \neq \lim_{T \rightarrow \infty} \int_0^T u_i dt / T \lim_{T \rightarrow \infty} \int_0^T u_j dt / T.$$

All of the preceding relations which were shown to hold for time averages hold, of course, for the other kinds of averages. Thus, for instance, if we consider ensemble averages and use equation (4-1), we find that

$$\overline{\overline{u_i u_j}} = \lim_{N \rightarrow \infty} \sum_{n=1}^N \overline{u_i u_j} / N = \overline{u_i u_j}, \quad (4-8a)$$

which is the same result as that obtained in equation (4-8) for time averages.

## 4.2 EQUATIONS IN TERMS OF MEAN AND FLUCTUATING COMPONENTS

Equations for mass, momentum, and energy conservation, as well as for the pressure, which are general enough for all of the work in this book are given by equations (3-4), (3-18a), (3-34), and (3-21a) respectively. We first rewrite those equations in slightly different forms and notations:

$$\frac{\partial \tilde{u}_i}{\partial x_i} = 0, \quad (4-10)$$

$$\frac{\partial \tilde{u}_i}{\partial t} = - \frac{\partial(\tilde{u}_i \tilde{u}_k)}{\partial x_k} - \frac{1}{\rho} \frac{\partial(\tilde{\sigma} - \sigma_e)}{\partial x_i} + \nu \frac{\partial^2 \tilde{u}_i}{\partial x_k \partial x_k} - \beta(\tilde{T} - T_e) g_i, \quad (4-11)$$

$$\frac{\partial \tilde{T}}{\partial t} = - \frac{\partial(\tilde{T} \tilde{u}_k)}{\partial x_k} + \alpha \frac{\partial^2 \tilde{T}}{\partial x_k \partial x_k}, \quad (4-12)$$

and

$$\frac{1}{\rho} \frac{\partial^2(\tilde{\sigma} - \sigma_e)}{\partial x_i \partial x_i} = - \frac{\partial^2(\tilde{u}_i \tilde{u}_k)}{\partial x_i \partial x_k} - \beta g_i \frac{\partial \tilde{T}}{\partial x_i}. \quad (4-13)$$

These equations are the same as equations (3-4), (3-18a), (3-34), and (3-21a), except that  $\tilde{\phantom{x}}$ 's have been placed over the instantaneous velocities  $u_i$ , mechanical pressures  $\sigma$ , and temperatures  $T$ , and the non-linear terms have been written in the so-called conservative form by using the continuity equation (4-10).

Following Reynolds (ref. 3), one can break the instantaneous quantities in equations (4-10) to (4-13) into mean and fluctuating (or turbulent) components. That process is known as Reynolds decomposition. Thus, set

$$\tilde{u}_i = U_i + u_i \quad (4-14)$$

$$\tilde{\sigma} = P + \sigma \quad (4-15)$$

and

$$\tilde{T} = T + \tau \quad (4-16)$$

where the first and second terms on the right sides of the equations are respectively mean and fluctuating components, and where

$$\overline{u_i} = \overline{\sigma} = \overline{\tau} = 0, \quad (4-17)$$

$$U_i = \overline{u_i}, \quad (4-18)$$

$$P = \overline{\sigma}, \quad (4-19)$$

and

$$T = \overline{\tau}. \quad (4-20)$$

As usual, the overbars designate averaged values. Equation (4-10) becomes, on using equations (4-14), (4-17), (4-18), and the properties of averaged values given in equations (4-6) to (4-8),

$$\frac{\partial U_k}{\partial x_k} = \frac{\partial u_k}{\partial x_k} = 0 \quad (4-21)$$

which shows that both the mean and fluctuating velocity components satisfy conservation of mass. Equations (4-11) to (4-13) become, on using equations (4-14) to (4-20) and (4-6) to (4-8), taking averages, and subtracting the averaged equations from the unaveraged ones,

$$\frac{\partial u_i}{\partial t} = -\frac{\partial(u_i u_k)}{\partial x_k} - \frac{1}{\rho} \frac{\partial(\sigma - \sigma_e)}{\partial x_i} + \nu \frac{\partial^2 u_i}{\partial x_k \partial x_k} - \beta g_i \tau - u_k \frac{\partial U_i}{\partial x_k} - U_k \frac{\partial u_i}{\partial x_k} + \frac{\partial \overline{u_i u_k}}{\partial x_k}, \quad (4-22)$$

$$\frac{\partial \tau}{\partial t} = -\frac{\partial(\tau u_k)}{\partial x_k} + \alpha \frac{\partial^2 \tau}{\partial x_k \partial x_k} - u_k \frac{\partial T}{\partial x_k} - U_k \frac{\partial \tau}{\partial x_k} + \frac{\partial \overline{\tau u_k}}{\partial x_k}, \quad (4-23)$$

and

$$\frac{1}{\rho} \frac{\partial(\sigma - \sigma_e)}{\partial x_i \partial x_i} = -\frac{\partial^2(u_i u_k)}{\partial x_i \partial x_k} - \beta g_i \frac{\partial \tau}{\partial x_i} - 2 \frac{\partial u_i}{\partial x_k} \frac{\partial U_k}{\partial x_i} + \frac{\partial^2 \overline{u_i u_k}}{\partial x_i \partial x_k}. \quad (4-24)$$

Equations (4-22) to (4-24) are useful for studying turbulence processes and for constructing evolution equations for correlations (e.g., for  $\overline{u_i u_j}$ ). The first five terms of equation (4-22), the first three of equation (4-23), and the first three of equation (4-24) are similar to the terms in equations (4-11) to (4-13) respectively, although their meanings are exactly the same only if  $U_i = T = P = 0$  (see eqs. (4-14) to (4-16)).

As was the case for equation (3-19) (or (4-11)), the first three terms on the right side of equation (4-22), which give contributions to the rate of change of the velocity fluctuation  $\partial u_i / \partial t$ , can be interpreted as an inertia-force (or turbulence self-interaction) term, a pressure-force term, and a viscous-force



term. The remaining terms are, respectively, a buoyancy-force term, a turbulence-production term, a mean-flow convection term, and a mean turbulent stress term, which may appear when the turbulence is statistically inhomogeneous (when mean turbulence quantities such as  $\overline{u_i u_k}$  are functions of position). (The reasons for referring to the production and convection terms as such will perhaps become clearer when the equivalent terms in the averaged equations are discussed.) It will be seen in the next chapter that when the mean-velocity gradient is not zero, the term  $-U_k \partial u_i / \partial x_k$  generates a small-scale structure in the turbulence by vortex stretching or by a breakup of eddies into smaller ones. The nonlinear self-interaction term  $-\partial(u_i u_k) / \partial x_k$  also produces a small-scale structure, and in addition produces randomization of the flow. This effect will also be considered in the next chapter.

The terms on the right side of equation (4-23), which give contributions to the rate of change of the temperature fluctuation  $\partial \tau / \partial t$ , are respectively a nonlinear temperature-velocity interaction term, a molecular diffusion term for temperature fluctuations, a production term for temperature fluctuations, a mean-flow convection term for temperature fluctuations, and a mean turbulent heat-transfer term which may be present when the turbulence is inhomogeneous.

The Poisson equation for the mechanical pressure fluctuations has four source terms—a nonlinear term, a buoyancy term, a mean-velocity-gradient term, and a mean-turbulent-stress term which appears when the turbulence is inhomogeneous.

### 4.3 AVERAGED EQUATIONS

Although the averaged equations for fluid motion do not form a closed (complete) set, they are very useful for studying the physical processes in turbulence. Moreover, approximate solutions can be obtained by introducing various closure schemes. Alternatively (or preferably), the terms in the averaged equations can often be calculated from a numerical solution of the *unaveraged* equations.

#### 4.3.1 Equations for Mean Flow and Mean Temperature

First consider the equations obtained by averaging each term in equations (4-11) to (4-13) after applying Reynolds decomposition (eqs. (4-14) to (4-20)) and using (4-21). This gives

$$\rho \frac{\partial U_i}{\partial t} = -\rho U_k \frac{\partial U_i}{\partial x_k} - \frac{\partial (P - \sigma_e)}{\partial x_i} + \frac{\partial}{\partial x_k} \left[ \rho \nu \left( \frac{\partial U_i}{\partial x_k} + \frac{\partial U_k}{\partial x_i} \right) - \rho \overline{u_i u_k} \right] - \rho \beta (T - T_e) g_i, \quad (4-25)$$

$$\rho c \frac{\partial T}{\partial t} = -\rho c U_k \frac{\partial T}{\partial x_k} - \frac{\partial}{\partial x_k} \left( -\rho c \alpha \frac{\partial T}{\partial x_k} + \rho c \overline{u_k \tau} \right), \quad (4-26)$$

and

$$\frac{\partial^2 (P - \sigma_e)}{\partial x_i \partial x_i} = -\rho \frac{\partial}{\partial x_i} \left( U_k \frac{\partial U_i}{\partial x_k} \right) - \rho \frac{\partial^2 \overline{u_i u_k}}{\partial x_i \partial x_k} - \rho \beta g_i \frac{\partial T}{\partial x_i}, \quad (4-27)$$

where the properties of averages given by equations (4-6) to (4-9) were used. One should note that time averages would not be appropriate in these equations unless averaged quantities change much more slowly with respect to time (preferably infinitely more slowly) than the unaveraged quantities. Otherwise, averages with respect to space variables in directions for which the turbulence is statistically stationary would be preferable. Equation (4-26) is written for a liquid; for a perfect gas  $c$  should be replaced by  $c_p$  (see equation (3-35)). Equations (4-25) to (4-27) look like (4-11) to (4-13) with instantaneous values replaced by average values, but with the important difference that an extra term involving  $\overline{u_i u_k}$  or  $\overline{u_k \tau}$  now appears in each of the equations. These terms arise from the nonlinear velocity and velocity-temperature terms in equations (4-11) to (4-13) and are a manifestation of the closure problem in turbulence. If those terms were absent, the set of equations (4-25) to (4-27) would contain as many unknowns as equations and so could be solved. In that case turbulent flows would be no more difficult to calculate than laminar ones. Note that barred quantities in equations (4-25) to (4-27) which contain lower-case letters are turbulent quantities. The term  $-\rho \overline{u_i u_k}$  was discovered by O. Reynolds (ref. 3), and is often called the Reynolds term or the Reynolds stress.

**4.3.1.1 Interpretation of the terms  $-\rho \overline{u_i u_k}$  and  $\rho c \overline{u_k \tau}$ .**—The forms of equations (4-25) and (4-26) suggest that the quantities  $-\rho \overline{u_i u_k}$  and  $\rho c \overline{u_k \tau}$  respectively augment the molecular (or viscous) stress tensor  $\rho \nu (\partial U_i / \partial x_k + \partial U_k / \partial x_i)$  and the molecular heat transfer vector  $-\rho c \alpha \partial T / \partial x_k$ . Since they involve fluctuating or turbulent components, we interpret  $-\rho \overline{u_i u_k}$  as a turbulent (or Reynolds) stress tensor and  $\rho c \overline{u_k \tau}$  as a turbulent heat transfer vector. (The quantity  $\overline{u_i u_k}$  is a second-order tensor, since it is the average value of the product of two vectors (the average value of a tensor is a tensor), and  $\overline{u_k \tau}$  is a vector, since it is the average value of the product of a vector and a scalar (the average value of a vector is a vector)). Thus in equations (4-25) and (4-26) we write

$$\bar{\tau}_{ki} = \rho \nu \left( \frac{\partial U_i}{\partial x_k} + \frac{\partial U_k}{\partial x_i} \right) - \rho \overline{u_i u_k} \quad (4-25a)$$

and

$$Q_k = -\rho c \alpha \frac{\partial T}{\partial x_k} + \rho c \overline{u_k \tau}, \quad (4-26a)$$

where  $\bar{\tau}_{ki}$  is the total stress tensor (the sum of the molecular and turbulent stress tensors), and  $Q_k$  is the total heat transfer vector (the sum of the molecular and turbulent heat transfer vectors).

We note that the expression for the turbulent stress corresponds exactly with that for the molecular stress obtained in the kinetic theory of gases (see, e.g., ref. 4). It is only necessary to replace the macroscopic turbulent velocity fluctuations in  $-\rho \overline{u_i u_k}$  by random molecular velocities. A similar correspondence exists in the expressions for the turbulent and molecular heat transfer, where the macroscopic velocity and temperature fluctuations in  $\rho c \overline{u_k \tau}$  are respectively replaced by a random molecular velocity and molecular kinetic energy (molecular temperature) (ref. 4).

Consider now the term  $-\rho \overline{u_i u_k}$  for  $i \neq k$ . Then, for instance,  $-\rho \overline{u_1 u_2}$  will, in the presence of a mean-velocity gradient  $\partial U_1 / \partial x_2$ , act like a turbulent shear stress on an  $x_1 - x_3$  plane. Similarly,  $\rho c \overline{u_2 \tau}$

will, in the presence of a mean-temperature gradient  $\partial T/\partial x_2$ , act like a turbulent heat transfer in the  $-x_2$ -direction.

To see how these effects come about, consider figure 4-1, where the curve represents either  $U_1$  or  $T$  plotted against  $x_2$ . Then if  $u_2$  is positive at a particular location, the fluid will instantaneously be moving into regions of higher  $U_1$  (if  $\partial U_1/\partial x_2$  is positive as shown), and so  $u_1$  will tend to be negative (the local velocity will tend to be less than  $U_1$ ). Similarly, if  $u_2$  is negative, the fluid will, instantaneously, be moving into regions of lower  $U_1$ , and so  $u_1$  will tend to be positive. In both cases the product  $u_1 u_2$  will tend to be negative, and so the average value  $\overline{u_1 u_2}$  will be nonzero and negative. That is, there will be a negative correlation between  $u_1$  and  $u_2$ . The quantity  $-\rho \overline{u_1 u_2}$  is the turbulent (Reynolds) shear stress acting on an  $x_1 - x_3$  plane and augments the molecular or viscous shear stress  $\rho \nu \partial U_1/\partial x_2$  on that plane. Of course if  $U_1$  is uniform,  $\overline{u_1 u_2}$  will be zero; there will be no correlation between  $u_1$  and  $u_2$ .

A similar interpretation applies to  $\rho \overline{u_2 \tau}$  if the curve in figure 4-1 represents the mean temperature  $T$  plotted against  $x_2$ . That is, when  $u_2$  is positive at a particular  $x_1$ , the fluid will, instantaneously, be moving into regions of higher  $T$  (if  $\partial T/\partial x_2$  is positive as shown), and so  $\tau$  will tend to be negative (the local temperature will tend to be less than  $T$ ). Similarly, when  $u_2$  is negative  $\tau$  will tend to be positive. In both cases the product  $u_2 \tau$  will tend to be negative. The average value  $\overline{u_2 \tau}$  will then be nonzero and negative, so that like the molecular conduction term,  $\rho \overline{u_2 \tau}$  will produce heat transfer in the  $-x_2$ -direction. If  $T$  is uniform there will, of course, be no correlation between  $u_2$  and  $\tau$ , and  $\overline{u_2 \tau}$  will be zero.

Finally, we should say something about  $-\rho \overline{u_i u_k}$  when  $i = k$ . In that case  $-\rho \overline{u_i u_{(i)}}$  (no sum on  $i$ ) will act like a normal turbulent stress and will augment the normal molecular stress  $\rho \nu \partial U_i/\partial x_{(i)}$ . For instance  $-\rho \overline{u_1^2}$  will be the normal stress on an  $x_2 - x_3$  plane.

The existence of the turbulent stress tensor  $-\rho \overline{u_i u_j}$  and heat transfer vector  $\rho \overline{c \tau u_j}$  is an important and physically significant deduction from the continuum equations for fluids (the Navier-Stokes, energy, and continuity equations). The deduction was obtained from those equations with no approximations by using only Reynolds decomposition and the rules for averaging. Unfortunately the procedure does not provide a way of calculating the values of the turbulent stresses and heat transfer, and so we are left with a closure problem (more unknowns than equations). Next we will consider some simple closure schemes.

#### 4.3.2 Simple Closures of the Equations for Mean Flow and Temperature

In order to close the system of equations (4-25) to (4-27), that is, to write it in a form in which the number of unknowns equals the number of equations, one must write the quantities  $\overline{u_i u_j}$  and  $\overline{u_k \tau}$  in terms of the mean velocity  $U_i$ , the mean temperature  $T$ , and  $x_i$ . To do that we necessarily introduce additional information into the equations, so that the theory is not deductive. However, because of the practical importance of obtaining solutions, a great many closure proposals have been made.

Probably the simplest way of closing the system of averaged equations would be to assume that  $\overline{u_i u_j}$  and  $\overline{u_k \tau}$  are respectively proportional to  $U_i U_j$  and  $U_k T$ . One might suppose that this is a reasonable assumption because  $U_i U_j$  and  $U_k T$  have the same dimensions as  $\overline{u_i u_j}$  and  $\overline{u_k \tau}$  and are respectively a second-order tensor and a vector (as are  $\overline{u_i u_j}$  and  $\overline{u_k \tau}$ ). But consider what happens to the turbulent stress terms in equations (4-25) and (4-27) for the simple case in which  $U_i = \delta_{i1} U_1$ , and  $U_1$  is independent of  $x_1$ ; that is, the flow is fully developed. In that case the suggested closure assumption gives, in equations (4-25) and (4-27),  $\partial(\rho \overline{u_i u_k}) / \partial x_k = \partial(\rho U_1 U_1) / \partial x_1 = 0$ , and  $\partial^2 \overline{u_i u_k} / \partial x_i \partial x_k = \partial^2 (U_1 U_1) / \partial x_1^2 = 0$ , where  $\rho$  is constant. Thus the assumed form for  $\overline{u_i u_j}$  would not appear in equations (4-25) and (4-27), and there would be no effect of turbulence on fully developed flow. Since that result is contrary to experience, the proposed closure assumption cannot be reasonable. Evidently the conditions of correct dimensionality and correct tensor properties, while necessary in a closure assumption, are not sufficient.

**4.3.2.1 Eddy diffusivities.**—Inadequacies such as that noted in the expression for  $\overline{u_i u_j}$  which was just considered can be avoided by introducing the so-called eddy diffusivities. This can be done formally by replacing molecular quantities in equations (3-13), (3-14), and (3-29) by turbulent quantities. Thus, in those equations,  $\sigma_{ij}/\rho \rightarrow -\overline{u_i u_j}$ ,  $\mu/\rho \rightarrow \epsilon$ ,  $q_i/(\rho c) \rightarrow \overline{\tau u_i}$ , and  $k/(\rho c) \rightarrow \epsilon_h$ , where the arrows are read "becomes." In addition, according to our notation for turbulent flow, the mean velocity is written as  $U_i$ . Then, for incompressible flow we get, for  $-\overline{u_i u_j}$  and  $\overline{\tau u_j}$ ,

$$-\overline{u_i u_j} = \epsilon \left( \frac{\partial U_i}{\partial x_j} + \frac{\partial U_j}{\partial x_i} \right) - \frac{1}{3} \overline{u_k u_k} \delta_{ij} \quad (4-28)$$

and

$$\overline{\tau u_j} = -\epsilon_h \frac{\partial T}{\partial x_j}, \quad (4-29)$$

where  $\epsilon$  is variously called the turbulent viscosity, eddy viscosity, or eddy diffusivity for momentum transfer, and  $\epsilon_h$  is the turbulent conductivity, eddy conductivity, or eddy diffusivity for heat transfer.

Unlike the molecular viscosity and conductivity in equations (3-13), (3-14), and (3-29), the eddy diffusivities are functions of the character and intensity of the turbulence. We notice that equations (4-28) and (4-29) do not suffer from the problems associated with the expressions given near the beginning of section 4.3.2; in general they give nonzero values for both the turbulent stress and heat-transfer terms in equations (4-25) to (4-27) for a fully developed flow in a channel or pipe. Moreover they give zero values for  $\overline{u_1 u_2}$  and  $\overline{\tau u_2}$  when the mean velocity and temperature gradients are zero, as they should at the center of symmetrical flows (see section 4.3.1.1). For unsymmetrical flows equations (4-28) and (4-29) may break down, but we shall not be concerned here with those flows. For statistically homogeneous flows without mean velocity gradients equation (4-28) gives  $\overline{u_i u_j} = \overline{u_k u_k} \delta_{ij} / 3$ , which is true only for isotropic turbulence. However for homogeneous turbulence we will use other methods. The eddy diffusivities in equations (4-28) and (4-29) are scalars. Other expressions, in which they are tensors, have also been proposed (ref. 5).

Equations (4-28) and (4-29) do not provide closures for the equations (4-25) to (4-27), since we still do not know  $\epsilon$  and  $\epsilon_h$  as functions of position and/or mean velocities. However they provide a framework

in which  $\overline{u_i u_j}$  and  $\overline{\tau u_j}$  are respectively a second-order tensor and a vector, as they should be, and in which reasonable expressions for  $\overline{u_i u_j}$  and  $\overline{\tau u_j}$  might be obtained. In general, expressions for those quantities must be tailored to the particular problem being considered.

**4.3.2.2 Mixing length.**—Before considering specific expressions for the eddy diffusivities, we will introduce Prandtl's mixing-length hypothesis (refs. 6 and 5) which gives a rough estimate of  $\epsilon_h/\epsilon$  and which gives an approximate picture of how momentum and heat might be transferred in a turbulent shear flow.

When turbulence exists in a flow, eddies or portions of fluid move about in an apparently random fashion. If a mean velocity gradient and/or temperature gradient exist in a direction transverse to the main flow, some of the eddies will move transversely into layers of different mean velocity and/or temperature (see fig. 4-1 and sec. 4.3.1.1). Consider the turbulent fluctuations  $u_1$ , and  $\tau$  at a point  $x_i$  (see eqs. (4-14) and (4-16)). The mean velocity and temperature at that point are respectively  $U_1$  and  $T$ , and the mean gradients are in the  $x_2$ -direction, as in figure 4-1.

According to mixing-length theory the fluctuations  $u_1$  and  $\tau$  at  $x_i$  are produced by an eddy or turbulent particle which originates from an instability at another point. We define the virtual origin of the eddy that produced the fluctuations  $u_1$  and  $\tau$  at  $x_i$  as the point  $x_{i,0}$  where the eddy would have been born with the mean velocity  $U_{1,0}$  and temperature  $T_0$  if the  $x_1$ -momentum and temperature of the eddy were conserved as it travels from  $x_{i,0}$  to  $x_i$  (see fig. 4-1). Note that actual conservation need not occur, since the virtual origin of the eddy can differ from its actual origin.

From equations (4-14) and (4-16), which define Reynolds decomposition, the fluctuations  $u_1$  and  $\tau$  at  $x_i$  are given by

$$u_1 = \tilde{u}_1 - U_1 \quad (4-30)$$

and

$$\tau = \tilde{T} - T, \quad (4-31)$$

where the  $\tilde{\phantom{x}}$ 's designate total instantaneous quantities at  $x_i$ , or mean values plus fluctuations. But mean values plus fluctuations in equations (4-30) and (4-31), designated by  $\tilde{u}_1$  and  $\tilde{T}$  respectively, are just the total  $x_1$ -velocity and temperature of the eddy considered in figure 4-1 and in the definition of virtual origin in the last paragraph. According to that definition, if the eddy were born at the virtual origin  $x_{i,0}$  with the mean  $x_1$ -velocity  $U_{1,0}$  and temperature  $T_0$ , then the  $x_1$ -momentum and temperature of that eddy would be effectively conserved as it moves from  $x_{i,0}$  to  $x_i$ . Thus  $\tilde{u}_1$  and  $\tilde{T}$  can be replaced by  $U_{1,0}$  and  $T_0$  respectively. Equations (4-30) and (4-31) then become

$$u_1 = U_{1,0} - U_1 \quad (4-32)$$

and

$$\tau = T_0 - T. \quad (4-33)$$

Substituting equations (4-32) and (4-33) into  $-\overline{u_1 u_2}$  and  $\overline{\tau u_2}$ , we get

$$-\overline{u_1 u_2} = \overline{(U_1 - U_{1,0}) u_2} \quad (4-34)$$

and

$$\overline{\tau u_2} = -(\overline{T - T_0})u_2. \quad (4-35)$$

Note that  $U_1 - U_{1,0} = u_1$  and  $T - T_0 = \tau$  are not removed from the bar since they vary with the averaging variable(s) ( $x_1$ ,  $x_3$ , and/or  $t$ ). If we expand  $U_1$  and  $T$  in Taylor series about  $U_{1,0}$  and  $T_0$  respectively and retain only the first two terms in each, we get

$$-\overline{u_1 u_2} = \overline{\ell_2 \frac{dU_1}{dx_2} u_2} = \overline{\ell_2 u_2} \frac{dU_1}{dx_2} \quad (4-36)$$

and

$$\overline{\tau u_2} = -\overline{\ell_2 \frac{dT}{dx_2} u_2} = \overline{\ell_2 u_2} \frac{dT}{dx_2}, \quad (4-37)$$

where  $\ell_2 = x_2 - x_{2,0}$  and is designated the mixing length. Let  $i = 1, j = 2$ , and the mean flow be in the  $x_1$ -direction in equations (4-28) and (4-29). Comparison of those equations with equations (4-36) and (4-37) then gives

$$\epsilon = \epsilon_h = \overline{\ell_2 u_2}. \quad (4-38)$$

The relation between  $\epsilon$  and  $\epsilon_h$  given by equation (4-38), besides following from mixing length theory, gives good agreement with experiment except at low Prandtl numbers  $c\mu/k$ . At low Prandtl numbers, as for liquid metals, the thermal conductivity  $k$  is generally so high that heat is conducted to or from an eddy as it moves transversely. The temperatures in equation (4-35) will then have to be replaced by values which are closer together, and  $|\overline{\tau u_2}|$  will decrease (refs. 7 to 9). In this chapter we will not be concerned with low Prandtl number fluids and will use equation (4-38).

Equations (4-36) and (4-37) have sometimes been criticized (often mercilessly) because they assume that  $\ell_2$  is small enough that  $U_1$  and  $T$  vary linearly over that distance, whereas in reality it may not be. That problem could be overcome by retaining more terms in the Taylor-series expansions for  $U_1 - U_{1,0}$  and  $T - T_0$ . For instance in the expansion for  $U_1 - U_{1,0}$ , we could retain an additional term  $(1/2)\ell_2^2 \partial^2 U_1 / \partial x_2^2$ . However that would complicate the analysis and may not be worth the effort, since one can probably absorb any second-order effects in the expressions which are assumed for the eddy diffusivity.

**4.3.2.3 The nonuniformity of turbulent mixing.**—A fundamental question about the nature of turbulence concerns how turbulent mixing takes place. Here we consider the *instantaneous* turbulent mixing which occurs in the presence of mean velocity and/or temperature gradients. We consider it at this point because of its relevance to mixing-length theory. It turns out that nonuniform mixing is a consequence of several known facts about turbulence.

Let us see what the presence of the turbulent stress and heat transfer terms in the equations for mean flow and heat transfer (eqs. (4-25) and (4-26)) implies about the instantaneous turbulent mixing. Instantaneous mixing refers here to the mixing one would see in a snapshot taken at a particular time.

Note first what would happen if the spatial pattern of instantaneous turbulent mixing were uniform, or nearly so. If that were the case, a portion of fluid as it moves transversely in mean velocity and temperature gradients (mean velocity in the  $x_1$ -direction) would have a uniform tendency (because of uniform mixing) to assume the mean  $x_1$ -momentum and temperature of the surrounding fluid at each point along its path. That tendency would be more pronounced at higher turbulence intensity or Reynolds number, because small-scale motions become excited with increasing turbulence intensity (ref. 10), and so the turbulent mixing (average or instantaneous) increases. (Note that turbulent mixing takes place most efficiently by small-scale motions, since those provide the most intimate contact of the fluid entering a region with that already there.)

Thus if the instantaneous turbulent mixing were spatially uniform, the tendency of a portion of fluid to assume the mean  $x_1$ -momentum and temperature of the surrounding fluid at each point as it moves transversely would increase with increasing turbulence intensity. That would, however, cause the fluctuations from the mean,  $u_1$  and  $\tau$  in the turbulent stress  $-\rho \overline{u_1 u_j}$  and heat transfer  $\rho c \overline{\tau u_j}$ , to decrease in magnitude with increasing turbulence intensity or Reynolds number. The stress component  $\overline{\rho u_1^2}$  would then decrease. But that trend is unphysical and does not occur. In fact, as might be expected, the opposite trend occurs; as turbulence intensity  $(\overline{u_1 u_j}/3)^{1/2}$  or Reynolds number increases,  $\overline{u_1^2}$  increases (ref. 11).

The instantaneous turbulent mixing therefore cannot be spatially uniform, or nearly so, as assumed in obtaining the above unphysical trend. There must be regions of relative quiescence if  $x_1$ -momentum and heat are to be transferred turbulently at high turbulence intensities. But in that case there must also be regions where the instantaneous mixing is relatively intense and localized, since that is the only way the average mixing could be high for high turbulence intensities when regions of quiescence are present. So the only sensible assumption about the instantaneous mixing is that it is small except in localized regions, where it is intense. Then the above unphysical trends do not occur, since the tendency of a portion of fluid, as it travels transversely, to assume the mean  $x_1$ -momentum and temperature of the surrounding fluid is sudden and is confined to localized regions. Note that even if the turbulence is statistically homogeneous, the instantaneous turbulent mixing tends to be highly inhomogeneous.

The fact that instantaneous turbulent mixing takes place mainly in localized regions means that the turbulence must be spatially intermittent in the small scales, since mixing, as mentioned before, takes place mainly by small-scale motions. Intermittency in the small scales has been found experimentally (ref. 12).

The localness or suddenness of the turbulent transfer considered in this section also seems to be in agreement with the concept of bursting coherent structures in shear flow near a wall. Much work has recently been done on that phenomenon (ref. 13).

Our result that instantaneous turbulent mixing is sudden and localized is congruous with mixing-length theory, which requires a certain suddenness in the turbulent mixing for turbulent transfer to take place. The mixing length can be thought of as the effective distance an eddy moves before mixing with the surrounding fluid. If the mixing took place continuously the mixing length would be zero, and the turbulent shear stress and heat transfer would be zero (eqs. (4-36) and (4-37)).

Thus, although fluid turbulence occurs in a continuum, changes in the momentum and temperature of a moving portion of fluid tend to be sudden and localized. In that respect turbulent systems are not unlike the systems considered in the kinetic theory of gases, where encounters between particles are sudden and localized. It is of interest that it was apparently kinetic theory that originally inspired

turbulent mixing-length theory; the mixing length was supposed to be something like the mean free path of kinetic theory (ref. 6).

4.3.2.4 *Some conditions satisfied by the turbulent shear stress and heat transfer near a wall.*—It may be helpful in obtaining models for the turbulent shear stress and heat transfer (or for the eddy diffusivities for momentum and heat transfer) to determine conditions which must be satisfied by those quantities in the region near a wall. Moreover the results obtained in this section, so far as they go, are exact, depending only on the continuity equation and the boundary conditions for the velocity and temperature fluctuations. The results for the turbulent shear stress have been given previously, for example in reference 14.

Consider an incompressible nonrarefied flow in the  $x_1$ -direction parallel to a wall. The normal to the wall is in the  $x_2$ -direction, with  $x_2 = 0$  at the wall. The continuity equation is

$$\frac{\partial u_i}{\partial x_i} = \frac{\partial u_1}{\partial x_1} + \frac{\partial u_2}{\partial x_2} + \frac{\partial u_3}{\partial x_3} = 0 . \quad (4-39)$$

Since the flow is nonrarefied, the nonslip condition holds at the wall, so that

$$(u_1)_{x_2=0} = (u_2)_{x_2=0} = (u_3)_{x_2=0} = 0 \quad (4-40)$$

at every point on the wall. Thus

$$\left( \frac{\partial u_1}{\partial x_1} \right)_{x_2=0} = \left( \frac{\partial u_3}{\partial x_3} \right)_{x_2=0} = 0 . \quad (4-41)$$

Equation (4-39) then gives, at the wall,

$$\left( \frac{\partial u_2}{\partial x_2} \right)_{x_2=0} = 0 . \quad (4-42)$$

Consider now the turbulent shear stress  $-\rho \overline{u_1 u_2}$ . Then

$$-\frac{\partial \overline{u_1 u_2}}{\partial x_2} = -\frac{\partial \overline{u_1 u_2}}{\partial x_2} = -\overline{u_1 \frac{\partial u_2}{\partial x_2}} - \overline{u_2 \frac{\partial u_1}{\partial x_2}} , \quad (4-43)$$

$$-\frac{\partial^2 \overline{u_1 u_2}}{\partial x_2^2} = -\overline{u_1 \frac{\partial^2 u_2}{\partial x_2^2}} - 2 \overline{\frac{\partial u_1}{\partial x_2} \frac{\partial u_2}{\partial x_2}} - \overline{u_2 \frac{\partial^2 u_1}{\partial x_2^2}} , \quad (4-44)$$



and

$$-\frac{\partial^3 \overline{u_1 u_2}}{\partial x_2^3} = -\overline{u_1 \frac{\partial^3 u_2}{\partial x_2^3}} - 3 \overline{\frac{\partial u_1}{\partial x_2} \frac{\partial^2 u_2}{\partial x_2^2}} - 3 \overline{\frac{\partial u_2}{\partial x_2} \frac{\partial^2 u_1}{\partial x_2^2}} - \overline{u_2 \frac{\partial^3 u_1}{\partial x_2^3}}, \quad (4-45)$$

where the properties of averages given by equations (4-6) and (4-7) were used. By using equations (4-40), (4-42), and (4-43) to (4-45) we get, at the wall,

$$-(\overline{u_1 u_2})_{x_2=0} = 0, \quad (4-46)$$

$$-\left( \frac{\partial \overline{u_1 u_2}}{\partial x_2} \right)_{x_2=0} = 0, \quad (4-47)$$

$$-\left( \frac{\partial^2 \overline{u_1 u_2}}{\partial x_2^2} \right)_{x_2=0} = 0, \quad (4-48)$$

and

$$-\left( \frac{\partial^3 \overline{u_1 u_2}}{\partial x_2^3} \right)_{x_2=0} = -3 \left( \frac{\partial u_1}{\partial x_2} \frac{\partial^2 u_2}{\partial x_2^2} \right)_{x_2=0}. \quad (4-49)$$

Since the zero'th, first, and second derivatives are zero at the wall,  $-\overline{u_1 u_2}$ , starting at zero, increases very slowly with  $x_2$  near the wall. The third derivative (see eq. (4-49)) gives no information, since at least at this stage, we do not know how to evaluate  $-(\partial u_1 / \partial x_2 \partial^2 u_2 / \partial x_2^2)_{x_2=0}$ . Thus

$$0 \leq \left| -\frac{\partial^3 \overline{u_1 u_2}}{\partial x_2^3} \right|_{x_2=0} \leq \infty. \quad (4-50)$$

A similar result holds for higher-order derivatives.

As an example, determine whether

$$-\overline{u_1 u_2} \propto x_2^{18/5} \quad (4-51)$$

is in agreement with equations (4-46) to (4-50). Equation (4-51) and its derivatives give, at the wall,  $-(\overline{u_1 u_2})_{x_2=0} = -(\partial \overline{u_1 u_2} / \partial x_2)_{x_2=0} = -(\partial^2 \overline{u_1 u_2} / \partial x_2^2)_{x_2=0} = 0$  and  $(\partial^3 \overline{u_1 u_2} / \partial x_2^3)_{x_2=0} = \infty$ . Since these evaluations are in agreement with equations (4-46) to (4-50), equation (4-51) satisfies continuity and the nonslip boundary conditions for  $u_1$  at the wall. In section 4.3.2.9 we will see that it also gives results in agreement with experiment.

Next consider the turbulent heat transfer  $\rho c \overline{\tau u_2}$ . Although the procedure is similar to that for the turbulent shear stress, the results can be different because the temperature fluctuation  $\tau$  at the wall may not be zero if the thermal conductivity of the wall material is not sufficiently high. Thus consider two cases,

$$\tau_{x_2=0} \neq 0 \quad (4-52)$$

for low thermal conductivity of the wall material, and

$$\tau_{x_2=0} = 0 \quad (4-53)$$

for high thermal conductivity of the wall material. Then, proceeding as for  $\overline{u_1 u_2}$ , we have

$$\frac{\partial \overline{\tau u_2}}{\partial x_2} = \overline{\frac{\partial \tau u_2}{\partial x_2}} = \overline{\tau \frac{\partial u_2}{\partial x_2}} + \overline{u_2 \frac{\partial \tau}{\partial x_2}}, \quad (4-54)$$

$$\frac{\partial^2 \overline{\tau u_2}}{\partial x_2^2} = \overline{\frac{\partial^2 \tau u_2}{\partial x_2^2}} = \overline{\tau \frac{\partial^2 u_2}{\partial x_2^2}} + 2 \overline{\frac{\partial \tau}{\partial x_2} \frac{\partial u_2}{\partial x_2}} + \overline{u_2 \frac{\partial^2 \tau}{\partial x_2^2}}, \quad (4-55)$$

and

$$\frac{\partial^3 \overline{\tau u_2}}{\partial x_2^3} = \overline{\frac{\partial^3 \tau u_2}{\partial x_2^3}} = \overline{\tau \frac{\partial^3 u_2}{\partial x_2^3}} + 3 \overline{\frac{\partial \tau}{\partial x_2} \frac{\partial^2 u_2}{\partial x_2^2}} + 3 \overline{\frac{\partial u_2}{\partial x_2} \frac{\partial^2 \tau}{\partial x_2^2}} + \overline{u_2 \frac{\partial^3 \tau}{\partial x_2^3}}. \quad (4-56)$$

Using equations (4-40), (4-42), (4-52), and (4-54) to (4-56), we get, for a wall with low thermal conductivity,

$$(\overline{\tau u_2})_{x_2=0} = 0, \quad (4-57)$$

$$\left( \frac{\partial \overline{\tau u_2}}{\partial x_2} \right)_{x_2=0} = 0, \quad (4-58)$$

$$\left( \frac{\partial^2 \overline{\tau u_2}}{\partial x_2^2} \right)_{x_2=0} = \left( \overline{\tau \frac{\partial^2 u_2}{\partial x_2^2}} \right)_{x_2=0}, \quad (4-59)$$

and

$$\left( \frac{\partial^3 \overline{\tau u_2}}{\partial x_2^3} \right)_{x_2=0} = \left( \overline{\tau \frac{\partial^3 u_2}{\partial x_2^3}} \right)_{x_2=0} + 3 \left( \overline{\frac{\partial \tau}{\partial x_2} \frac{\partial^2 u_2}{\partial x_2^2}} \right)_{x_2=0}.$$

Again, since we cannot evaluate the right side of equation (4-59),

$$0 \leq \left| \frac{\partial^2 \overline{\tau u_2}}{\partial x_2^2} \right|_{x_2=0} \leq \infty. \quad (4-60)$$

A similar result holds for the third and higher derivatives.

On the other hand, equations (4-40), (4-42), (4-53), and (4-54) to (4-56) give, for a wall with high thermal conductivity,

$$-\overline{(\tau u_2)}_{x_2=0} = 0, \quad (4-61)$$

$$-\left( \frac{\partial \overline{\tau u_2}}{\partial x_2} \right)_{x_2=0} = 0, \quad (4-62)$$

$$-\left( \frac{\partial^2 \overline{\tau u_2}}{\partial x_2^2} \right)_{x_2=0} = 0, \quad (4-63)$$

$$-\left( \frac{\partial^3 \overline{\tau u_2}}{\partial x_2^3} \right)_{x_2=0} = -3 \left( \overline{\frac{\partial \tau}{\partial x_2} \frac{\partial^2 u_2}{\partial x_2^2}} \right)_{x_2=0}, \quad (4-64)$$

and

$$0 \leq \left| -\frac{\partial^3 \overline{\tau u_2}}{\partial x_2^3} \right|_{x_2=0} \leq \infty. \quad (4-65)$$

A result similar to equation (4-65) holds for the fourth and higher derivatives.

So, like the turbulent shear stress, the turbulent heat transfer is zero at a wall and increases very slowly with  $x_2$  near a wall. However  $|\overline{\tau u_2}|$  may increase slightly more rapidly than  $|\overline{u_1 u_2}|$  if the wall thermal conductivity is low, since in that case  $(\partial^2 \overline{\tau u_2} / \partial x_2^2)_{x_2=0}$  may be nonzero. But since an effect of wall thermal conductivity on turbulent heat transfer does not seem to have been measured, and since equality of eddy diffusivities for heat and momentum transfer gives good results, this possible difference may not be significant in most situations. Of course, new work may show otherwise.

**4.3.2.5 Specialization of equations (4-25) and (4-26) for fully developed parallel mean flow and fully developed heat transfer without buoyancy.**—For simplicity consider a turbulent flow between two infinite parallel walls, which may or may not be moving. The flow is fully developed in space and time and is in the  $x_1$ -direction. The direction normal to the walls is  $x_2$ . Fully developed flow is here taken to mean that all of the dependent variables in equation (4-25) except the pressure are independent of time and  $x_1$ . The pressure may vary with  $x_1$ . If we neglect buoyancy effects by letting  $g_i = 0$ , equation (4-25) becomes, for  $i = 1$  and  $2$ ,

$$0 = -\frac{\partial P}{\partial x_1} + \frac{d}{dx_2} \left( \rho \nu \frac{dU_1}{dx_2} - \rho \overline{u_1 u_2} \right) \quad (4-66)$$

and

$$0 = -\frac{\partial P}{\partial x_2} - \rho \frac{d\overline{u_2^2}}{dx_2}. \quad (4-67)$$

Note that by virtue of the equation following (3-22),  $\sigma_e$  drops out of equation (4-25) for  $g_i = 0$ . Differentiating equation (4-67) with respect to  $x_1$  gives

$$\frac{\partial}{\partial x_2} \left( \frac{\partial P}{\partial x_1} \right) = -\rho \frac{\partial}{\partial x_1} \left( \frac{d\overline{u_2^2}}{dx_2} \right) = 0, \quad (4-68)$$

since  $\overline{u_2^2} = \overline{u_2^2}(x_2)$  does not change with  $x_1$  for fully developed flow. Integrating equation (4-66) with respect to  $x_2$  (using eqs. (4-68) and (4-25a)) then gives

$$\frac{\partial P}{\partial x_1} x_2 + C_1 = \rho \nu \frac{dU_1}{dx_2} - \rho \overline{u_1 u_2} = \bar{\tau}_{21}, \quad (4-69)$$

where  $C_1$  is a constant of integration whose value depends on the boundary conditions, and  $\bar{\tau}_{21}$  is the total averaged shear stress (the sum of the molecular and turbulent parts). According to equation (4-69) the total shear stress varies linearly with  $x_2$ .

For the case where both walls are stationary,  $dU_1/dx_2 = \overline{u_1 u_2} = \bar{\tau}_{21} = 0$  at the channel center (at  $x_2 = (x_2)_c$ ), and

$$C_1 = -(x_2)_c \frac{\partial P}{\partial x_1}. \quad (4-70)$$

Using that value for  $C_1$ , equation (4-69) becomes, at  $x_2 = 0$ ,

$$-(x_2)_c \frac{\partial P}{\partial x_1} = (\bar{\tau}_{21})_w \equiv \bar{\tau}_w$$

and

$$1 - \frac{x_2}{(x_2)_c} = \frac{\rho \nu}{\bar{\tau}_w} \frac{dU_1}{dx_2} - \frac{\rho}{\bar{\tau}_w} \overline{u_1 u_2} = \frac{\bar{\tau}_{21}}{\bar{\tau}_w}. \quad (4-71)$$

Thus the total shear stress  $\bar{\tau}_{21}$  varies linearly with distance from the wall, being a maximum at the wall and zero at the channel center. Since the turbulent shear stress  $-\rho \overline{u_1 u_2}$  is much greater than the molecular shear stress  $\rho \nu dU_1/dx_2$ , except in the immediate vicinity of the wall,  $-\overline{u_1 u_2}$  also varies linearly with  $x_2$  over most of the channel cross-section. At the wall, of course, unlike the total shear stress  $\bar{\tau}_{21}$ ,  $-\overline{u_1 u_2}$  is zero because the velocity fluctuations are zero.

Next consider the energy equation (eq. (4-26)) for the case to which equation (4-69) applies (a steady, turbulent, unidirectional, fully developed mean flow between infinite parallel walls). The mean temperature is also steady, and the flow is fully developed thermally. Equation (4-26) can then be written using equation (4-26a), as

$$\rho c U_1 \frac{\partial T}{\partial x_1} = \frac{\partial}{\partial x_1} \left( \rho c \alpha \frac{\partial T}{\partial x_1} - \rho c \overline{u_1 \tau} \right) + \frac{\partial}{\partial x_2} \left( \rho c \alpha \frac{\partial T}{\partial x_2} - \rho c \overline{u_2 \tau} \right) = -\frac{\partial Q_1}{\partial x_1} - \frac{\partial Q_2}{\partial x_2}, \quad (4-72)$$

where  $Q_1$  and  $Q_2$  are respectively the total (time-averaged) heat transfer (molecular plus turbulent) in the  $x_1$ - and  $x_2$ -directions. Fully developed thermally is here taken to mean that the molecular and turbulent heat-transfer vectors are independent of  $x_1$ . This definition is consistent with equation (4-72), as can be seen by differentiation of that equation with respect to  $x_1$ . (Note that although the left side of equation (4-72) was not assumed independent of  $x_1$ , that independence follows from the independence of  $x_1$  of the molecular heat-transfer vector.) Then equation (4-72) becomes, for fully developed heat transfer,

$$\rho c U_1 \frac{\partial T}{\partial x_1} = \frac{d}{dx_2} \left( \rho c \alpha \frac{\partial T}{\partial x_2} - \rho c \overline{u_2 \tau} \right) = - \frac{dQ_2}{dx_2}, \quad (4-73)$$

or

$$\frac{\partial T}{\partial x_1} \int U_1(x_2) dx_2 + C_2 = \alpha \frac{\partial T}{\partial x_2} - \overline{u_2 \tau} = - \frac{Q_2}{\rho c}, \quad (4-74)$$

where  $\partial T / \partial x_1$  is written outside the integral sign, since the flow is fully developed thermally ( $(\partial / \partial x_1)(\alpha \partial T / \partial x_2) = 0 = (\partial / \partial x_2)(\partial T / \partial x_1)$ ).

4.3.2.6 *Law of the wall.*—Equations (4-11) and (4-13) can be written in dimensionless form for  $g_i = 0$  as

$$\frac{\partial \tilde{u}_i^+}{\partial t^+} = - \frac{\partial(\tilde{u}_i^+ \tilde{u}_k^+)}{\partial x_k^+} - \frac{\partial \tilde{\sigma}^+}{\partial x_i^+} + \frac{\partial^2 \tilde{u}_i^+}{\partial x_k^+ \partial x_k^+} \quad (4-75)$$

and

$$\frac{\partial^2 \tilde{\sigma}^+}{\partial x_i^+ \partial x_i^+} = - \frac{\partial^2(\tilde{u}_i^+ \tilde{u}_k^+)}{\partial x_i^+ \partial x_k^+}, \quad (4-76)$$

where  $\tilde{\phantom{x}}$  over a quantity indicates a total instantaneous value (mean plus fluctuating), and where

$$\tilde{u}_i^+ \equiv \frac{\tilde{u}_i}{\sqrt{\bar{\tau}_w / \rho}}, \quad x_i^+ \equiv \frac{x_i \sqrt{\bar{\tau}_w / \rho}}{\nu}, \quad \tilde{\sigma}^+ \equiv \frac{\tilde{\sigma} / \rho}{\bar{\tau}_w / \rho}, \quad \text{and} \quad t^+ \equiv \frac{t \bar{\tau}_w}{\rho \nu}. \quad (4-77)$$

(The quantity  $\sigma_e$  drops out of the set of equations since  $g_i = 0$  (see equation following (3-22)).)

The set of equations (4-75) and (4-76) contains four equations in the four unknowns  $u_1^+$ ,  $u_2^+$ ,  $u_3^+$ , and  $\tilde{\sigma}^+$ . Thus one could do a thought experiment, starting from given initial conditions. Using appropriate boundary conditions at the walls (e.g.,  $u_1^+ = 0$  for  $x_2^+ = 0, 2(x_2^+)_c$ ), a solution of equations (4-75) and (4-76) could, in principle, be obtained. For fully developed statistically steady flow one would have to consider a region far from the channel entrance and times large enough for the solution to become independent of initial conditions. The parameter in this system is  $(x_2^+)_c$ , which appears as  $1/2$  the maximum value of  $x_2^+$  (the walls are  $2(x_2^+)_c$  units apart). The quantity  $(x_2^+)_c \equiv (x_2)_c \sqrt{\bar{\tau}_w / \rho} / \nu$  is a kind of Reynolds number, since  $\sqrt{\bar{\tau}_w / \rho}$  is a velocity (called the friction velocity). The solution of equations (4-75) and (4-76), with boundary conditions at  $x_2^+ = 0$  and  $2(x_2^+)_c$ , gives

$$\hat{u}_1^+ = \hat{u}_1^+ [x_k^+, t^+, (x_2^+)_c]$$

and

$$\tilde{\sigma}^+ = \tilde{\sigma}^+ [x_k^+, t^+, (x_2^+)_c].$$

However, since mean values are steady and fully developed,  $\overline{u_1^+ u_2^+}$  (see eq. (4-14)), and  $\overline{\hat{u}_1^+} = U_1^+$  (see eq. (4-18)), are not functions of  $x_1^+$ ,  $x_3^+$ , or  $t^+$ . Thus,

$$\overline{u_1^+ u_2^+} = \overline{u_1^+ u_2^+} [x_2^+, (x_2^+)_c], \quad (4-78)$$

and

$$\overline{\hat{u}_1^+} = U_1^+ = U_1^+ [x_2^+, (x_2^+)_c]. \quad (4-79)$$

Next let  $(x_2^+)_c \rightarrow \infty$ . Then for the region where  $x_2^+ \ll (x_2^+)_c$ , the parameter  $(x_2^+)_c$  drops out of the determining boundary conditions. That occurs because the only boundary condition determining the turbulence at  $x_2^+ \ll (x_2^+)_c$  is the one at the near wall, the boundary condition at  $x_2^+ = 2(x_2^+)_c \rightarrow \infty$  having no effect. So equations (4-78) and (4-79) become, for  $(x_2^+)_c \rightarrow \infty$  and  $x_2^+ \ll (x_2^+)_c$ ,

$$\overline{u_1^+ u_2^+} = \overline{u_1^+ u_2^+} (x_2^+), \quad (4-80)$$

and

$$U_1^+ = U_1^+ (x_2^+). \quad (4-81)$$

For the present fully developed unidirectional flow, the eddy viscosity from equation (4-28) is

$$\epsilon = - \frac{\overline{u_1^+ u_2^+}}{dU_1^+/dx_2^+}, \quad (4-82)$$

or

$$\frac{\epsilon}{\nu} = - \frac{\overline{u_1^+ u_2^+}}{dU_1^+/dx_2^+}. \quad (4-83)$$

So, from equations (4-78) and (4-79),

$$\frac{\epsilon}{\nu} = \frac{\epsilon}{\nu} [x_2^+, (x_2^+)_c], \quad (4-84)$$

or, from equations (4-80) and (4-81),

$$\frac{\varepsilon}{\nu} = \frac{\varepsilon}{\nu}(x_2^+) \quad (4-85)$$

for  $x_2^+ \ll (x_2^+)_c$  and  $(x_2^+)_c \rightarrow \infty$ .

The fact that equations (4-80), (4-81), and (4-85) hold for  $x_2^+ \ll (x_2^+)_c$  and  $(x_2^+)_c \rightarrow \infty$  is often called the law of the wall. Although that is usually considered to be an empirical law, we have obtained it here by using the Navier-Stokes equations in a thought experiment. Note that if one considers the region so close to the wall that  $\overline{u_1^+ u_2^+} \rightarrow 0$ , the so-called laminar sublayer, equations (4-71) and (4-77) give (for  $x_2 \ll (x_2^+)_c$ )

$$\frac{dU_1^+}{dx_2^+} = 1, \quad (4-86)$$

or

$$U_1^+ = x_2^+. \quad (4-87)$$

**4.3.2.7 The velocity-defect law.**—Consider now the central region of the channel, sometimes referred to as the region away from the wall. As in the last section the flow is fully developed and statistically steady. We write equations (4-75) and (4-76) as

$$\frac{\partial \tilde{u}_i^+}{\partial t^*} = -\frac{\partial(\tilde{u}_i^+ \tilde{u}_k^+)}{\partial x_k^*} - \frac{\partial \tilde{\sigma}^+}{\partial x_i^*} + \frac{1}{(x_2^+)_c} \frac{\partial^2 \tilde{u}_i^+}{\partial x_k^* \partial x_k^*} \quad (4-88)$$

and

$$\frac{\partial^2 \tilde{\sigma}^+}{\partial x_i^* \partial x_i^*} = -\frac{\partial^2(\tilde{u}_i^+ \tilde{u}_k^+)}{\partial x_i^* \partial x_k^*}, \quad (4-89)$$

where

$$x_i^* \equiv \frac{x_i}{(x_2)_c}, \quad (x_2^+)_c \equiv \frac{(x_2)_c \sqrt{\tau_w/\rho}}{\nu}, \quad \text{and} \quad t^* \equiv \frac{t \sqrt{\tau_w/\rho}}{(x_2)_c}. \quad (4-90)$$

The quantities  $\tilde{u}_i^+$  and  $\tilde{\sigma}^+$  are defined in equation (4-77). Proceeding as for the law of the wall in the last section, we note that equations (4-88) and (4-89) constitute a set of four equations in the four unknowns  $\tilde{u}_1^+$ ,  $\tilde{u}_2^+$ ,  $\tilde{u}_3^+$ , and  $\tilde{\sigma}^+$ . Here the walls where the boundary conditions are set are at  $x_2^+ = 0, 2$  (e.g.,  $\tilde{u}_1^+ = 0$  at  $x_2^+ = 0, 2$ ). As in the last section we do a thought experiment, starting with given initial conditions. We consider a cross section where the mean flow is fully developed and continue the



solution until the flow is statistically steady. Then equations (4-88) and (4-89), or their solution, show that

$$\hat{u}_1^+ = \hat{u}_1^+ [x_k^*, t^*, (x_2^+)_c] \quad (4-91)$$

and

$$\hat{\sigma}^+ = \hat{\sigma}^+ [x_k^*, t^*, (x_2^+)_c]. \quad (4-92)$$

Note that whereas in the last section  $(x_2^+)_c$  was included in the functional relations because of its use for the location of the boundary condition at  $x_2^+ = 0$ ,  $2(x_2^+)_c$ , here it is included because of its appearance in the differential equation (4-88);  $(x_2^+)_c$  is not needed for the location of the boundary condition at  $x_2^+ = 2$ .

Since mean values are steady and fully developed,  $\overline{\hat{u}_2^+} = U_1^+$  (see eq. (4-18)) is not a function of  $x_1^*$ ,  $x_3^*$ , or  $t^*$ , as are the unaveraged quantities in equations (4-91) and (4-92). Thus

$$\overline{\hat{u}_1^+} = U_1^+ = U_1^+ [x_2^*, (x_2^+)_c]. \quad (4-93)$$

Now we confine our attention to the region away from the wall and let  $(x_2^+)_c \rightarrow \infty$ , so that the viscous term, including  $(x_2^+)_c$ , drops out of equation (4-88). Batchelor explains this loss of the influence of viscosity in the context of Fourier analysis (ref. 12). He notes that the region of wavenumber space which is affected by the action of viscous forces moves out from the origin toward a wavenumber of infinity as the Reynolds number increases. In the limit of infinite Reynolds number (infinite  $(x_2^+)_c$  in our case) the sink of energy is displaced to infinity, and the influence of viscous forces is negligible for wavenumbers (reciprocal eddy sizes) of finite magnitude. (See chapter V for a discussion of Fourier analysis.) Thus, for  $(x_2^+)_c \rightarrow \infty$ , equation (4-93) can be written, for the region away from the wall, as

$$[U_1^+ - (U_1^+)_c] = [U_1^+ - (U_1^+)_c](x_2^*), \quad (4-94)$$

where  $(U_1^+)_c$  is the value of  $U_1^+$  at the channel midpoint. Equation (4-94) is written with  $U_1^+ - (U_1^+)_c$  as the dependent variable to ensure that curves for different Reynolds numbers will collapse at the channel midpoint. According to equation (4-94) they will then also collapse at points *near* the midpoint. The quantity  $U_1^+ - (U_1^+)_c$  is called the dimensionless velocity defect, and equation (4-94), which applies in the central region of the channel when viscous forces are negligible there (when  $(x_2^+)_c \rightarrow \infty$ ), is known as the velocity-defect law.<sup>1</sup> As in the case of the law of the wall, equation (4-94) is usually considered to be an empirical law, but it is obtained here by using the Navier-Stokes equations in a thought experiment.

---

<sup>1</sup>Note that letting  $(x_2^+)_c \rightarrow \infty$  and neglecting the viscous terms in equations (4-88) destroys the accuracy of the solution near the wall, since viscous effects are not negligible there. But as already shown, letting  $(x_2^+)_c \rightarrow \infty$  preserves the accuracy in the region away from the wall, the region we are interested in here, since viscous effects are negligible away from the wall.

4.3.2.8 *The logarithmic law.*—Next we want to determine the form of the mean velocity profile required in a possible overlap region, where equation (4-81) (the law of the wall), and equation (4-94) (the velocity defect law), both apply. From equations (4-71), (4-83), and (4-84), which apply over a whole channel cross section in the fully developed region, we get

$$1 - \frac{x_2^+}{(x_2^+)_c} = \left\{ 1 + \frac{\varepsilon}{\nu} [x_2^+, (x_2^+)_c] \right\} \frac{dU_1^+}{dx_2^+}. \quad (4-95)$$

It is known that, except in the immediate vicinity of the wall, where  $x_2^+$  is less than say 70, the molecular shear stress is much smaller than the turbulent. We will show later in this section that our results are consistent with that statement. Thus, neglecting the molecular shear stress in equation (4-95) we have

$$1 - \frac{x_2^+}{(x_2^+)_c} = \frac{\varepsilon}{\nu} [x_2^+, (x_2^+)_c] \frac{dU_1^+}{dx_2^+}. \quad (4-96)$$

In order that equation (4-81) (the law of the wall) will hold, we confine the range of equation (4-96) to  $x_2^+/(x_2^+)_c \ll 1$ , but at the same time keep  $x_2^+/(x_2^+)_c$  large enough that the turbulent stress is large compared with the molecular stress.<sup>2</sup> For that range we can use equation (4-85) in equation (4-96). The latter then becomes

$$1 = \frac{\varepsilon}{\nu} (x_2^+) \frac{dU_1^+}{dx_2^+}. \quad (4-97)$$

Note that equation (4-97), when integrated from  $x_2 = 0$  (at the near wall) to  $x_2$ , is in the form of equation (4-81), and is thus an expression of the law of the wall.

To ensure that equation (4-97) will also satisfy equation (4-94), the velocity-defect law, we first write the former in terms of  $x_2^* \equiv x_2/(x_2)_c = x_2^+/(x_2^+)_c$ ,  $(x_2^+)_c$ , and the dimensionless velocity defect  $(U_1^+)_c - U_1^+$ . That gives

$$1 = - \frac{\varepsilon}{\nu} [(x_2^+)_c x_2^*] \frac{d[(U_1^+)_c - U_1^+]}{(x_2^+)_c dx_2^*}, \quad (4-98)$$

---

<sup>2</sup>The range of  $x_2^+$  for which that is possible increases as  $(u_2^+)_c \rightarrow \infty$ ; the latter was assumed for obtaining the velocity-defect law and the law of the wall.

where the subscript  $c$  refers to values at the channel center. If equation (4-98) is to agree with equation (4-94), then  $(x_2^+)_c$  must cancel out of equation (4-98). For that to happen,  $\epsilon/\nu$  must be proportional to  $(x_2^+)_c$ , so that

$$\frac{\epsilon}{\nu}(x_2^+) = \frac{\epsilon}{\nu}[(x_2^+)_c x_2^*] = K(x_2^+)_c x_2^* = Kx_2^+, \quad (4-99)$$

where  $K$  is a constant (called the Kármán constant). Then equation (4-98) becomes

$$1 = -Kx_2^* \frac{d[(U_1^+)_c - U_1^+]}{dx_2^*}, \quad (4-100)$$

which, when integrated from  $x_2^* = 1$  (at the channel center) to  $x_2^*$ , is in agreement with equation (4-94). Thus, only when  $\epsilon/\nu$  is given by equation (4-99) does equation (4-97) satisfy both equations (4-81) and (4-94), as it must in an overlap region.<sup>3</sup> Substituting equation (4-99) into equation (4-97) gives

$$1 = Kx_2^+ \frac{dU_1^+}{dx_2^+}, \quad (4-101)$$

or, on integration,

$$U_1^+ = \frac{1}{K} \ln x_2^+ + C. \quad (4-102)$$

Equation (4-102) is the well known logarithmic velocity distribution which applies to the portion of the law-of-the-wall region where the turbulent shear stress is much greater than the molecular. It can be obtained in a number of ways (e.g., ref. 15), but is obtained here from equations (4-81) and (4-94) by assuming an overlap region. That was first done by Millikan, but in a somewhat different way (ref. 16). Besides obtaining the logarithmic law, we have shown that any expression for  $\epsilon/\nu$  which satisfies both the law of the wall and the velocity defect law in some overlap region must, according to our analysis, reduce to  $Kx_2^+$  in that region (eq. (4-99)).

We can now see whether the assumption that the turbulent shear stress is much greater than the molecular shear stress except very close to the wall, where  $x_2^+$  is less than about 70, is in agreement with our results. Substituting the expression for  $\epsilon/\nu$  in equation (4-99) into equation (4-95) gives

---

<sup>3</sup>Actually, there are expressions for  $\epsilon/\nu$  which satisfy both equations (4-81) and (4-94) but which have an appearance which differs from that of equation (4-99). However, they reduce to equation (4-99). For example, Prandtl's mixing-length expression (ref. 6) and von Kármán's similarity expression (ref. 15) are both of the form  $(\epsilon/\nu) = (\epsilon/\nu)(U_1^+, x_2^+)$  and satisfy equations (4-81) and (4-94). But  $(\epsilon/\nu) = (\epsilon/\nu)(U_1^+, x_2^+) = (\epsilon/\nu)[U_1^+(x_2^+), x_2^+] = (\epsilon/\nu)(x_2^+)$ . This agrees with equation (4-85) and leads to equation (4-99). Equation (4-99) is simpler than the other expressions for  $\epsilon/\nu$  and, since the other expressions reduce to it, may be more fundamental.

$$1 - \frac{x_2^+}{(x_2^+)_c} = (1 + Kx_2^+) \frac{dU_1^+}{dx_2^+}, \quad (4-103)$$

so that the ratio of turbulent to molecular shear stress is  $Kx_2^+/1$ . Since  $K \approx 0.4$  the turbulent shear stress is more than an order of magnitude greater than the molecular stress for  $x_2^+ > 70$ .

**4.3.2.9 An expression for  $\epsilon/\nu$  for fully developed flow which applies at all distances from a wall.**—We now give a general expression for the eddy diffusivity which satisfies conditions given in sections 4.3.2.4 and 4.3.2.6 to 4.3.2.8, and which applies across the whole channel in the fully developed region. The expression is

$$\frac{\epsilon}{\nu} = Lx_2^+ \left[ 1 - \frac{x_2^+}{(x_2^+)_c} \right]^{5/4}, \quad (4-104)$$

where

$$L = \begin{cases} aU_1^{+13/5} & \text{for } aU_1^{+13/5} \leq 2/5 \\ 2/5 & \text{for } aU_1^{+13/5} > 2/5 \end{cases} \quad (4-105)$$

$$\text{and } a = 3 \times 10^{-4}.$$

Using equation (4-104) to close equation (4-95), a fully developed form of the equation for the mean flow, we get

$$1 - \frac{x_2^+}{(x_2^+)_c} = \left\{ 1 + Lx_2^+ \left[ 1 - \frac{x_2^+}{(x_2^+)_c} \right]^{5/4} \right\} \frac{dU_1^+}{dx_2^+}, \quad (4-106)$$

where  $L$  is given by equation (4-105).

Consider now whether the conditions obtained in sections 4.3.2.4 and 4.3.2.6 to 4.3.2.8 are satisfied by equations (4-104) to (4-106). First note that those equations satisfy equations (4-79) and (4-84) for  $0 \leq x_2^+ < \infty$ . Then for  $x_2^+ \ll (x_2^+)_c$  they agree with the law-of-the-wall equations (4-81) and (4-85). As  $x_2^+ \rightarrow 0$ , equation (4-86) or (4-87) is satisfied. That is, as  $x_2^+ \rightarrow 0$ ,  $U_1^+$  becomes equal to  $x_2^+$ . An additional condition satisfied as  $x_2^+ \rightarrow 0$  is that  $\epsilon/\nu \rightarrow x_2^{+18/5}$ , which is equivalent to equation (4-51). This follows from evaluating equations (4-104) and (4-105) for small values of  $x_2^+$  and using equation (4-87). Then by using equations (4-83) and (4-86), we get equation (4-51), which in turn satisfies equations (4-46) to (4-50). These last equations are consequences of continuity and the nonslip boundary condition at the wall, so the expression for  $\epsilon/\nu$  given by equations (4-104) and (4-105) is also in agreement with those consequences.

Next consider whether equation (4-106) satisfies the velocity defect law (eq. (4-94)) for the region away from the wall, where the turbulent shear stress is much greater than the molecular (where  $x_2^+$  is greater than say 70). For that region equation (4-106) can be written as

$$1 = -\frac{2}{5}x_2^+(1 - x_2^+)^{1/4} \frac{d[(U_1^+)_c - U_1^+]}{dx_2^+}, \quad (4-107)$$

where  $x_2^+ = x_2^+/(x_2^+)_c$ . But equation (4-107) when integrated from the channel center to  $x_2^+$ , is in the form of equation (4-94). Thus equation (4-106), from which equation (4-107) is obtained for the region away from the wall, satisfies the velocity-defect law in that region. Integration of equation (4-107) gives

$$(U_1^+)_c - U_1^+ = \frac{5}{2} \ln \left[ \frac{1 + (1 - x_2^+)^{1/4}}{1 - (1 - x_2^+)^{1/4}} \right] - 5 \tan^{-1} (1 - x_2^+)^{1/4} \quad (4-108)$$

for our velocity-defect law.

Finally, for the law-of-the-wall region, where  $x_2^+ \ll (x_2^+)_c$ , equation (4-106) becomes

$$1 = \left( 1 + \frac{2}{5}x_2^+ \right) \frac{dU_1^+}{dx_2^+}. \quad (4-109)$$

Then for the part of that region where the turbulent shear stress is much greater than the molecular (the region away from the wall), we have

$$1 = \frac{2}{5}x_2^+ \frac{dU_1^+}{dx_2^+} \quad (4-110)$$

which, when integrated, becomes

$$U_1^+ = \frac{5}{2} \ln x_2^+ + C, \quad (4-111)$$

which agrees with the logarithmic distribution in equation (4-102).

Equation (4-106) is plotted semilogarithmically for several values of  $(x_2^+)_c$  in figure 4-2. Also included in the plot are some experimental data from references 11 and 15, and a numerical solution (direct numerical simulation) of the unaveraged Navier-Stokes equations from reference 17. Although the experimental data are for a pipe, and equation (4-106) was obtained for a flat channel, a similar equation is obtained for a pipe by letting  $(x_2^+)_c$  be the radius of the pipe. For the region close to a wall, the flow in a pipe should be similar to that in a channel, since, for that region the pipe wall could be considered

flat. Also, for a pipe, as well as for a channel, the total shear stress varies linearly with wall distance, as can be shown by writing a force balance on an element of fluid for both configurations. It is conceivable that the eddy diffusivity for the central region might be different for the two configurations, but such differences are not apparent in figure 4-2. Equation (4-106) appears to represent both the data and the numerical solution quite well.

We can calculate friction factor as a function of Reynolds number by using the velocity distribution from equation (4-106). Since we will be comparing the calculated friction factors with those obtained experimentally for a pipe, the quantity  $(x_2)_c$  will be the pipe radius (see the last paragraph). The friction factor  $f$  is given by

$$f \equiv \frac{\bar{\tau}_w}{\rho U_a^2 / 2} = \frac{2}{U_a^{+2}}, \quad (4-112)$$

and the Reynolds number  $Re$  is obtained from

$$Re \equiv 2(x_2)_c \frac{U_a}{\nu} = 2(x_2)_c U_a^+, \quad (4-113)$$

where  $U_a^+$  is a dimensionless bulk or mixed-mean velocity and is given by

$$U_a^+ \equiv \frac{U_a}{\sqrt{\tau_w / \rho}} = \left[ 2 / (x_2)_c \right] \int_0^{(x_2)_c} [(x_2)_c - x_2^+] U_1^+ dx_2^+ \quad (4-114)$$

for a pipe.

A plot of friction factor versus Reynolds number, as obtained from equations (4-106), (4-112), and (4-113), is compared with experimental data for turbulent flow in a pipe in figure 4-3. As in the case of the velocity distribution in figure 4-2 the agreement is quite good.

**4.3.2.10 Thermal law of the wall, temperature-defect law, and temperature logarithmic law.**—Laws analogous to those obtained for the mean velocity distribution in sections 4.3.2.6 to 4.3.2.8 can be obtained for the mean temperature distribution when fully developed heat transfer, in addition to fully developed flow, occurs in a passage. The procedures are similar, and so this section will not be detailed. The main difference here is that the energy equation (4-12) (in appropriate dimensionless forms) is added to the lists of unaveraged equations used in the thought experiments. Thus, in addition to equations (4-75) and (4-76) we use

$$\frac{\partial \tilde{T}^+}{\partial t^+} = - \frac{\partial(\tilde{T}^+ \hat{u}_k^+)}{\partial x_k^+} + \frac{1}{Pr} \frac{\partial^2 \tilde{T}^+}{\partial x_i^+ \partial x_i^+},$$

and in addition to equations (4-88) and (4-89) we have

$$\frac{\partial \tilde{T}^+}{\partial t^*} = - \frac{\partial(\tilde{T}^+ \hat{u}_k^*)}{\partial x_k^*} + \frac{1}{(x_2^*)_c Pr} \frac{\partial^2 \tilde{T}^+}{\partial x_i^* \partial x_i^*},$$

where  $\tilde{T}^+ \equiv \frac{(\tilde{T}_w - \tilde{T})c\bar{\tau}_w}{(Q_2)_w \sqrt{\bar{\tau}_w/\rho}}$ ,  $Pr \equiv \frac{\nu}{\alpha}$  is the Prandtl number, and  $(Q_2)_w$  is the time-averaged normal

heat transfer at the wall. The rest of the dimensionless quantities have already been defined in equations (4-77) and (4-90). Then one obtains the thermal law of the wall, the temperature-defect law, and the temperature logarithmic law in place of equations (4-81), (4-94), and (4-102) respectively. These are

$$T^+ = T^+(x_2^+, Pr),$$

$$(T_c^+ - T^+) = (T_c^+ - T^+)(x_2^+),$$

and for an overlap region, where both the thermal law of the wall and the temperature defect law apply,

$$T^+ = \frac{1}{K_1} \ln y^+ + C(Pr),$$

where  $T^+ = \bar{T}^+$  is the time-averaged dimensionless temperature difference, and  $K_1 = K$  (see eq. (4-102)) if  $\epsilon_h = \epsilon$  as in equation (4-38). Note that the Prandtl number  $Pr$  does not appear in the temperature-defect law because the term  $\left\{1/[(x_2^+)Pr]\right\} \partial^2 \tilde{T}^+ / \partial x_i^+ \partial x_i^+$  drops out of the dimensionless energy equation used for the temperature-defect law when  $(x_2^+)_c \rightarrow \infty$ . (This loss of the influence of thermal conduction (or of thermal smearing) can be explained by an argument similar to that for the influence of viscosity, as given after equation (4-93).) On the other hand,  $Pr$  appears in the thermal law of the wall because the term  $(1/Pr) \partial^2 \tilde{T}^+ / \partial x_i^+ \partial x_i^+$  does not drop out of the dimensionless energy equation used for the law of the wall when  $(x_2^+)_c \rightarrow \infty$ . Finally, note that in getting the logarithmic law for the temperature distribution we use, as obtained from equations (4-29) and (4-74)

$$\frac{Q_2}{(Q_2)_w} = \left( \frac{1}{Pr} + \frac{\epsilon_h}{\nu} \right) \frac{dT^+}{dx_2^+} \quad (4-115)$$

in place of equation (4-95), where  $\epsilon_h$  is the eddy diffusivity for heat transfer. As a result of this change  $\epsilon$  is replaced by  $\epsilon_h$  and/or  $U_1^+$  by  $T^+$  in equations (4-97) to (4-102). Note that, as for equation (4-95), and except for very small Prandtl numbers, if one lets  $(x_2^+)_c \rightarrow \infty$  there will be an extensive region where the turbulent term is much greater than the molecular term, and where the term on the left side can be replaced by 1. The results in this section, like those in sections 4.3.2.6 to 4.3.2.8 follow from a thought experiment with the unaveraged continuum equations.

**4.2.3.11 A calculation of fully developed convective heat transfer.**—Consider next a treatment of the fully developed heat transfer which can occur when temperature gradients exist in a flowing fluid. If, in accordance with equation (4-38) we set  $\epsilon_h = \epsilon$ , equation (4-115) becomes

$$\frac{Q_2}{(Q_2)_w} = \left( \frac{1}{Pr} + \frac{\epsilon}{\nu} \right) \frac{dT^+}{dx_2^+}, \quad (4-116)$$

where, again,

$$T^+ \equiv \frac{(T_w - T)c\bar{\tau}_w}{(Q_2)_w \sqrt{\bar{\tau}/\rho}}$$

and

$$Pr \equiv \frac{\nu}{\alpha}$$

is the Prandtl number of the fluid. As for the velocity distribution (eq. (4-106)),  $\epsilon/\nu$  in equation (4-116) is obtained from equation (4-104). Equation (4-116) applies to either a channel or a pipe, as does equation (4-106). However, the quantity  $Q_2/(Q_2)_w$  in equation (4-116) is different for the two configurations, although the effect of the difference on the heat-transfer coefficients is small except for liquid metals (which are not considered here). Since we will be comparing our results mainly with experimental heat-transfer (and mass-transfer) data for a pipe, we use  $Q_2/(Q_2)_w$  for a pipe (ref. 7 or 9):

$$\frac{Q_2}{(Q_2)_w} = \frac{(x_2^+)_c}{(x_2^+)_c - x_2^+} - \frac{2}{[(x_2^+)_c - x_2^+](x_2^+)_c U_a^+} \int_0^{x_2^+} [(x_2^+)_c - \xi] U_1^+(\xi) d\xi. \quad (4-117)$$

The quantity  $(x_2^+)_c$  is defined as  $(x_2)_c \sqrt{\bar{\tau}_w/\rho} / \nu$ , where  $(x_2)_c$  is now the pipe radius,  $U_1^+$  is obtained from equation (4-106) and  $U_a^+$  is given by equation (4-114). (Compare eq. (4-117) with that obtained for a channel by using the first and last members of eq. (4-74)).

We want to calculate the Stanton number as a function of Reynolds and Prandtl number. The Stanton number is given by

$$St \equiv \frac{h}{\rho c U_a} = \frac{1}{U_a^+ T_a^+}, \quad (4-118)$$

where the heat-transfer coefficient  $h$  is defined as

$$h \equiv \frac{(Q_2)_w}{T_w - T_a}, \quad (4-119)$$

and the dimensionless mixed-mean temperature difference  $T_a^+$  is obtained from

$$T_a^+ = \frac{\int_0^{(x_2^+)_c} [(x_2^+)_c - x_2^+] T^+ U_1^+ dx_2^+}{\int_0^{(x_2^+)_c} [(x_2^+)_c - x_2^+] U_1^+ dx_2^+}, \quad (4-120)$$



where  $U_1^+$  is calculated from equation (4-106), and  $T^+$  is obtained from equations (4-116) and (4-104). Finally the Reynolds number  $Re$  is given by equation (4-113). By varying the parameter  $(x_2^+)_c$ , Stanton number can be calculated as a function of Reynolds number and Prandtl number from these equations.

Figure 4-4 shows plots of calculated Stanton number versus Prandtl number for three Reynolds numbers. Included for comparison are experimental data for heat and mass transfer. The mass-transfer data are included by replacing temperatures by concentrations and molecular thermal diffusivities by molecular diffusivities for mass transfer. The agreement of the experimental data with the solid curves calculated by using velocity and temperature distributions from equations (4-106), (4-116), and (4-104) is good over the entire range of variables shown.

Of some interest is the fact that the good agreement with experiment was obtained by setting the eddy diffusivity for heat transfer (or for mass transfer)  $\epsilon_h$  equal to that for momentum transfer  $\epsilon$ , as obtained from the mixing-length theory (see eq. (4-38)). By contrast, the agreement obtained by setting  $\epsilon/\epsilon_h$  equal to the molecular Prandtl number (about 0.7 for air), as is often done, is much poorer. This is indicated by the dashed curve in figure 4-4c. These results do not, of course, prove that  $\epsilon/\epsilon_h = 1$  at all points in the flow, since  $\epsilon/\epsilon_h$  may vary with position. They only show that the mean effective value of  $\epsilon/\epsilon_h$  is very close to 1.

**4.3.2.12 Some other closure assumptions for fully developed or nearly fully developed (equilibrium) flows.**—The results in the last section utilized an approximate expression for the eddy viscosity which was, however, based partially on exact information. Here we review briefly some earlier approaches.

A reasonable expression for the region away from walls is the von Kármán similarity expression (ref. 33). That expression is most easily obtained by assuming that, away from boundaries, the turbulence at a point is a function only of conditions in the vicinity of the point, in particular, of the first and second derivatives at the point. Then by dimensional analysis we obtain for the eddy viscosity

$$\epsilon = \epsilon \left( \frac{\partial U_1}{\partial x_2}, \frac{\partial^2 U_1}{\partial x_2^2} \right) = K^2 \frac{\left( \frac{\partial U_1}{\partial x_2} \right)^3}{\left( \frac{\partial^2 U_1}{\partial x_2^2} \right)^2}, \quad (4-121)$$

where  $K$  is the Kármán constant.

Von Kármán's hypothesis (eq. (4-121)) has been proposed for the region away from a wall. Close to a wall we assume that the eddy viscosity is a function only of quantities measured relative to a wall,  $U_1$  and  $x_2$ , and of  $\nu$ . The simplest assumption consistent with dimensional analysis and the requirement that the effect of  $\nu$  should become small for large  $x_2$  is then (ref. 33)

$$\epsilon = \epsilon(U_1, x_2, \nu) = n^2 U_1 x_2 \left[ 1 - \exp \left( \frac{-n^2 U_1 x_2}{\nu} \right) \right], \quad (4-122)$$

where  $n$  is an experimental constant ( $n = 0.124$ ). Equations (4-121) and (4-122) give results for flow and heat (or mass) transfer in tubes which are almost as good as those in figure 4-4 (see ref. 33). The use of those equations also gives good results for the boundary layer on a flat plate (ref. 34).

By making a small modification in the derivation of equation (4-121) we can obtain an expression for  $\epsilon$  which should be applicable to a vortex. We assume that the turbulence at a point is dependent only on the shearing deformation rate at the point and in the vicinity of the point; that is, it is a function of the deformation rate and its derivatives. If we exclude derivatives of the deformation rate higher than the first we get, for a parallel flow (eq. (4-121)). However, for a circular vortex, we get

$$\epsilon = \epsilon \left[ \frac{dv}{dr} - \frac{v}{r}, \frac{d}{dr} \left( \frac{dv}{dr} - \frac{v}{r} \right) \right] = \frac{-K^2 \left( \frac{dv}{dr} - \frac{v}{r} \right)^3}{\left[ \frac{d}{dr} \left( \frac{dv}{dr} - \frac{v}{r} \right) \right]^2}, \quad (4-123)$$

where  $v$  is the tangential velocity and  $r$  is the radius. For a vortex flow,  $v = v_0 r_0 / r$ , where the subscripts 0 refer to values at some arbitrary radius. Equation (4-123) then becomes

$$\epsilon = \frac{K^2 v_0 r_0}{2}. \quad (4-124)$$

Equation (4-124) has been used profitably for turbulent vortex flows in vortex tubes (ref. 35), in astrophysical clouds (ref. 36), and in the atmosphere (ref. 37).

Finally we mention closures based on Prandtl's mixing-length  $\ell_2$  (ref. 6), where  $\ell_2$  is defined by

$$\overline{u_1 u_2} = -\ell_2^2 \left( \frac{\partial U_1}{\partial x_2} \right)^2. \quad (4-125)$$

Prandtl assumed that  $\ell_2 = Kx_2$ , where  $x_2$  is the distance from a wall. Van Driest (ref. 38) has modified that assumption by introducing a damping factor which reduces  $\ell_2$  in the region close to a wall:

$$\ell_2 = Kx_2 \left[ 1 - \exp \left( \frac{-x_2^+}{A} \right) \right], \quad (4-126)$$

where  $A$  is an additional experimental constant. Equation (4-126) appears to be reasonably applicable to the regions both close to and away from a wall, as is our equation (4-104). Equation (4-104) gives, in addition, a velocity profile which is accurate in the so-called wake region, where  $x_2 \sim (x_2)_c$  (see fig. 4-2). Although the use of an equation which is applicable to two or more regions in a flow may be somewhat more convenient than the use of a separate equation for each region, there is basically no reason why one equation should apply to more than one region; the turbulence mechanism is likely different in the different regions.

A word should perhaps be said about the value of the Kármán constant  $K$ . If  $U_1^+ = U_1^+[x_2^+, (x_2^+)_c]$ , as in figure 4-2, then a value of  $K = 0.4$ , or  $2/5$ , (see eq. (4-105)) gives good results. On the other hand, if it is assumed that  $U_1^+ = U_1^+(x_2^+)$ , so that a single curve is obtained instead of the multiple curves in figure 4-2, then  $K = 0.36$  gives better agreement with the data (ref. 33). Finally, for a vortex (eq. (4-124)),  $K$  seems to be close to 0.3 (ref. 35). It is not surprising that the value of  $K$  appears to be slightly different for a vortex than for a parallel flow, since, as for all closures, the ones considered here are approximate and correspond only partially to reality. Thus the constants in a closure scheme must often be "fine-tuned" when the flow configuration is changed.

**4.3.2.13 A treatment of moderately short highly accelerated turbulent boundary layers.**—The last few sections considered closure schemes for fully developed or nearly fully developed turbulent flows. We turn now to a problem which is in some ways the opposite of those just considered: Given a fully developed or nearly fully developed turbulent flow and transverse heat transfer to which the boundary-layer assumptions are applicable, to determine the streamwise evolution when the flow is subjected to a severe streamwise pressure gradient. A boundary layer subjected to a severe pressure gradient can be considered to be the same thing as a highly accelerated boundary layer. According to Bernoulli's equation, which applies outside the boundary layer, where viscous and turbulence stresses are negligible,

$$-\frac{1}{\rho} \frac{dP}{dx_1} = U_\infty \frac{dU_\infty}{dx_1}, \quad (4-127)$$

where  $U_\infty$  is the velocity just outside the boundary layer. For a thin steady-state two-dimensional boundary layer with constant properties and without buoyancy, equations (4-25), (4-26), and (4-21) become respectively

$$U_1 \frac{\partial U_1}{\partial x_1} = -U_2 \frac{\partial U_1}{\partial x_2} - \frac{1}{\rho} \frac{dP}{dx_1} + \nu \frac{\partial^2 U_1}{\partial x_2^2} - \frac{\partial}{\partial x_2} \overline{u_1 u_2}, \quad (4-128)$$

$$U_1 \frac{\partial T}{\partial x_1} = -U_2 \frac{\partial T}{\partial x_2} + \alpha \frac{\partial^2 T}{\partial x_2^2} - \frac{\partial}{\partial x_2} \overline{\tau u_2}, \quad (4-129)$$

and

$$\frac{\partial U_2}{\partial x_2} = -\frac{\partial U_1}{\partial x_1}, \quad (4-130)$$

where  $x_1$  and  $x_2$  are respectively in the direction along and normal to the wall. The pressure gradient is written as a total derivative  $dP/dx_1$  because  $P$  is not a function of  $x_2$  for a thin boundary layer. Equations (4-128) to (4-130) apply to a boundary layer even when the flow is along a curved wall (ref. 39).

In order to solve equations (4-128) to (4-130) to obtain the evolution of  $U_1$  and  $T$ ,  $\overline{u_1 u_2}$  and  $\overline{\tau u_2}$  must be known at each point in the flow. The experiments of Blackwelder and Kovasznay (ref. 40) suggest that although severe pressure gradients caused the mean flow in those experiments to change considerably along streamlines, the Reynolds stresses, at least in the important intermediate region of wall distances, were relatively unaffected. This leads us to the hypothesis of frozen Reynolds stresses and

turbulent heat transfer along streamlines in a moderately short highly accelerated turbulent boundary layer. We gave theoretical arguments for that hypothesis in references 41 and 42, where we showed that it gives good agreement with experiment when applied to equations (4-128) to (4-130). Launder (ref. 43) had earlier used the concept of a frozen Reynolds stress, but in an approximate integral approach to the boundary layer rather than in the solution of the partial differential equations (4-128) and (4-130).

Changes along streamlines, if not zero, should be smaller than say changes at constant  $x_2$ , since flow along streamlines tends to involve the same fluid or eddies at various streamwise points. In applying the hypothesis of frozen  $\overline{u_1 u_2}$  and  $\overline{\tau u_2}$  along streamlines it is convenient to transform equations (4-128) to (4-130) from  $(x_1, x_2)$  to  $(x_1, \psi)$  coordinates (von Mises coordinates), where the stream function  $\psi$  is given by

$$\frac{\partial \psi}{\partial x_1} = -U_2, \quad \frac{\partial \psi}{\partial x_2} = U_1, \quad (4-131)$$

so that

$$\left( \frac{\partial}{\partial x_1} \right)_{x_2} = \left( \frac{\partial}{\partial x_1} \right)_{\psi} - U_2 \left( \frac{\partial}{\partial \psi} \right)_{x_1}, \quad \left( \frac{\partial}{\partial x_2} \right)_{x_1} = \left( \frac{\partial}{\partial \psi} \right)_{x_1} U_1, \quad (4-132)$$

where the subscripts are quantities held constant. Equations (4-128) to (4-130) then become

$$U_1 \left( \frac{\partial U_1}{\partial x_1} \right)_{\psi} = -\frac{1}{\rho} \frac{dP}{dx_1} + \frac{1}{2} \nu U_1 \frac{\partial^2 U_1^2}{\partial \psi^2} - U_1 \frac{\partial \overline{u_1 u_2}}{\partial \psi} \quad (4-133)$$

and

$$\left( \frac{\partial T}{\partial x_1} \right)_{\psi} = \alpha \frac{\partial}{\partial \psi} \left( U_1 \frac{\partial T}{\partial \psi} \right) - \frac{\partial \overline{\tau u_2}}{\partial \psi}, \quad (4-134)$$

where the subscripts  $\psi$  indicate changes along a streamline (at constant  $\psi$ ). By virtue of equation (4-131), equations (4-133) and (4-134) satisfy continuity automatically.

The equations for the evolution of  $\overline{u_1 u_2}$  and of  $\overline{\tau u_2}$  will be obtained later in this chapter (see eqs. (4-140) and (4-141)). For our purpose the important point is that those equations do not contain  $dP/dx_1$ , in contrast to equation (4-133) for the evolution of  $U_1$  or to equation (4-127) for the evolution of  $U_{\infty}$ , the latter of which is a special case of equation (4-133). Taking that fact into account, as well as the discussion in the paragraph preceding equation (4-131), one would expect, for large  $dP/dx_1$ , that there would be large gradients of  $U_{\infty}$  or of  $U_1$  along streamlines without correspondingly large streamwise gradients of  $\overline{u_1 u_2}$  and  $\overline{\tau u_2}$ . Then if the boundary layer is moderately short, the hypothesis that the turbulent shear stress and transverse heat transfer are frozen at their initial values as one proceeds along a streamline in a flow with large streamwise gradients of  $U_{\infty}$  or  $P$  should be a good approximation.

Rescaling the variables in equations (4-133) and (4-134) so as to convert them to dimensionless form, and introducing the frozen turbulent stress/heat-transfer hypothesis give

$$\frac{1}{2} \left( \frac{\partial U_1^2}{\partial x_1} \right)_\psi = - \frac{dP}{dx_1} + \frac{1}{2} U_1 \frac{\partial^2 U_1^2}{\partial \psi^2} - U_1 \frac{\partial (\overline{u_1 u_2})_0}{\partial \psi} \quad (4-135)$$

and

$$\left( \frac{\partial T}{\partial x_1} \right)_\psi = \frac{1}{Pr} \frac{\partial}{\partial \psi} \left( U_1 \frac{\partial T}{\partial \psi} \right) + \frac{\partial (\overline{\tau u_2})_0}{\partial \psi}, \quad (4-136)$$

where

$$\begin{aligned} \frac{U_i}{U_0} &\rightarrow U_i, \quad \frac{(x_1 - x_0)}{\nu} U_0 \rightarrow x_1, \quad \frac{\psi}{\nu} \rightarrow \psi, \\ \frac{\nu}{\rho U_0^3} \frac{dP}{dx_1} &\rightarrow \frac{dP}{dx_1}, \quad \frac{(\overline{u_1 u_2})_0}{U_0^2} \rightarrow (\overline{u_1 u_2})_0, \\ \frac{T_w - T}{(T_w)_0 - T_\infty} &\rightarrow T, \quad \frac{(\overline{\tau u_2})_0}{[(T_w)_0 - T_\infty] U_0} \rightarrow (\overline{\tau u_2})_0, \end{aligned} \quad (4-137)$$

and the arrow  $\rightarrow$  means "has been replaced by." The quantity  $x_0$  is the value of  $x_1$  at the initial station,  $U_0$  is the velocity outside the boundary layer at the initial station,  $(T_w)_0$  is the wall temperature at the initial station,  $T_\infty$  is the constant temperature outside the thermal boundary layer, and  $Pr$  is the Prandtl number. The quantities  $(\overline{u_1 u_2})_0$  and  $(\overline{\tau u_2})_0$  are, respectively, the values of  $\overline{u_1 u_2}$  and  $\overline{\tau u_2}$  on the same streamline as  $\overline{u_1 u_2}$  and  $\overline{\tau u_2}$  but at the initial station.

The frozen turbulent stress/heat-transfer hypothesis can be tested by numerically integrating equations (4-135) and (4-136) along streamlines (at constant  $\psi$ ) and comparing the results with experiments for the same conditions. Upstream of the regions of severe streamwise pressure gradients the pressure gradients were essentially zero.

Velocity profiles ( $U_1/U_\infty$  against  $\psi/\nu$ ) are plotted and compared with experiment in figure 4-5. (Note the shifted vertical scales.) In all cases the effect of the pressure gradient and the total normal strain parameter  $U_\infty/U_0$  is to flatten the profiles. The agreement between theory and experiment is considered good.

Semi-logarithmic plots of  $U_1/(\overline{\tau_w}/\rho)^{1/2}$  against  $(\overline{\tau_w}/\rho)^{1/2} x_2/\nu$  (law-of-the-wall plots) are given in figure 4-6. These profiles show the inner region of the boundary layer much better than does figure 4-5. The shear stress  $\overline{\tau_w}$  at the wall for the theoretical curves was obtained from the slope of the velocity profile at the wall by using points very close to the wall ( $(\overline{\tau_w}/\rho)^{1/2} x_2/\nu \ll 1$ ). Points very close to the wall were necessary because of the nonlinearity of the profile close to the wall in the presence of a severe pressure gradient. It might be pointed out that this nonlinearity makes the experimental determination of the shear stress at the wall extremely difficult. Both theory and experiment indicate that the original logarithmic and wake regions are destroyed by the pressure-gradient and normal-strain effects, although a new logarithmic layer of smaller slope seems to form eventually. Also, the thickness of the sublayer approximately doubles, indicating an apparent "relaminarization," as observed experimentally by many

investigators. However, it is not a true relaminarization since, at least in the theory,  $\overline{u_1 u_2}$  is constant along streamlines. The agreement between theory and experiment appears to be quite good. For values of  $U_\infty/U_0$  larger than those shown, the approximation of a frozen Reynolds stress apparently begins to break down.

In order to see how sensitive the development of the mean profile is to the Reynolds shear stress, results were calculated for  $\overline{u_1 u_2} = 0$  and are shown dashed in figures 4-5(b) and 4-7. The effect of  $\overline{u_1 u_2}$  on the profiles in figure 4-5(b) is slight. The law-of-the-wall plots in figure 4-7, on the other hand, show a significant quantitative effect of  $\overline{u_1 u_2}$  on the profiles, but qualitatively the curves for  $\overline{u_1 u_2} = 0$  and  $\overline{u_1 u_2} \neq 0$  are much the same. In both cases the original logarithmic and wake regions are destroyed and the sublayer is thickened. The difference between the indicated quantitative effects of  $\overline{u_1 u_2}$  on the profiles in figures 4-5(b) and 4-7 is evidently due to the difference in scales and in scaling parameters in the two figures.

Figure 4-8 shows, for a large value of the pressure-gradient parameter, the contributions of various terms in equation (4-128) to the rate of change of the nondimensional mean kinetic energy  $(1/2)\partial(U_1/U_0)^2/\partial(x_1 U_0/\nu)$ . (The energy in the transverse velocity component is negligible for a boundary layer.) The contribution of the Reynolds stress term is very large in a narrow region near the wall. However, that tends to be offset by the viscous contribution. Comparison of the curves for  $\overline{u_1 u_2} = 0$  and  $\overline{u_1 u_2} \neq 0$  shows that the viscous contribution adjusts its value so as to offset the effect of the Reynolds stress. The viscous term is not zero at the wall but balances the pressure-gradient term so that  $U_1$  can remain zero at the wall. Thus, the present velocity profile, in contrast to the case of zero pressure gradient, is nonlinear at the wall. (If it were linear the viscous term in equation (4-128) would be zero at the wall.)

The pressure-gradient term is independent of wall distance and, for the case shown in figure 4-8, becomes dominant for  $(\overline{\tau_w}/\rho)^{1/2} x_2/\nu > 40$ . Thus, the destruction of the logarithmic and wake regions is due mainly to the pressure-gradient term, rather than to a change in the structure of the turbulence (although some change in structure may occur (ref. 45)). Also, the thickening of the sublayer is mostly, although not entirely, due to the pressure-gradient contribution, since as mentioned, viscous effects tend to offset the Reynolds stress contribution.

The results in figure 4-8 are, of course, for a large pressure-gradient parameter. For regions of lower pressure gradient, the Reynolds stress will have a greater effect, as shown in figure 4-7. Also, the velocity profile at any position depends on the whole distribution of pressure gradients up to that position; that is,  $U_1$  is a functional of  $dP/dx_1$ , or

$$U_1 = U_1 \left[ \frac{dP}{dx_1}(\xi) \right], \quad (4-138)$$

where  $0 < \xi < x_1$ . Thus, there is a quantitative (but not a qualitative) effect of  $\overline{u_1 u_2}$  on the velocity profile, even at those positions where the pressure-gradient parameter is large.

The analysis can be easily extended to include mass injection at the wall by transforming equation (4-135) from  $(x_1, \psi)$  to  $(x_1, \psi')$  coordinates, where  $\psi' = \psi - \psi_w$ , and  $\psi_w$  is the stream function at the wall. The latter will vary with  $x_1$  in accordance with equation (4-131). Equation (4-135), when

written in  $(x_1, \psi')$  coordinates, has the additional term  $-(1/2)(U_2)_w \partial U_1^2 / \partial \psi'$  on the right side, where  $(U_2)_w$  is the dimensionless normal velocity at the wall, and where, as in equation (4-135), all quantities have been nondimensionalized by  $U_0$  and  $\nu$  (see eq. (4-137)). As before, we use the simplification that  $\overline{u_1 u_2}$  remains frozen as it is convected along streamlines (along lines of constant  $\psi$ , not constant  $\psi'$ ). The injected fluid is assumed to be turbulence-free.

To show the effect of mass injection on a boundary layer with severe pressure gradients, mass injection was added in the theoretical calculations in figure 4-6. For positive mass injection figure 4-9 shows that the normal flow quickly raises the  $U_1/(\tau_w/\rho)^{1/2}$  curve, particularly in the wake region, after which the favorable pressure gradient lowers and flattens the curve. The resulting curve still lies above the initial profile. For negative injection, the normal flow and pressure gradient lower and flatten the initial profile. These trends are similar to those observed in the experiments of Julien, Kays, and Moffat (ref. 46).

All of the results so far were for favorable pressure gradients, but the analysis should apply as well to severe unfavorable gradients. Figure 4-10 shows a comparison between theory and experiment for the results of Kline et al. (ref. 45) for a severe unfavorable pressure gradient (their fig. 9(a)). The results indicate that the adverse pressure gradients produce an exaggerated wake region, but that the logarithmic and sublayer regions are relatively unaffected. The agreement between theory and experiment is good. It might be mentioned that the results for adverse pressure gradients were more sensitive to the  $\overline{u_1 u_2}$  distribution than were those for favorable gradients. In particular, when  $\overline{u_1 u_2}$  was taken as zero, separation occurred upstream for the run shown in figure 4-10 for  $U_\infty/U_0 = 0.92$ . Thus the presence of turbulence appears to delay separation. This is evidently because the Reynolds stress term in equation (4-128) is positive close to the wall and thus tends to increase  $U_1$  in that region.

Figure 4-11 shows theoretical Stanton-number and skin-friction-coefficient variations with dimensionless longitudinal distance for run 12 from reference 47. The shear stress and heat transfer at the wall for the theoretical curves were obtained from the slopes of the velocity and temperature profiles at the wall by using points very close to the wall  $\sqrt{(\tau_w/\rho)} x_2/\nu \ll 1$ . Also included in the plot are experimental values for  $U_\infty/U_0$ . Initial conditions were taken at  $x_0 = 4.32$  ft. The difference between the Stanton number and skin-friction-coefficient variations is rather striking and indicates that Reynolds analogy (see, e.g., ref. 33) does not apply in regions of severe pressure gradients. This difference is also indicated in the experimental results of references 40 and 47.

The effect of favorable pressure gradients on velocity and temperature distributions is illustrated in figure 4-12, where theoretical values of  $T^+$  and  $U_1^+$  are plotted against  $x_2^+$  for a low and a high value of pressure-gradient parameter  $K = (\nu/\rho U_\infty^3) dP/dx_1$ . The results are again for run 12 from reference 47. The effect of the pressure gradient on the  $T^+$  profile tends to be opposite to that on the  $U_1^+$  profile. Whereas the pressure gradient flattens the  $U_1^+$  profile in the outer region of the boundary layer, it steepens the  $T^+$  profile in that region. The same trends have been observed experimentally in references 44 and 48. The difference between the velocity and temperature results (or the skin friction and heat transfer results) is evidently due to the fact that the equation for the evolution of the mean velocity contains a pressure-gradient term (eq. (4-128)) whereas that for the mean temperature does not (eq. (129)). Although the temperature equation does not contain a pressure gradient term, the pressure gradient can still affect the temperature through the mean velocity.

A comparison between theory and experiment for the evolution of Stanton number in severe favorable pressure gradients is presented in figure 4-13 for three values of maximum pressure-gradient parameter  $K_m$ . The value of  $x_0$  (the initial station for each run was taken at the point where the local

pressure-gradient parameter  $K_L$  starts to increase rapidly). For the smaller values of  $K_m$  good agreement between theory and experiment is indicated for values of  $U_\infty/U_0$  which are not too large. It appears that the range of values of  $U_\infty/U_0$  for which the theory applies increases as the pressure-gradient or acceleration parameter increases. For values of  $U_0(x_1 - x_0)/\nu$  (or of  $U_\infty/U_0$ ) greater than those shown in figure 4-13, the theory appears to break down because the total streamwise strain becomes too great and/or the local pressure-gradient parameter  $K_L$  becomes too small.

Figure 4-13 also shows Stanton numbers calculated for turbulent initial velocity and temperature profiles, but for  $\overline{\tau u_2} = \overline{u_1 u_2} = 0$ . It is seen that the turbulent stresses and fluxes have a very large effect on the evolution of the Stanton number. The large effect of turbulence on Stanton number perhaps raises questions about calling regions such as those shown in figure 4-13 "relaminarization regions," although at the large values of  $K_m$  and  $U_0(x_1 - x_0)/\nu$  there is some tendency for the zero-turbulence curves to approach those for turbulence. The effects of turbulence on the velocity and temperature distributions are also considerable, although the general trends without turbulence are similar to those in figure 4-12.

It should, of course, be remembered that, as is the case for  $U_1$  (eq. (4-138)), Stanton number, as well as  $C_f$  and  $T$  at any longitudinal position depend on the whole distribution of pressure gradients up to that position. That is, Stanton number, for instance, is a functional of  $dP/dx_1$ , or

$$St = St \left[ \frac{dP}{dx_1}(\xi) \right], \quad (4-139)$$

where  $0 < \xi \leq x_1$ .

### 4.3.3 One-Point Correlation Equations

Sections 4.3.1 and 4.3.2 considered the equation for the evolution of the mean flow (eq. (4-25)) and that for the mean temperature (eq. (4-26)). Those were obtained by averaging the equations for the instantaneous velocity and temperature (eqs. (4-11) and (4-12)) after applying Reynolds decomposition, and contained the important but undetermined turbulent stress tensor  $-\rho \overline{u_i u_j}$  and turbulent heat transfer vector  $\rho c \overline{u_i \tau}$ . This was our first encounter with the closure problem, and sections 4.3.2 to 4.3.2.13 considered some simple closure schemes.

One can construct equations for the evolution of the undetermined quantities  $\overline{u_i u_j}$  in equations (4-25) and (4-27) from equation (4-22) for  $g_i = 0$  and the following similar equation for the component  $u_j$ :

$$\frac{\partial u_j}{\partial t} = - \frac{\partial}{\partial x_k} (u_j u_k) - \frac{1}{\rho} \frac{\partial \sigma}{\partial x_j} + \nu \frac{\partial^2 u_j}{\partial x_k \partial x_k} - u_k \frac{\partial U_j}{\partial x_k} - U_k \frac{\partial u_j}{\partial x_k} + \frac{\partial}{\partial x_k} \overline{u_j u_k}.$$

Note once again that  $\sigma_e$  drops out the equations of motion for  $g_i = 0$  by virtue of the equation following equation (3-22). Next multiply equation (4-22) by  $u_j$  and the above equation for  $u_j$  by  $u_i$ , add the two equations, and average. This gives, using continuity (eq. (4-21)),



$$\begin{aligned} \frac{\partial}{\partial t} \overline{u_i u_j} = & - \left( \overline{u_j u_k} \frac{\partial U_i}{\partial x_k} + \overline{u_i u_k} \frac{\partial U_j}{\partial x_k} \right) - U_k \frac{\partial}{\partial x_k} \overline{u_i u_j} - \frac{\partial}{\partial x_k} \overline{u_i u_j u_k} - \frac{1}{\rho} \left( \frac{\partial}{\partial x_i} \overline{\sigma u_j} + \frac{\partial}{\partial x_j} \overline{\sigma u_i} \right) \\ & + \nu \frac{\partial^2 \overline{u_i u_j}}{\partial x_\ell \partial x_\ell} + \frac{1}{\rho} \left( \overline{\sigma \frac{\partial u_j}{\partial x_i}} + \overline{\sigma \frac{\partial u_i}{\partial x_j}} \right) - 2\nu \frac{\partial u_i}{\partial x_\ell} \frac{\partial u_j}{\partial x_\ell}. \end{aligned} \quad (4-140)$$

Similarly, multiplying equation (4-22) by  $\tau$ , equation (4-23) by  $u_i$ , adding the two equations, and averaging, give

$$\begin{aligned} \frac{\partial}{\partial t} \overline{u_i \tau} = & - \left( \overline{\tau u_k} \frac{\partial U_i}{\partial x_k} + \overline{u_i u_k} \frac{\partial \tau}{\partial x_k} \right) - U_k \frac{\partial}{\partial x_k} \overline{u_i \tau} - \frac{\partial}{\partial x_k} \overline{\tau u_i u_k} - \frac{1}{\rho} \frac{\partial}{\partial x_i} \overline{\sigma \tau} \\ & + \frac{1}{\rho} \overline{\sigma \frac{\partial \tau}{\partial x_i}} + \nu \overline{\tau \frac{\partial^2 u_i}{\partial x_k \partial x_k}} + \alpha \overline{u_i \frac{\partial^2 \tau}{\partial x_k \partial x_k}}, \end{aligned} \quad (4-141)$$

where continuity is again used and buoyancy is neglected. Equations (4-140) and (4-141) are known as moment or correlation equations. Setting  $j = i$  in equation (4-140) and using continuity, we get, for the rate of change of the kinetic energy per unit mass,

$$\begin{aligned} \frac{\partial}{\partial t} \left( \frac{\overline{u_i u_i}}{2} \right) = & - \overline{u_i u_k} \frac{\partial U_i}{\partial x_k} - U_k \frac{\partial}{\partial x_k} \left( \frac{\overline{u_i u_i}}{2} \right) - \frac{\partial}{\partial x_k} \left( \frac{\overline{u_i u_i} u_k}{2} \right) - \frac{1}{\rho} \frac{\partial}{\partial x_k} (\overline{\sigma u_k}) \\ & + \nu \frac{\partial^2 \left( \frac{\overline{u_i u_i}}{2} \right)}{\partial x_\ell \partial x_\ell} - \nu \frac{\partial u_i}{\partial x_\ell} \frac{\partial u_i}{\partial x_\ell}. \end{aligned} \quad (4-142)$$

As in equations (4-25) to (4-27), barred quantities in equations (4-140) to (4-142) which contain lower-case letters are turbulent quantities.

The one-point correlation equations (4-140) and (4-141) give expressions for the rate of change of  $\overline{u_i u_j}$  and  $\overline{u_i \tau}$  which might be used in conjunction with equations (4-25) to (4-27). But the situation with respect to closure is now worse than before. Whereas without equations (4-140) and (4-141) we had only to determine  $\overline{u_i u_j}$  and  $\overline{u_i \tau}$ , with it we have to determine quantities like  $\overline{u_i u_j u_k}$ ,  $\overline{\tau u_i u_k}$ ,  $\overline{\sigma u_j}$ ,  $\overline{\sigma \tau}$ ,  $\overline{\sigma \frac{\partial u_j}{\partial x_i}}$ ,  $(\frac{\partial u_i}{\partial x_\ell})(\frac{\partial u_j}{\partial x_\ell})$ ,  $\overline{\sigma \frac{\partial \tau}{\partial x_i}}$ , and  $\overline{\tau \frac{\partial^2 u_i}{\partial x_k \partial x_k}}$ . One might use equation (4-24) to obtain the pressure correlations, but that would only introduce more unknowns. However, equations (4-140)

to (4-142) are very useful for studying the processes in turbulence, in that most of the terms have clear physical meanings. Moreover, one may be able to calculate terms in those equations from numerical solutions of the unaveraged equations.

An additional one-point equation can be obtained by multiplying equation (4-23) by  $\tau$ , averaging, and again neglecting buoyancy. This gives

$$\frac{\partial \overline{\tau^2}}{\partial t} = -2\overline{\tau u_k} \frac{\partial T}{\partial x_k} - U_k \frac{\partial \overline{\tau^2}}{\partial x_k} - \frac{\partial \overline{\tau^2 u_k}}{\partial x_k} + \alpha \frac{\partial^2 \overline{\tau^2}}{\partial x_k \partial x_k} - 2\alpha \frac{\partial \overline{\tau}}{\partial x_k} \frac{\partial \overline{\tau}}{\partial x_k}, \quad (4-143)$$

where  $\overline{\tau^2}$  is the variance of the temperature fluctuation.

**4.3.3.1 Physical interpretation of terms in one-point equations.**—Consider first equations (4-140) and (4-142), since physically meaningful interpretations of all the terms in those equations can be given. As in the case of equation (3-19) it is helpful, for purposes of interpretation, to multiply the terms in equations (4-140) and (4-142) through by  $\rho$  and by a volume element  $dx_1 dx_2 dx_3$ . Then the term on the left side of equation (4-140) or (4-142) gives the time rate of change of  $\overline{\rho u_i u_j}$ , or of the kinetic energy  $\overline{\rho u_i u_j}/2$ , within the element. This rate of change is contributed to by the terms on the right sides of the equations. The first of those terms is equal to the net work done on the element by turbulent stresses acting in conjunction with mean-velocity gradients. It is therefore called a turbulence production term; it equals the rate of production of  $\overline{\rho u_i u_j}$  or of  $\overline{\rho u_i u_j}/2$  within the volume element by work done on the element. A somewhat abbreviated interpretation suggested by the form of the term, which is often given, is that it represents work done on the turbulent stress  $\overline{\rho u_i u_j}$  by the mean-velocity gradient.

The next term in each of the equations describes the convection or net flow of turbulence or turbulent energy into a volume element by the mean velocity  $U_k$ . It moves the turbulence bodily, rather than doing work on it by deforming it, as in the case of the production term. It vanishes when either  $U_k$  is zero (no mean flow) or when the turbulence is homogeneous  $[\overline{u_i u_j} \neq \overline{u_i u_j}(x_k)]$ . In the latter case there is no accumulation of turbulence within a volume element, even with a mean flow.

The next three terms in equation (4-140) and in equation (4-142) also vanish for homogeneous turbulence. Since they do not contain the mean velocity they do not convect the turbulence bodily or do work on it. Therefore, we interpret them as diffusion terms which diffuse net turbulence from one part of the turbulent field to another by virtue of its inhomogeneity. The pressure-velocity-gradient terms in equation (4-140) drop out of the contracted equation (4-142) because of continuity (eq. (4-21)). Therefore, they give zero contribution to the rate of change of the total energy  $\overline{u_i u_i}/2$ , but they can distribute the energy among the three directional components  $\overline{u_{(i)}^2}/2$  (no sum on  $i$ ). The last term in equations (4-140) and (4-142) is the viscous dissipation term, which dissipates turbulence by the presence of fluctuating velocity gradients.

Consider next, equation (4-141) which, on multiplication by  $\rho c$  and the volume element  $dx_1 dx_2 dx_3$ , gives the time rate of change of  $\overline{\rho c u_i \tau}$  within the element. The first term on the right side gives the production of turbulent heat transfer  $\overline{\rho c u_i \tau}$  by the interaction of  $\overline{\tau u_k}$  with the mean velocity gradient and by the interaction of  $\overline{u_i u_k}$  with the mean temperature gradient. The next term gives the net flow of  $\overline{\rho c u_i \tau}$  into the volume element by convection. It changes  $\overline{\rho c u_i \tau}$  within the element by moving that quantity

bodily. The term vanishes for homogeneous turbulence. The next two terms in equation (4-141) also vanish for homogeneous turbulence, but since they do not contain the mean velocity, they do not convect  $\rho \overline{cu_i \tau}$  bodily or produce  $\rho \overline{cu_i \tau}$ . Therefore, as in the analogous terms in equation (4-140), we interpret them as diffusion terms which diffuse a turbulence quantity from one part of the turbulence field to another by virtue of its inhomogeneity. The next term changes  $\rho \overline{cu_i \tau}$  by the interaction of the pressure fluctuation  $\sigma$  with the temperature-fluctuation gradient. The last two terms change  $\rho \overline{cu_i \tau}$  by molecular action. For  $\alpha = \nu$  (for a Prandtl number of 1) they can be interpreted by writing them as  $\nu \frac{\partial^2 \overline{u_i \tau}}{\partial x_\ell \partial x_\ell} - 2\nu \frac{\partial \overline{u_i}}{\partial x_\ell} \frac{\partial \tau}{\partial x_\ell}$ . Comparing these terms with analogous terms in equation (4-140), we interpret the first as a diffusion term and the second as a dissipation term.

Finally, consider the equation for the evolution of the temperature variance  $\overline{\tau^2}$  (eq. (4-143)). The terms on the right side of that equation are similar to terms already considered in the other evolution equations. They are, respectively, a production term, a convection term, two diffusion terms which diffuse  $\overline{\tau^2}$  by virtue of the inhomogeneity of the turbulence field, and a dissipation term which dissipates  $\overline{\tau^2}$  by fluctuating temperature gradients.

**4.3.3.2 Some direct numerical simulations of terms in one-point moment equations.**—In section 4.3.3 we obtained averaged one-point moment (or correlation) equations which give the time-evolution of quantities such as  $\overline{u_i u_j}$ ,  $\overline{u_i \tau}$ , and  $\overline{u_i u_i}$ . Also, in the last section we gave interpretations of the terms in those equations. However, because of the closure problem which arises in connection with averaged equations, particularly with one-point moment equations, we have not been able to solve those equations or calculate terms. Those terms have, however, been calculated by numerical solution of the unaveraged equations (eqs. (4-11) to (4-13) (or by eqs. (4-22) to (4-24) together with eqs. (4-25) to (4-27).)

The cases to be considered here will be concerned with the evolution of the mean turbulent kinetic energy according to equation (4-142). The averaged values in that equation will vary only in the direction  $x_2$ , one of the directions normal to the mean velocity  $U_1$ . In that case equation (4-142) becomes

$$\frac{\partial}{\partial t} \left( \frac{\overline{u_k u_k}}{2} \right) = -\overline{u_1 u_2} \frac{\partial U_1}{\partial x_2} - \frac{1}{\rho} \frac{\partial}{\partial x_2} \overline{\sigma u_2} - \frac{\partial}{\partial x_2} \left( \frac{\overline{u_k u_k}}{2} u_2 \right) + \nu \frac{\partial^2}{\partial x_2^2} \left( \frac{\overline{u_k u_k}}{2} \right) - \nu \frac{\partial \overline{u_k}}{\partial x_\ell} \frac{\partial \overline{u_k}}{\partial x_\ell}. \quad (4-144)$$

Mansour, Kim, and Moin (ref. 49) have calculated the terms in equation (4-144) from a numerical solution of the unaveraged Navier-Stokes equations for a steady fully developed turbulent channel flow. The boundary condition was  $u_i = 0$  at the walls. The results, which correspond to the numerical solution plotted in figure 4-2, are shown in figure 4-14. The corresponding turbulence kinetic energy profile is plotted in figure 4-15. Since the turbulence is steady-state, the sum of the terms on the right side of equation (4-144) is zero.

The production term  $-\overline{u_1 u_2} dU_1/dx_2$ , whose form shows that turbulent energy is produced by work done on the Reynolds shear stress by the mean velocity gradient, is largest in the region close to the wall and peaks at an  $x_2^+$  of about 12. According to figure 4-2, the mean velocity profile at that point is just beginning to deviate appreciably from a laminar ( $U_1^+ = x_2^+$ ) profile. Note that the production term

$-\overline{u_1 u_2} \, dU_1/dx_2$  in figure 4-14 is positive as it should be, since according to the argument in section 4.3.1.1 and figure 4-1, when  $dU_1/dx_2$  is positive  $\overline{u_1 u_2}$  is negative, and vice versa. Similarly the dissipation term  $-\nu \overline{\partial u_k / \partial x_\ell} \, \partial u_k / \partial x_\ell$  is always negative, because it is the negative of the sum of the squares of velocity gradients. The remaining three terms in equation (4-144), and which are plotted in figure 4-14, are diffusion terms. They are the kinetic-energy diffusion term  $\partial \overline{u_2 u_k u_k} / 2 \partial x_2$ , the viscous diffusion term  $\nu \partial^2 \overline{u_k u_k} / 2 \partial x_2^2$ , and the pressure diffusion term  $-(\partial \overline{\sigma u_2} / \partial x_2) / \rho$ . The plots of those terms show that all three of them are positive near  $x_2 = 0$ , where a large energy sink occurs because of the boundary condition  $u_i = 0$  at  $x_2 = 0$  (see fig. 4-15). Farther away from the wall they become negative. Thus they remove turbulent energy from the region where the energy is large and deposit it where the energy is smaller. All of the diffusion terms therefore tend to make the turbulence more homogeneous. Far from the wall there is a region of small positive  $\partial \overline{u_2 u_k u_k} / 2 \partial x_2$ , apparently because the energy in that region decreases gradually with increasing  $x_2$ .

A comparison of the turbulence diffusion processes with spectral transfer processes (to be discussed in the next chapter) and the directional-transfer processes arising from the pressure velocity-gradient correlations (see sect. 4.3.3.1) is instructive. The spectral-transfer processes remove energy from wave-number (or eddy size) regions where the energy is large and deposit it in regions of smaller energy. The directional-transfer processes remove energy from large-energy directional components and deposit it in a directional component (or components) where the energy is smaller. The turbulence diffusion processes, as shown here, remove energy from regions of space where the energy is large and deposit it in regions of smaller energy. The spectral transfer, directional transfer, and turbulence diffusion processes tend, respectively, to make the turbulence more uniform in wavenumber space, more isotropic, and more homogeneous in physical space.

Terms in equation (4-144) have also been calculated for a developing turbulent free shear layer, where the mean quantities were functions only of  $x_2$  and time (ref. 50). The terms were calculated from a numerical solution of the unaveraged equations, where the boundary conditions were periodic. Results were similar to those just considered for a fully developed channel flow, insofar as the kinetic-energy and pressure-diffusion terms diffused turbulence kinetic energy from regions where the energy was high to regions where it was lower. As expected (see the discussion for the channel flow) the production term was positive. The viscous dissipation and the viscous diffusion terms were, however, negligibly small, unlike those terms for the channel. That was apparently because the presence of walls in the channel produced larger mean gradients there than those in the free shear layer.

#### 4.3.4 Two-Point Correlation Equations

As shown in section 4.3.3 the use of one-point correlation or moment equations in conjunction with the equations for the mean flow causes the number of unknowns to go up faster than the number of available equations, so that the closure problem, in effect, gets worse. This leads one to consider the use of two-point equations, where one might be able to at least eliminate terms containing instantaneous gradients, such as  $\overline{\sigma \partial u_i / \partial x_i}$  and  $\overline{\partial u_i / \partial x_\ell} \, \partial u_j / \partial x_\ell$ . In that case the use of higher-order equations might be expected to increase the number of unknowns at the same rate as the number of available equations. Since an assumption for still undetermined higher-order quantities (e.g., triple correlations) might be expected to affect the flow to a lesser extent than an assumption for lower-order quantities (e.g.,  $\overline{u_i u_j}$ ), there might be some advantage in this procedure. Moreover the use of two-point equations enables us to consider the important spectral-transfer problem of turbulence, as we will see in the next chapter.

Before obtaining the two-point correlation equations, consider the structure of the two-point correlations. Some of those correlations have been obtained by Kim, Moin, and Moser (ref. 17) in a numerical solution of the unaveraged Navier-Stokes equations and are plotted in figure 4-16. As the separation  $r_k$  between the defining points increases, the correlation between the velocities at those points goes to zero (as  $r_k \rightarrow \infty$ ). This might be considered a consequence of the mixing property of turbulence; although mixing is generally associated with temporal separation (sect. 4.1.1), the effects of temporal and spatial separations appear to be similar. In connection with the spanwise separations, note that the correlations go negative before becoming asymptotically zero as  $r_2$  increases, in contrast to the correlations with point separation in the streamwise direction. More will be said about that phenomenon in the next chapter, where it will be predicted theoretically.

In this section we will consider only two-point equations obtained from the Navier-Stokes equations and will neglect heat-transfer and buoyancy effects. Then equation (4-22) for  $u_i$  at a point  $P$  and a similar equation for  $u'_j$  at a point  $P'$  can be written as

$$\frac{\partial u_i}{\partial t} + u_k \frac{\partial U_i}{\partial x_k} + U_k \frac{\partial u_i}{\partial x_k} + \frac{\partial}{\partial x_k} (u_i u_k) - \frac{\partial}{\partial x_k} \overline{u_i u_k} = -\frac{1}{\rho} \frac{\partial \sigma}{\partial x_i} + \nu \frac{\partial^2 u_i}{\partial x_k \partial x_k} \quad (4-145)$$

and

$$\frac{\partial u'_j}{\partial t} + u'_k \frac{\partial U'_j}{\partial x'_k} + U'_k \frac{\partial u'_j}{\partial x'_k} + \frac{\partial}{\partial x'_k} (u'_j u'_k) - \frac{\partial}{\partial x'_k} \overline{u'_j u'_k} = -\frac{1}{\rho} \frac{\partial \sigma'}{\partial x'_j} + \nu \frac{\partial^2 u'_j}{\partial x'_k \partial x'_k} \quad (4-146)$$

Multiplying equation (4-145) by  $u'_j$  and equation (4-146) by  $u_i$ , adding, taking averages, using the fact that quantities at one point are independent of the position of the other point, and introducing the new variables  $r_k \equiv x'_k - x_k$  and  $(x_k)_n \equiv n x'_k + (1-n)x_k$  ( $0 \leq n \leq 1$ , see fig. 4-17), results in

$$\begin{aligned} & \frac{\partial}{\partial t} \overline{u_i u'_j} + \overline{u_k u'_j} \frac{\partial U_i}{\partial x_k} + \overline{u_i u'_k} \frac{\partial U'_j}{\partial x'_k} + (U'_k - U_k) \frac{\partial}{\partial r_k} \overline{u_i u'_j} + [(1-n)U_k + nU'_k] \frac{\partial}{\partial (x_k)_n} \overline{u_i u'_j} \\ & + \frac{1}{\rho} \left[ \frac{\partial}{\partial (x_i)_n} \overline{\sigma u'_j} + \frac{\partial}{\partial (x_j)_n} \overline{u_i \sigma'} \right] + \frac{\partial}{\partial (x_k)_n} [n \overline{u_i u'_j u'_k} + (1-n) \overline{u_i u_k u'_j}] + \frac{\partial}{\partial r_k} (\overline{u_i u'_j u'_k} - \overline{u_i u_k u'_j}) \\ & = \frac{1}{\rho} \left[ n \frac{\partial}{\partial (x_i)_n} \overline{\sigma u'_j} + (1-n) \frac{\partial}{\partial (x_j)_n} \overline{u_i \sigma'} - \frac{\partial}{\partial r_j} \overline{u_i \sigma'} + \frac{\partial}{\partial r_i} \overline{\sigma u'_j} \right] \\ & + (1-2n+2n^2) \nu \frac{\partial^2 \overline{u_i u'_j}}{\partial (x_k)_n \partial (x_k)_n} - 2(1-2n) \nu \frac{\partial^2 \overline{u_i u'_j}}{\partial (x_k)_n \partial r_k} + 2\nu \frac{\partial^2 \overline{u_i u'_j}}{\partial r_k \partial r_k}, \end{aligned} \quad (4-147)$$

where the following transformations were used:

$$\begin{aligned}\frac{\partial}{\partial x_k} &= (1 - n) \frac{\partial}{\partial (x_k)_n} - \frac{\partial}{\partial r_k}, \\ \frac{\partial}{\partial x'_k} &= n \frac{\partial}{\partial (x_k)_n} + \frac{\partial}{\partial r_k}, \\ \frac{\partial^2}{\partial x_k \partial x_k} + \frac{\partial^2}{\partial x'_k \partial x'_k} &= (1 - 2n + 2n^2) \frac{\partial^2}{\partial (x_k)_n \partial (x_k)_n} - 2(1 - 2n) \frac{\partial^2}{\partial (x_k)_n \partial r_k} + 2 \frac{\partial^2}{\partial r_k \partial r_k}.\end{aligned}$$

To obtain the general two-point equations for the pressure-velocity correlations, take the divergence of equations (4-145) and (4-146) and use the continuity equation. Thus, from equation (4-146), one obtains

$$\frac{1}{\rho} \frac{\partial^2 \sigma'}{\partial x'_j \partial x'_j} = -2 \frac{\partial u'_k}{\partial x'_j} \frac{\partial U'_j}{\partial x'_k} - \frac{\partial^2 u'_j u'_k}{\partial x'_j \partial x'_k} + \frac{\partial^2 \overline{u'_j u'_k}}{\partial x'_j \partial x'_k}. \quad (4-148)$$

Multiplying by  $u_i$ , taking averages, and introducing the variables  $r_k$  and  $(x_k)_n$ , as in equation (4-147), gives

$$\begin{aligned}\frac{1}{\rho} \left[ n^2 \frac{\partial^2 \overline{u_i \sigma'}}{\partial (x_j)_n \partial (x_j)_n} + 2n \frac{\partial^2 \overline{u_i \sigma'}}{\partial (x_j)_n \partial r_j} + \frac{\partial^2 \overline{u_i \sigma'}}{\partial r_j \partial r_j} \right] &= -2 \frac{\partial U'_j}{\partial x'_k} \left[ n \frac{\partial \overline{u_i u'_k}}{\partial (x_j)_n} + \frac{\partial \overline{u_i u'_k}}{\partial r_j} \right] \\ &\quad - n^2 \frac{\partial^2 \overline{u_i u'_j u'_k}}{\partial (x_j)_n \partial (x_k)_n} - n \frac{\partial^2 \overline{u_i u'_j u'_k}}{\partial (x_j)_n \partial r_k} - n \frac{\partial^2 \overline{u_i u'_j u'_k}}{\partial (x_k)_n \partial r_j} - \frac{\partial^2 \overline{u_i u'_j u'_k}}{\partial r_j \partial r_k}.\end{aligned} \quad (4-149)$$

Similarly, from equation (4-145),

$$\begin{aligned}\frac{1}{\rho} \left[ (1 - n)^2 \frac{\partial^2 \overline{\sigma u'_j}}{\partial (x_i)_n \partial (x_i)_n} - 2(1 - n) \frac{\partial^2 \overline{\sigma u'_j}}{\partial (x_i)_n \partial r_i} + \frac{\partial^2 \overline{\sigma u'_j}}{\partial r_i \partial r_i} \right] &= -2 \frac{\partial U_i}{\partial x_k} \left[ (1 - n) \frac{\partial \overline{u_k u'_j}}{\partial (x_i)_n} - \frac{\partial \overline{u_k u'_j}}{\partial r_i} \right] \\ &\quad - (1 - n)^2 \frac{\partial^2 \overline{u_i u'_k u'_j}}{\partial (x_i)_n \partial (x_k)_n} + (1 - n) \frac{\partial^2 \overline{u_i u'_k u'_j}}{\partial (x_i)_n \partial r_k} + (1 - n) \frac{\partial^2 \overline{u_i u'_k u'_j}}{\partial (x_k)_n \partial r_i} - \frac{\partial^2 \overline{u_i u'_k u'_j}}{\partial r_i \partial r_k}\end{aligned} \quad (4-150)$$

The equation for the mean velocity (eq. (4-25)) with buoyancy neglected) is

$$\frac{\partial U_i}{\partial t} + U_k \frac{\partial U_i}{\partial x_k} = -\frac{1}{\rho} \frac{\partial P}{\partial x_i} + \frac{\partial}{\partial x_k} \left( \nu \frac{\partial U_i}{\partial x_k} - \overline{u_i u'_k} \right) \quad (4-151)$$

Equations (4-147), (4-149), and (4-150) constitute the two-point correlation equations for inhomogeneous turbulence with mean velocity gradients. A possible solution for these equations is that all the correlations are zero. In that case no turbulence exists, and the flow is laminar. We are mainly interested here in nontrivial turbulent solutions.

The terms on the right side of the Poisson equations (4-149) and (4-150) are source terms associated with the mean velocity and triple correlations. Most of the terms in equations (4-147) are similar to terms in the one-point equation (4-140). Thus equation (4-147) contains turbulence-production, convection, viscous, and diffusion terms. The sum of the pressure-velocity correlation terms on the right side of the equation transfers energy among directional components. That can be seen by using the relations following equation (4-147) (the first for  $\partial \overline{u_i \sigma_j} / \partial r_j$  and the second for  $\partial \overline{\sigma u_j} / \partial r_i$ , and using continuity, since the sum of the terms is zero for  $i = j$ ; the terms give zero contribution to the rate of change of energy  $\overline{u_i u_i} / 2$ , but they can transfer energy among directional components. The remaining terms in equation (4-147),  $\partial(\overline{u_i u_j u_k'} - \overline{u_i u_k u_j'}) / \partial r_k$  and  $(U_k' - U_k) \partial \overline{u_i u_j'} / \partial r_k$ , are new terms which do not have counterparts in the one-point equations. One may interpret them by converting equation (4-147) to spectral form by taking its Fourier transform. We will postpone doing that until the next chapter, where the spectral form of the equations will be discussed. Note that no averaged quantities containing instantaneous gradients appear in those equations, as they do in the one-point equations, so that the number of unknowns, in comparison with the number of available equations, is reduced. However, the two-point correlation equations, together with the equation for the mean velocity (eq. (4-151)) and the continuity equation (eq. (4-21)) still do not form a determinate set for turbulent flow because of the unknown triple correlations.

If the turbulence is weak (low Reynolds number), and/or if the mean velocity gradients are generally very large, it may be possible to neglect terms containing triple correlations. Higher Reynolds numbers might be considered by constructing general three- and four-point equations. In each case the set of equations would be made determinate by neglecting terms containing the highest-order correlations. However, even for the case of a fully developed flow at low Reynolds number, the difficulties of solution are extremely great. For that reason modelers of inhomogeneous turbulence have generally preferred to use the one-point equations (see e.g., refs. 51 and 52).<sup>4</sup>

Still, it appears that the present scheme should, formally, constitute a solution to the turbulent shear-flow problem. But the direct numerical solution of the unaveraged equations, as in references 17, 49, and 50, may be simpler. One can, however, get an approximate solution for sustained inhomogeneous turbulence and study, to some extent, the sustaining mechanism (ref. 53).

Turbulence is essentially a nonlinear phenomenon.<sup>5</sup> The nonlinear character of the two-point correlation equations (4-147), (4-149), and (4-150), even when the triple correlation terms are neglected, is made evident when the mean velocities in those equations are eliminated by introducing equation (4-151) into them. A simplified problem is considered, where the mean velocity is in the  $x_1$ -direction and mean quantities are steady and can change only in the  $x_2$ -direction (ref. 53). Then if the mean velocity is eliminated by equation (4-151) and the turbulence is weak enough (and/or the mean velocity gradients are generally large enough) for triple-correlation terms to be neglected, the set of simultaneous correlation

---

<sup>4</sup>The two-point equations can, of course be profitably used for statistically *homogeneous* turbulence, as in the next chapter.

<sup>5</sup>The action in turbulence is somewhat similar to that of a clock, a violin bow, or an electronic oscillator in that in each of these a steady flow of energy is converted into oscillating energy by a nonlinear mechanism.

equations which must be considered consists of four nonlinear partial differential equations in four independent and four dependent variables. Although these equations might appear to be too complicated to be of use, some results can be obtained by expanding them in power series in each of the space variables to obtain algebraic expressions for the correlations, some of which are nonlinear (quadratic). The solutions so obtained will be accurate only for small values of the space variables.

The reduction of the partial differential equations to a set of algebraic equations, some of which contain quadratic terms, shows the importance of the nonlinear terms in the original equations. The quadratic terms in the algebraic equations come, of course, from the nonlinear terms in the differential equations. If those terms were absent, the algebraic equations would all be linear and homogeneous (no constant terms), since the original equations contained no constant terms. In that case the only solution would be that all the turbulence correlations are zero, so that the flow would be laminar. On the other hand, in the presence of nonlinear terms the system of algebraic equations is quadratic, so that nonzero steady-state turbulence correlations can exist (ref. 53).

Reference 53 also shows the importance of the pressure-velocity correlations in sustaining turbulence. The nonlinear production term is absent in the equation for  $\overline{u_2 u_2'}$  ( $i = j = 2$  in eq. (4-147)), since  $U_i = \delta_{i1} U_1$  in our problem. Thus the energy for sustaining  $\overline{u_2 u_2'}$  must be transferred from the other components of  $\overline{u_i u_j'}$ . The equations for the other components do, of course, contain nonlinear production terms, and energy can be transferred among the directional components by the pressure-velocity correlations (see discussion following eq. (4-151)).

The set of algebraic equations obtained by expanding the correlation equations in power series in the independent variables has been reduced to a single quadratic equation

$$N_c^2 = \left[ N + (\overline{u_1 u_2'})_0^* \right] \left[ N + a(\overline{u_1 u_2'})_0^* \right], \quad (4-152)$$

where

$$(\overline{u_1 u_2'})_0^* = \frac{\ell^2 (\overline{u_1 u_2'})_0}{\nu^2}, \quad N = \frac{\bar{\tau} \ell^2}{\rho \nu^2},$$

$N_c$  is the critical value of  $N$  (at which  $\overline{u_1 u_2'} = 0$ ), the subscript 0 designates the point in  $x_2, r_k$  space about which the series expansions are made,  $\bar{\tau}$  is the shear stress, which is uniform in the present problem,  $\ell$  is a measure of the scale of the turbulence, and  $a$  is a constant. Equation (4-152) might be used to estimate the variation of  $\overline{u_1 u_2'}$  with  $\bar{\tau}$  and  $\ell$ , preferably over a limited range; otherwise  $a$  might not be constant. For values of  $N$  below the critical value the correlation changes sign, according to equation (4-152). In that case one should use the no-turbulence solution of equations (4-147) and (4-149) to (4-151). Note that the no-turbulence solution is valid when  $N$  is above its critical value as well as when it is below it. Thus the fluid could be either turbulent or nonturbulent when  $N$  is above  $N_c$ .

In order to make a rough comparison of our results with experiment we can recast equation (4-152) so as to obtain an approximate expression for the friction factor for low Reynolds-number fully developed pipe flow. Actually, equation (4-152) is more nearly applicable to Couette flow than to pipe flow; however, because of the similarity of trends in pipe and Couette flows and the availability of experimental data for transition pipe flow, the comparison will be made with pipe-flow data. The approximate equation obtained in reference 53 is



$$f = \left(16 + B \text{Re}_c^{-2}\right) \text{Re}^{-1} - B \text{Re}^{-3}, \quad (4-153)$$

where  $f = 2\tau_w/(\rho U_a^2)$  is the friction factor,  $\text{Re} = U_a D/\nu$ ,  $U_a$  is the averaged pipe velocity,  $D$  is the pipe diameter,  $\text{Re}_c$  is the critical Reynolds number, and  $B$  is considered constant. For  $\text{Re} = \text{Re}_c$ ,  $f = 16/\text{Re}_c$ , which is the value of  $f$  for laminar flow at  $\text{Re}_c$ .

Equation (4-153) and the solution for laminar flow, together with experimental data from reference 54, are plotted in figure 4-18. The transition Reynolds number  $\text{Re}_c$  was taken as 2200, and  $B$  was set equal to  $0.21 \times 10^9$ . With these values for  $\text{Re}_c$  and  $B$ , equation (4-143) is in reasonable agreement with the data for the turbulent region up to a Reynolds number of about 5500. The deviation of the curve from the data at higher Reynolds numbers is probably caused mainly by the neglect of triple correlations. The laminar solution is, of course, part of the present solution, since the case of no turbulence satisfies the correlation equations. For  $\text{Re} < \text{Re}_c$  the laminar solution is appropriate because the turbulent solution goes below it and thus becomes unphysical.

#### 4.4 REMARKS

We began this chapter by considering kinds of averages and their properties, together with some notions of randomness from ergodic theory. Next, averaging was applied to the continuum equations derived in the last chapter. It was noted that when the equations are averaged, random chaotically fluctuating variables are replaced by variables which change in a smoother fashion. However, the closure problem then arises. Whereas the original unaveraged equations, together with appropriate initial and boundary conditions could, in principle, be completely solved, the solution of the averaged equations is indeterminate. That is, because of the nonlinearity of the basic equations, there are more unknowns than equations in the set of *averaged equations*. The addition of higher-order moment equations does not alleviate the problem; the number of unknowns goes up as fast as the number of equations when the added moment equations are multipoint, whereas if the added equations are single-point, the number of unknowns goes up *faster*. However, the use of those equations enables one to study the processes in turbulence. In particular, the numerical solution of the instantaneous (unaveraged) equations enables one to calculate terms in the averaged evolution equations. That procedure, in fact, provides a means of closing the system of averaged equations without introducing information which is supplemental to the basic continuum equations.

Because of the engineering importance of obtaining solutions for turbulent flows at high Reynolds numbers (where accurate numerical simulations cannot yet be carried out), much effort has been devoted to modeling the undetermined terms in the averaged equations. To this end, we obtained some approximate solutions for a simple fully developed flow and heat transfer which were, however, based partially on exact information. Other approximate solutions and closure schemes, including a frozen stress model for highly accelerated flows, were also discussed. The basis for a mixing-length theory and the nature of turbulent mixing were considered. Finally, the functional forms of the velocity and temperature profiles near and away from a wall, and the logarithmic profiles for the velocity and temperature were derived.

However, the only turbulent solutions considered which could be called completely deductive are numerical solutions of the unaveraged equations. As discussed, it is necessary to use supplementary information if the equations are averaged, unless, of course, they are closed by a numerical solution of the original unaveraged equations. Attempts to obtain analytical solutions of the unaveraged equations have not been successful, mostly because of the nonlinearity of those equations. Sensitive dependence of those

equations on initial conditions, in fact, appears to preclude an analytical solution. It is mentioned by Herring (ref. 55) that the simplest turbulence theory is just the Navier-Stokes equations; since most turbulence calculations are numerical anyway, no insight is lost by considering direct integration of the Navier-Stokes equations forward in time, starting with some suitable initial data. Because of its relevance and importance in turbulence research, we give here a few additional remarks on direct numerical solution.

Although numerical solution (or numerical simulation) bears some similarity to experiment there is an important difference. The former uses directly, and attempts to solve, a given set of mathematical equations (say the Navier-Stokes equations). The latter ordinarily does not, although both methods may arrive at the same description of nature. A numerical solution is, in fact, much closer to a theoretical solution than to experiment. A numerical solution differs from a theoretical one only in the tools that are used; numerical methods and high-speed computers may take place of, or supplement, analytical tools. A significant difference is not, as sometimes stated, that the numerical solution is discrete; as many points as desired can be calculated if a suitable interpolation formula is provided.

Because of the small scale of some of the turbulent eddies, accuracy is a problem in the numerical study of turbulence. Smaller and smaller eddies are generated as the Reynolds number (strength) of the turbulence increases. One can always pick a Reynolds number large enough that the results will be quantitatively inaccurate, no matter how fine the numerical mesh. On the other hand, turbulence at any fixed Reynolds number could, in principle, be calculated, given the availability of a powerful enough computer. Note that there does not seem to be a qualitative difference (no bifurcations) between low and high Reynolds-number turbulence; in the latter the turbulent energy is just spread out over a (much) wider range of eddy sizes. The mathematical or computational methods used may of course, be different for higher Reynolds numbers.

Although we started this section with a discussion of averages and averaged equations, it has been appropriate to close it with a discussion of numerical solutions of the original unaveraged equations, those being the only completely deductive turbulent solutions considered thus far (see, e.g., refs. 17 and 49). (Deductive refers here to solutions of the continuum equations which do not require an input of supplementary information.) Note that, as mentioned earlier, a deductive solution of an unclosed averaged equation (e.g., the evolution equation for the turbulent energy) can be obtained by using it in conjunction with unaveraged equations, the terms in the averaged equation being calculated from the numerical solution of the determinate unaveraged equations. As a final remark, it seems unlikely that a turbulent *analytical* solution of the unaveraged equations could ever be obtained, because the solution would have to be sensitively dependent on initial conditions (see chapter VI).

In order to continue with the analysis of turbulence, it will be necessary, or at least convenient, to introduce Fourier analysis. That will be done in the next chapter.

## REFERENCES

1. Lebowitz, J.L.; and Penrose, O.: Modern Ergodic Theory. Phys. Today, vol. 26, no. 2, Feb. 1973, pp. 23-29.
2. Lichtenberg, A.J.; and Lieberman, M.A.: Regular and Stochastic Motion. Springer-Verlag, New York, 1983.
3. Reynolds, O.: On the Dynamical Theory of Incompressible Viscous Fluids and the Determination of the Criterion. Philos. Trans. R. Soc. London, vol. 186, 1895, pp. 123-164.

4. Tanenbaum, B.S.: Plasma Physics. McGraw-Hill, New York, 1967, pp. 162-164.
5. Hinze, J.O.: Turbulence. McGraw-Hill, New York, 1975.
6. Prandtl, L.: The Mechanics of Viscous Fluids; in Aerodynamic Theory, A General Review of Progress, Vol. III, edited by W.F. Durand. Springer-Verlag, Berlin, Germany, 1934, pp. 34-208.
7. Deissler, R.G.: Analysis of Fully Developed Turbulent Heat Transfer at Low Peclet Numbers in Smooth Tubes with Application to Liquid Metals. NACA RME52F05, 1952.
8. Jenkins, R.: Variation of the Eddy Conductivity with Prandtl Modulus and its Use in Prediction of Turbulent Heat Transfer Coefficients. Preprints of Papers—Heat Transfer and Fluid Mechanics Institute. Stanford University Press, Stanford, CA, 1951, pp. 147-158.
9. Jakob, M.: Heat Transfer, Vol. II. John Wiley and Sons, New York, 1957, pp. 507-529.
10. Deissler, R.G.: On the Decay of Homogeneous Turbulence Before the Final Period. Phys. Fluids, vol. 1, no. 2, Mar.-Apr. 1958, pp. 111-121.
11. Laufer, J.: The Structure of Turbulence in Fully Developed Pipe Flow. NACA TN-2954, 1953.
12. Batchelor, G.K.: The Theory of Homogeneous Turbulence. Cambridge University Press, New York, 1953, pp. 107, 108, 183-187.
13. Hussain, A.K.M.F.: Coherent Structures—Reality and Myth. Phys. Fluids, vol. 26, no. 10, Dec. 1983, pp. 2816-2850.
14. Townsend, A.A.: The Structure of Turbulent Shear Flow. Cambridge University Press, New York, 1956, pp. 218-221.
15. Deissler, R.G.: Analytical and Experimental Investigation of Adiabatic Turbulent Flow in Smooth Tubes. NACA TN-2138, 1950.
16. Millikan, C.B.: A Critical Discussion of the Turbulent Flows in Channels and Circular Tubes. Proceedings of the Fifth International Congress for Applied Mechanics, J.P. Den Hartog and M. Peters, eds., Wiley & Sons, New York, 1938, pp. 386-392.
17. Kim, J.; Moin, P.; and Moser, R.: Turbulence Statistics in Fully Developed Channel Flow at Low Reynolds Number. J. Fluid Mech., vol. 177, 1987, pp. 133-166.
18. Nikuradse, J.: Gesetzmässigkeiten der Turbulenten Strömung in Glatten Rohren. VDI-Forschungsheft, no. 356, Sept.-Oct. 1932, p. 36.
19. Stanton, T.E.; and Pannell, J.R.: Similarity of Motion in Relation to the Surface Friction of Fluids. Philos. Trans. R. Soc. London, ser. A, vol. 214, 1914, pp. 199-224.
20. Bernardo, E.; and Eian, C.S.: Heat Transfer Tests of Aqueous Ethylene Glycol Solutions in an Electrically Heated Tube. NACA WR E-136, 1945.

21. Kaufman, S.J.; and Isely, F.D.: Preliminary Investigation of Heat Transfer to Water Flowing in an Electrically Heated Inconel Tube. NACA RM E50G31, 1950.
22. Kreith, F.; and Summerfield, M.: Pressure Drop and Convective Heat Transfer with Surface Boiling at High Heat Flux; Data for Aniline and n-Butyl Alcohol. Trans. ASME, vol. 72, no. 6, Aug. 1950, pp. 869-879.
23. Deissler, R.G.; and Eian, C.S.: Analytical and Experimental Investigation of Fully Developed Turbulent Flow of Air in a Smooth Tube with Heat Transfer with Variable Fluid Properties. NACA TN-2629, 1952.
24. Grele, M.D.; and Gedeon, L.: Forced-Convection Heat-Transfer Characteristics of Molten Sodium Hydroxide. NACA RM E53L09, 1953.
25. Hoffman, H.W.: Turbulent Forced Convection Heat Transfer in Circular Tubes Containing Molten Sodium Hydroxide. ORNL-1370, Oak Ridge National Laboratories, Oak Ridge, TN, 1952.
26. Bonilla, C.F.: Mass Transfer in Liquid Metal and Fused Salt Systems. NYO-3086, First Quarterly Progress Report. U.S. Atomic Energy Commission, Technical Information Service, Oak Ridge, TN, 1951.
27. Linton, W.H., Jr.; and Sherwood, T.K.: Mass Transfer from Solid Shapes to Water in Streamline and Turbulent Flow. Chem. Eng. Prog., vol. 46, no. 5, May 1950, pp. 258-264.
28. Barnet, W.I.; and Kobe, K.A.: Heat and Vapor Transfer in a Wetted-Wall Tower. Ind. Eng. Chem., vol. 33, no. 4, Apr. 1941, pp. 436-442.
29. Chilton, T.H.; and Colburn, A.P.: Mass Transfer (Absorption) Coefficients. Ind. Eng. Chem., vol. 26, no. 11, Nov. 1934, pp. 1183-1187.
30. Jackson, M.L.; and Ceaglske, N.H.: Distillation, Vaporization, and Gas Absorption in a Wetted-Wall Column. Ind. Eng. Chem., vol. 42, no. 6, June 1950, pp. 1188-1198.
31. Lin, C.S., et al.: Diffusion-Controlled Electrode Reactions. Ind. Eng. Chem., vol. 43, no. 9, Sept. 1951, pp. 2136-2143.
32. Eagle, A.E.; and Ferguson, R.M.: On the Coefficient of Heat Transfer from the Internal Surface of Tube Walls. Proc. R. Soc. London, ser. A, vol. 127, 1930, pp. 540-566.
33. Deissler, R.G.: Turbulent Heat Transfer and Friction in Smooth Passages. Turbulent Flows and Heat Transfer, C.C. Lin, ed., Princeton University Press, Princeton, NJ, 1959, pp. 288-313.
34. Deissler, R.G., and Loeffler, A.L.: Analysis of Turbulent Flow and Heat Transfer on a Flat Plate at High Mach Numbers with Variable Fluid Properties. NASA Rept. TR R-17, 1959.
35. Deissler, R.G.; and Perlmutter, M.: Analysis of the Flow and Energy Separation in a Turbulent Vortex. Int. J. Heat Mass Transfer, vol. 1, no. 2-3, 1960, pp. 173-191.
36. Deissler, R.G.: Gravitational Collapse of a Turbulent Vortex with Application to Star Formation. Astrophys. J., vol. 209, Oct. 1, 1976, pp. 190-204.

37. Deissler, R.G.: Models for Some Aspects of Atmospheric Vortices. *J. Atmos. Sci.*, vol. 34, Oct. 1977, pp. 1502-1517.
38. Van Driest, E.R.: On Turbulent Flow Near a Wall. *J. Aeronaut. Sci.*, vol. 23, 1956, pp. 1007-1011.
39. Goldstein, S.: Modern Developments in Fluid Dynamics. Vol. 1. Clarendon Press, Oxford, England, 1938, pp. 119-120.
40. Blackwelder, R.F.; and Kovasznay, L.S.G.: Large-Scale Motion of a Turbulent Boundary Layer During Relaminarization. *J. Fluid Mech.*, vol. 53, May 9, 1972, pp. 61-83.
41. Deissler, R.G.: Evolution of a Moderately Short Turbulent Boundary Layer in a Severe Pressure Gradient. *J. Fluid Mech.*, vol. 64, July 24, 1974, pp. 763-774.
42. Deissler, R.G.: Evolution of the Heat Transfer and Flow in Moderately Short Turbulent Boundary Layers in Severe Pressure Gradients. *Int. J. Heat Mass Transfer*, vol. 17, Sept. 1974, pp. 1079-1085.
43. Launder, B.E.: Laminarization of the Turbulent Boundary Layer by Acceleration. Massachusetts Institute of Technology Gas Turbine Laboratory Rept. 77, Nov. 1964.
44. Patel, V.C.; and Head, M.R.: Reversion of Turbulent to Laminar Flow. *J. Fluid Mech.*, vol. 34, no. 2, 1968, pp. 371-392.
45. Kline, S.J., et al.: The Structure of Turbulent Boundary Layers. *J. Fluid Mech.*, vol. 30, no. 4, 1967, pp. 741-773.
46. Julien, H.L.; Kays, W.M.; and Moffat, R.J.: Experimental Hydrodynamics of the Accelerated Turbulent Boundary Layer With and Without Mass Injection. *J. Heat Transfer*, vol. 93, Nov. 1971, pp. 373-379.
47. Moretti, P.M.; and Kays, W.M.: Heat Transfer to a Turbulent Boundary Layer with Varying Free Stream Temperature—An Experimental Study. *Int. J. Heat Mass Transfer*, vol. 8, Sept. 1965, pp. 1187-1202.
48. Back, L.H.; and Cuffell, R.F.: Turbulent Boundary layer and Heat Transfer Measurements Along a Convergent-Divergent Nozzle. *J. Heat Transfer*, vol. 93, Nov. 1971, pp. 397-407.
49. Mansour, N.N.; Kim, J.; and Moin, P.: Reynolds-Stress and Dissipation—Rate Budgets in a Turbulent Channel Flow. *J. Fluid Mech.*, vol. 194, 1988, pp. 15-44.
50. Deissler, R.G.: Turbulent Solutions of the Equations of Fluid Motion. *Rev. Mod. Phys.*, vol. 56, no. 1, 1984, pp. 223-254.
51. Rodi, W.: Turbulence Models for Practical Applications. Introduction to the Modeling of Turbulence. Von Kármán Institute for Fluid Dynamics, Rhode-Saint-Genese, Belgium, 1987, p. 27.
52. Launder, B.E.; Reynolds, W.C.; and Rodi, W.: Turbulence Models and Their Applications. Vol. 2, Editions Eyrolles, Paris, France, 1984.

53. Deissler, R.G.: Problem of Steady-State Shear-Flow Turbulence. *Phys. Fluids*, vol. 8, no. 3, 1965, pp. 391-398.
54. Deissler, R.G.; Weiland, W.F.; and Lowdermilk, W.H.: Analytical and Experimental Investigation of Temperature Recovery Factors for Fully Developed Flow of Air in a Tube. NACA TN-4376, 1958.
55. Herring, J.R.: Statistical Turbulence Theory and Turbulence Phenomenology; in Free Turbulent Shear Flows. Vol. 1: Conference Proceedings. NASA SP-321, 1973, pp. 41-66.

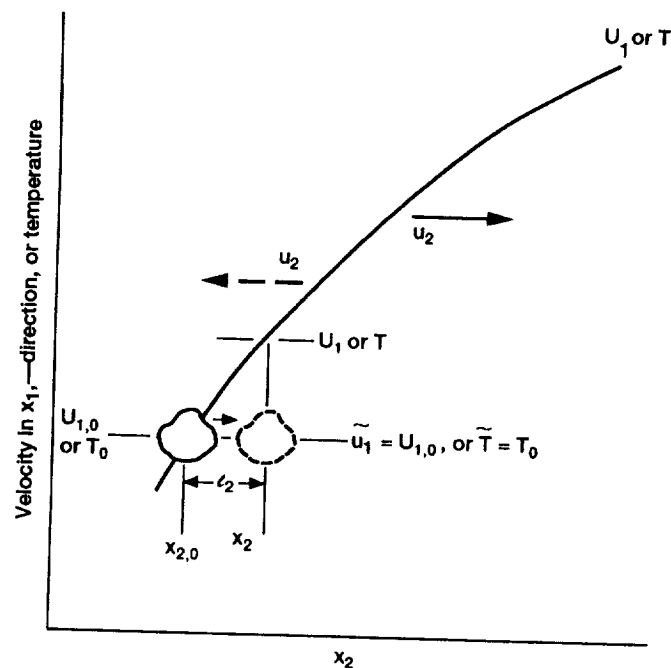


Figure 4-1.—Sketch illustrating development of turbulent shear stress  $-\rho \bar{u}_1 u_2$  or heat transfer  $\rho c \bar{u}_1 \bar{u}_2$  in presence of a mean velocity or temperature gradient. Regardless of whether the velocity fluctuation  $u_2$  is positive or negative, the product  $\bar{u}_1 u_2$  (or  $\bar{u}_1 \bar{u}_2$ ) is negative (see section 4.3.1.1). Also illustrated (in the lower part of the figure) is a mixing-length theory, where  $l_2$  is the mixing length and  $x_{2,0}$  is at the virtual origin of an eddy (see section 4.3.2.2).

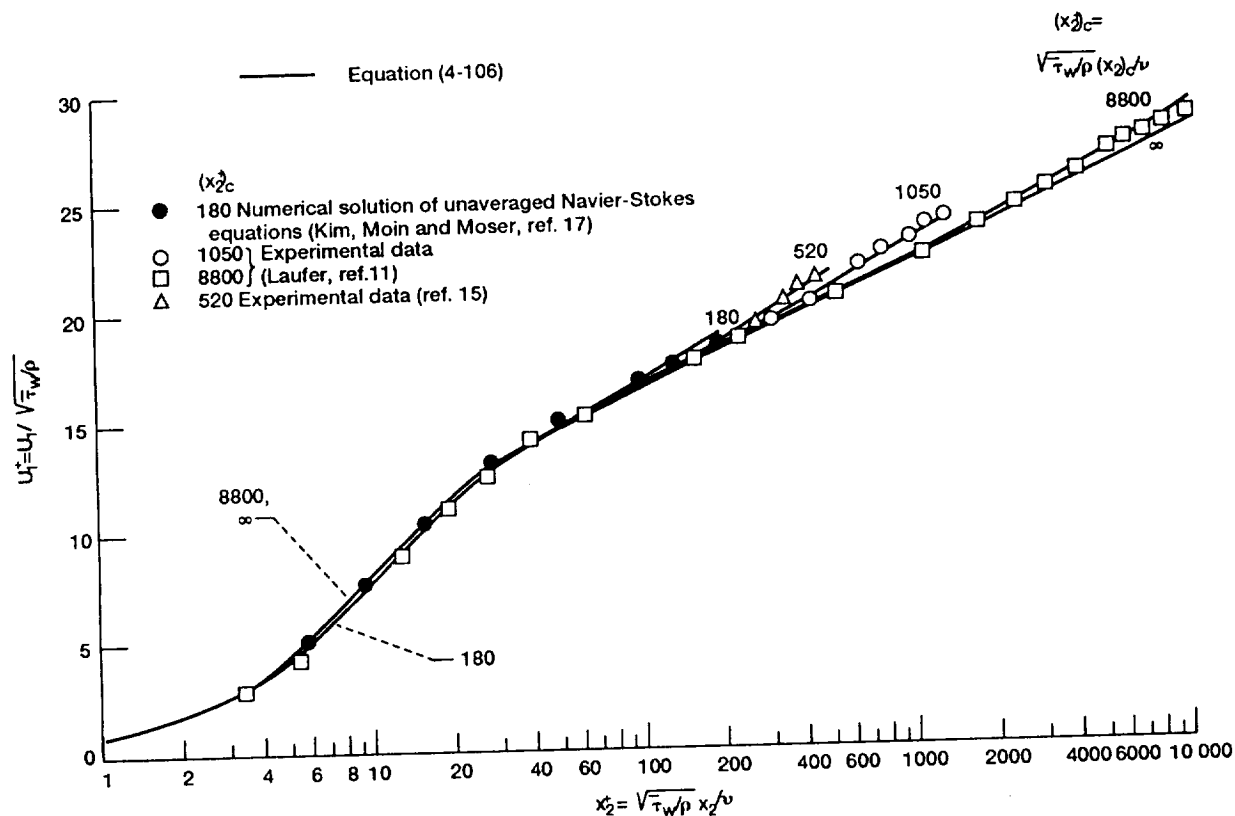


Figure 4-2.—Velocity distribution for turbulent flow through a channel or pipe.

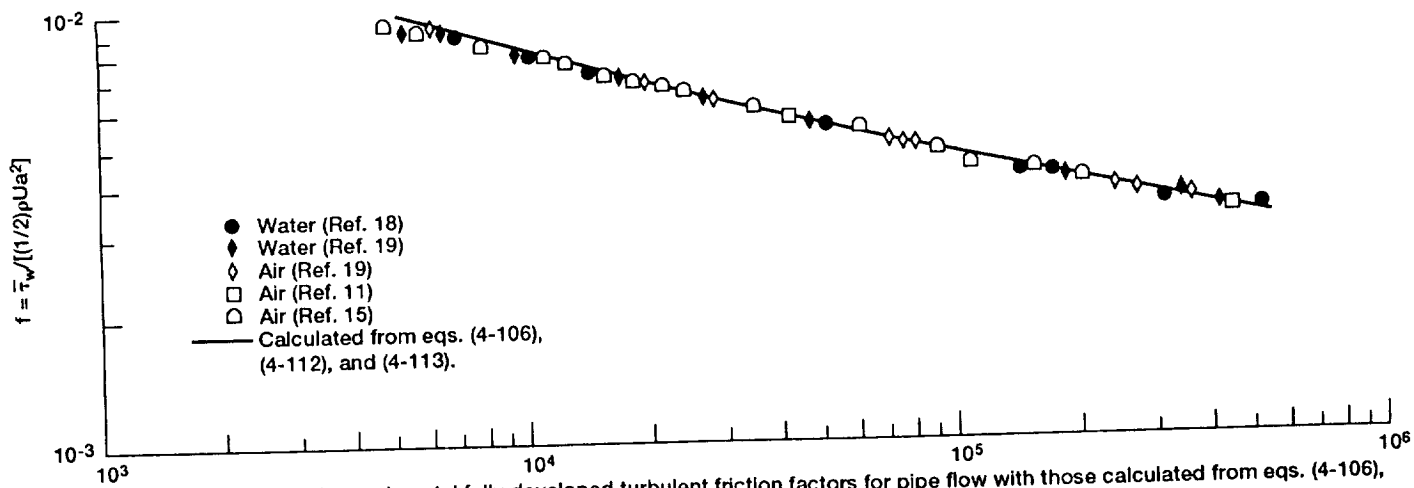


Figure 4-3. —Comparison of experimental fully developed turbulent friction factors for pipe flow with those calculated from eqs. (4-106), (4-112) and (4-113).

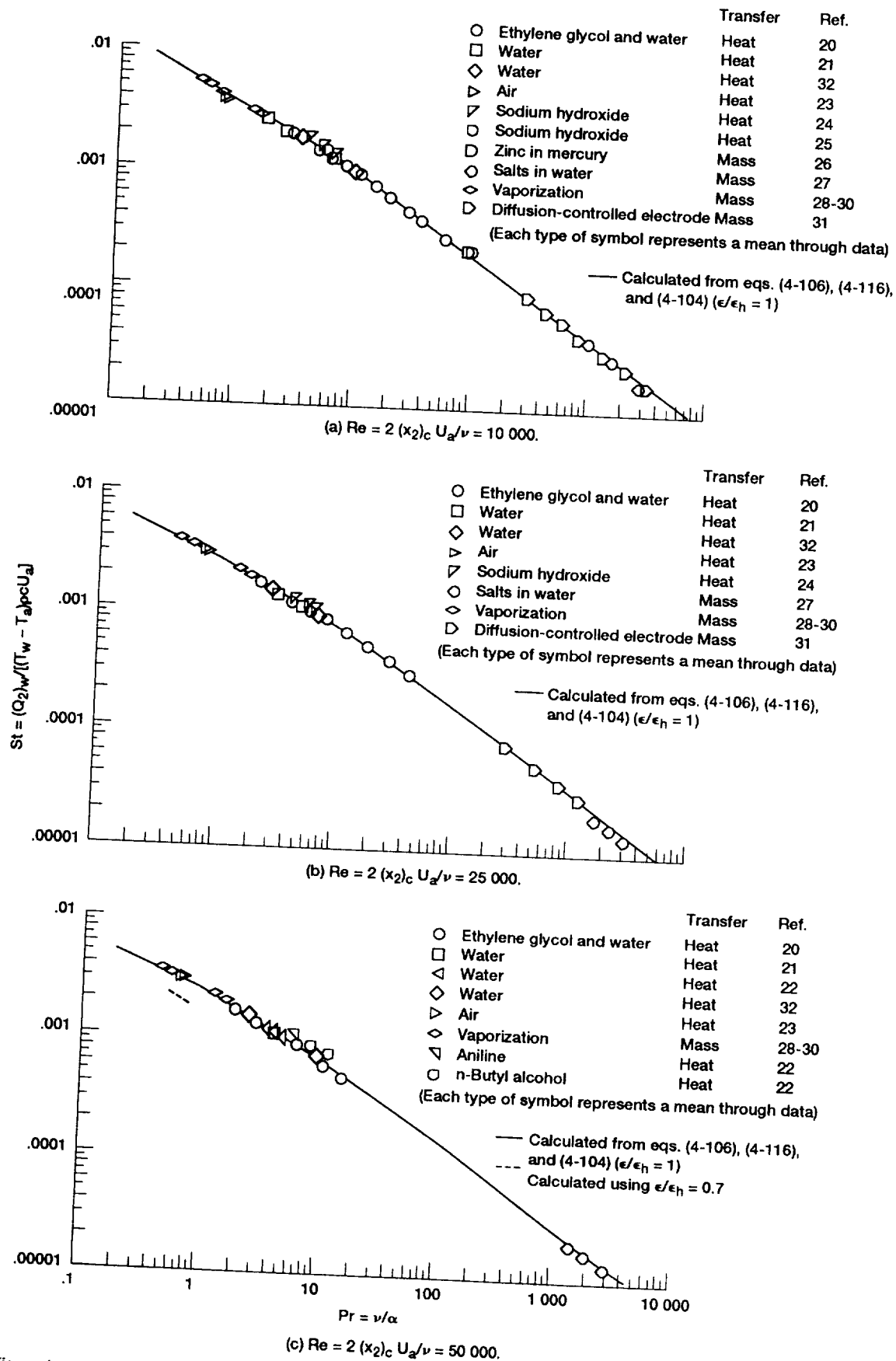
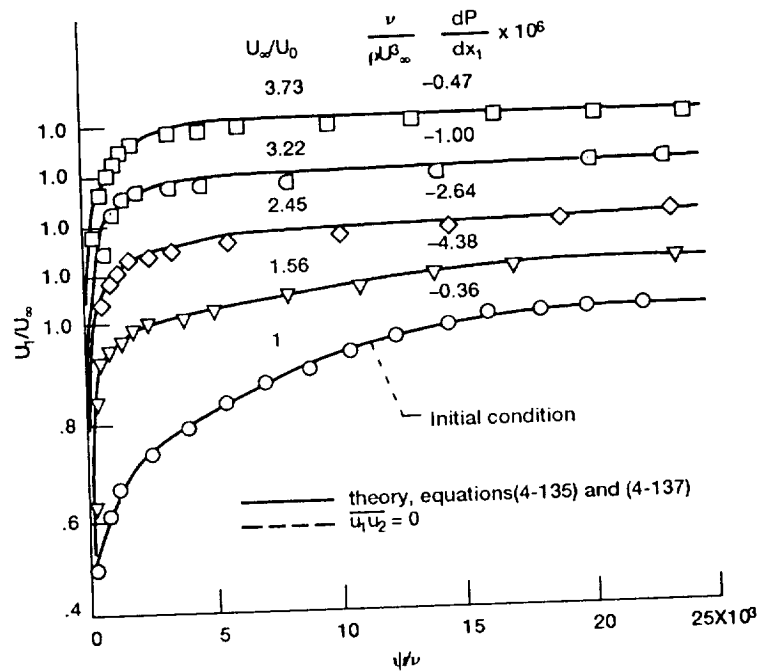
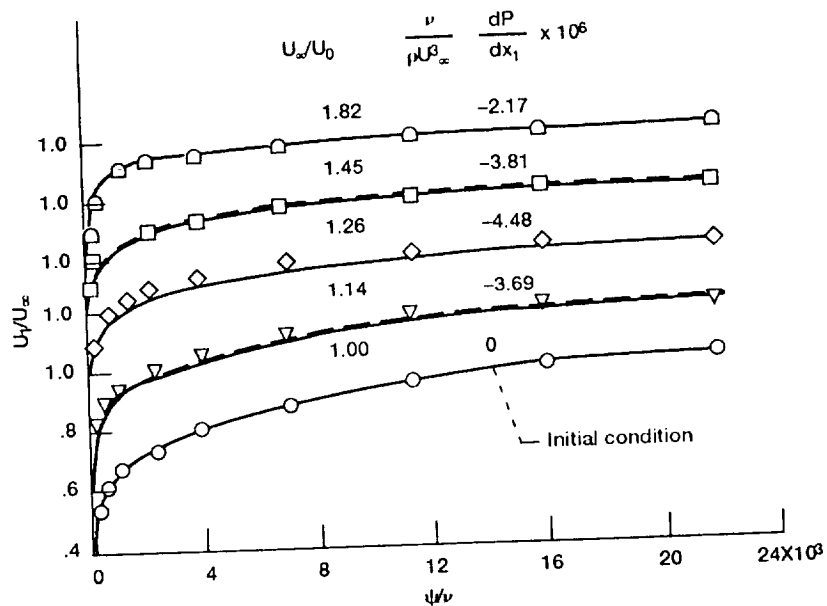


Figure 4-4.—Comparison of calculated Stanton numbers with experiment. (For the mass-transfer data the temperatures  $T_w$  and  $T_a$  are replaced by concentrations, and the molecular thermal diffusivity  $\alpha$  is replaced by a diffusivity for mass transfer.)





(a) Blackwelder & Kovaszny (ref. 40).



(b) Patel & Head (ref. 44) (Note shifted vertical scales).

Figure 4-5.—Predicted early and intermediate development of mean velocity profile in a turbulent boundary layer with severe favorable pressure gradients and comparison with experiments. Symbols indicate experimental data points.

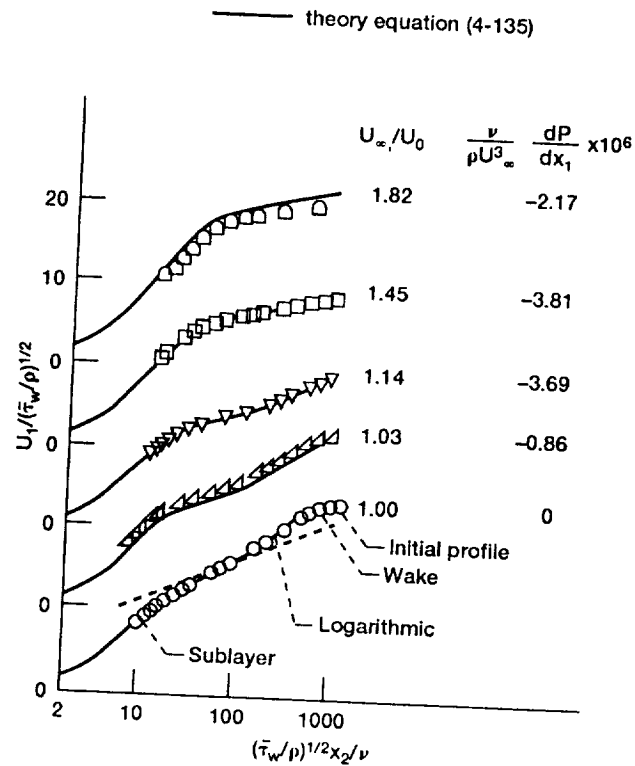


Figure 4-6. —Semi-logarithmic law-of-the-wall plot of theoretical velocity profiles for severe favorable pressure gradients and comparison with experiment of Patel & Head (ref. 44). (Note shifted vertical scales.) Symbols indicate experimental data points.

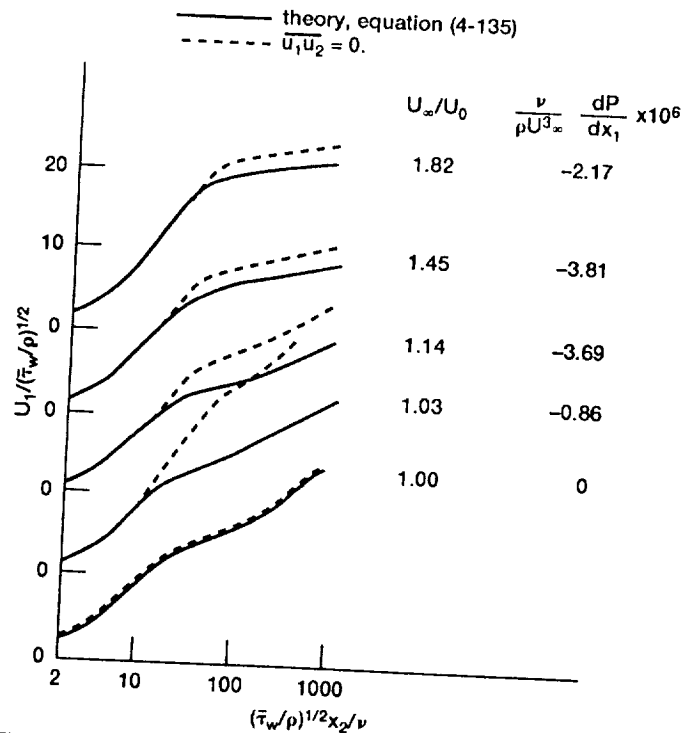


Figure 4-7. —Effect of neglecting Reynolds shear stress on theoretical law-of-the-wall plot for experimental conditions of figure 4-5. (Noted shifted vertical scales.)

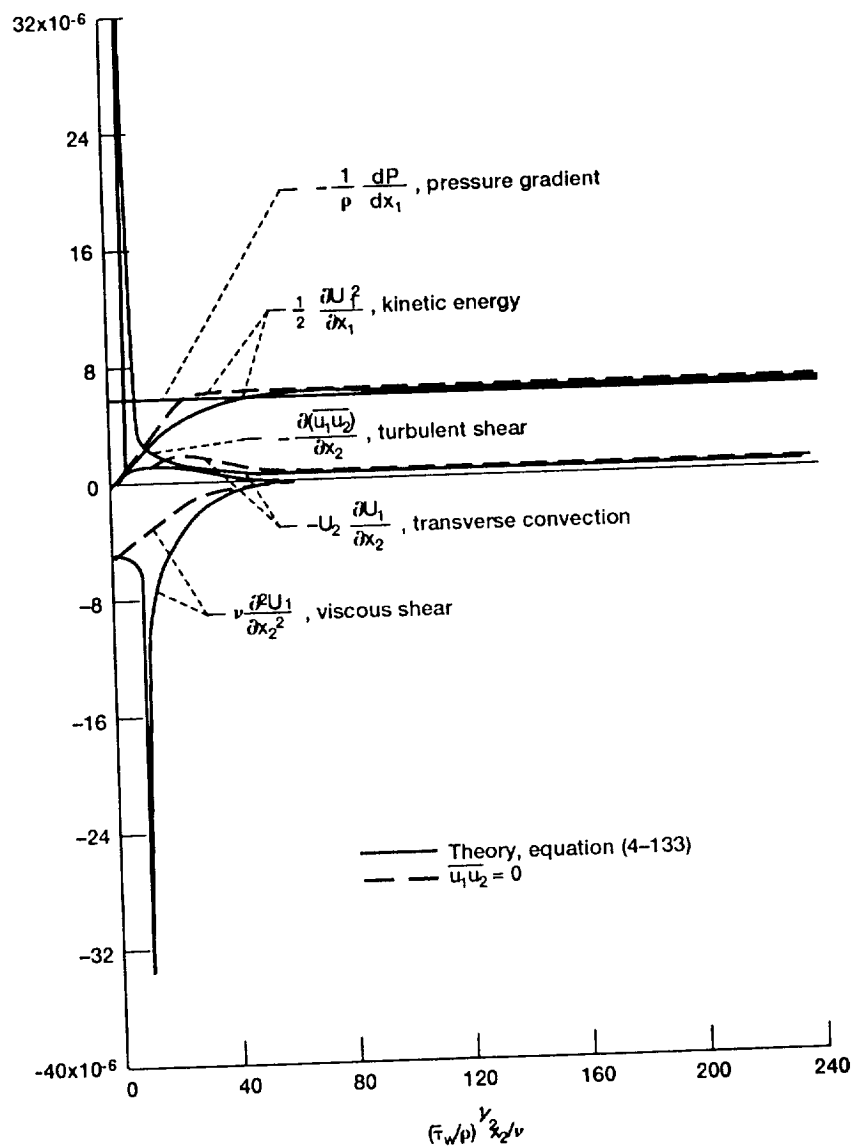


Figure 4-8.—Contribution of various terms in eq. (4-128) to streamwise rate of change of dimensionless kinetic energy of mean flow for initial conditions of figure 4-6. Terms in eq. (4-128) nondimensionalized by  $U_0$  and  $\nu$ .  $U_w/U_0 = 1.14$ . Note that transverse component of kinetic energy is negligible for a boundary layer.

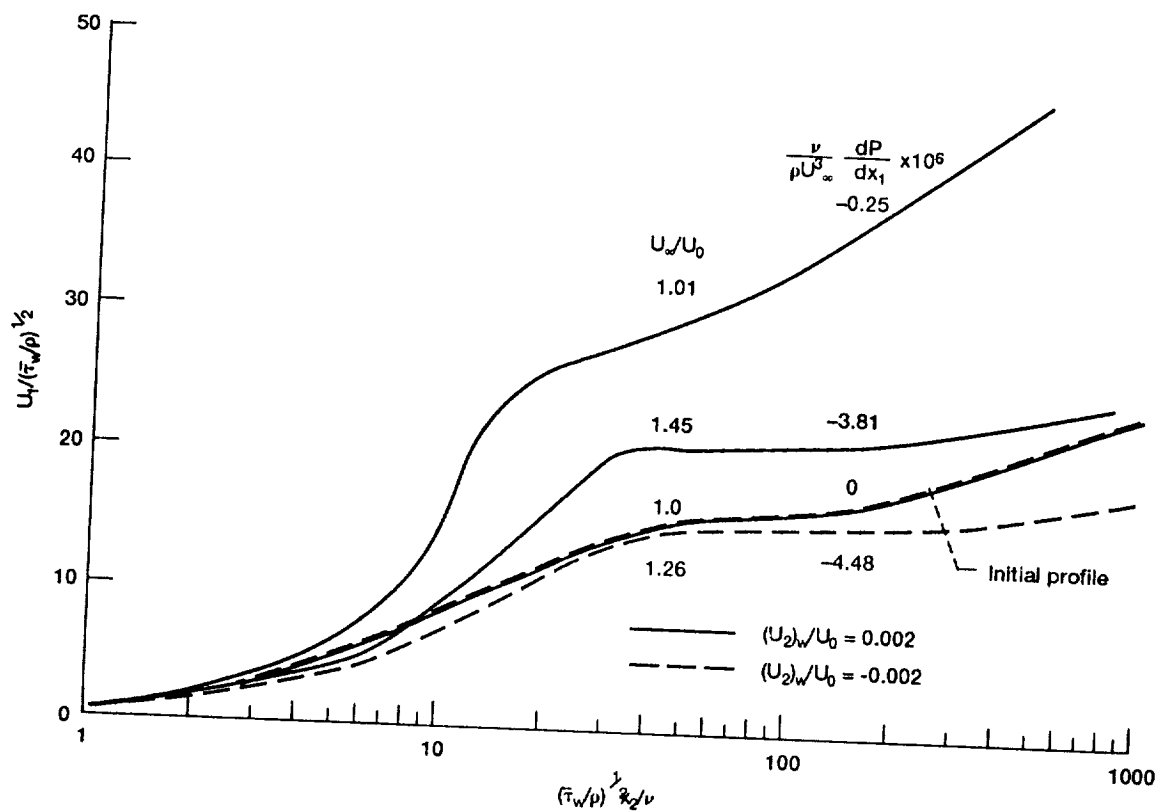


Figure 4-9.—Effect of mass injection normal to wall on theoretical velocity profiles for severe favorable pressure gradients. (Initial conditions and pressure gradients correspond to figure 4-6)

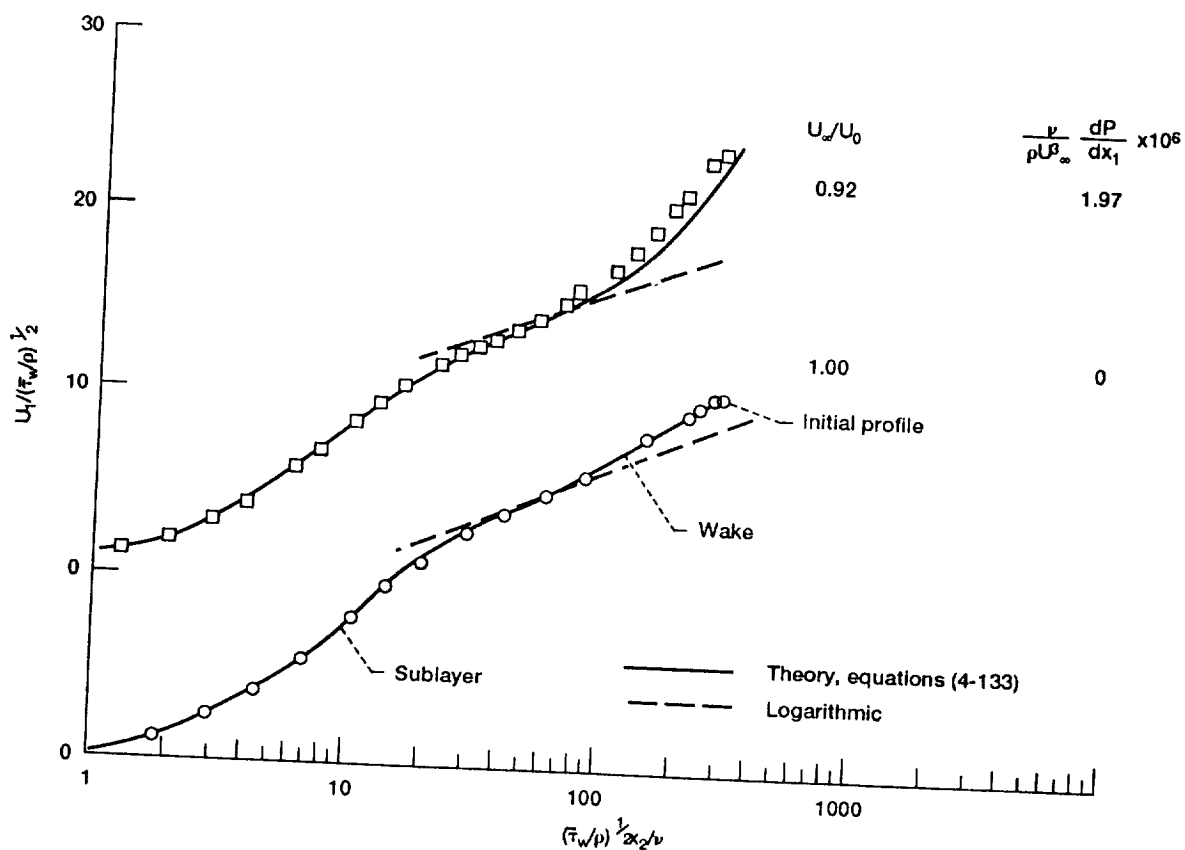


Figure 4-10.—Theoretical velocity profiles for severe adverse pressure gradients and comparison with experiment of Kline et al. (ref. 45). (Note shifted vertical scales).

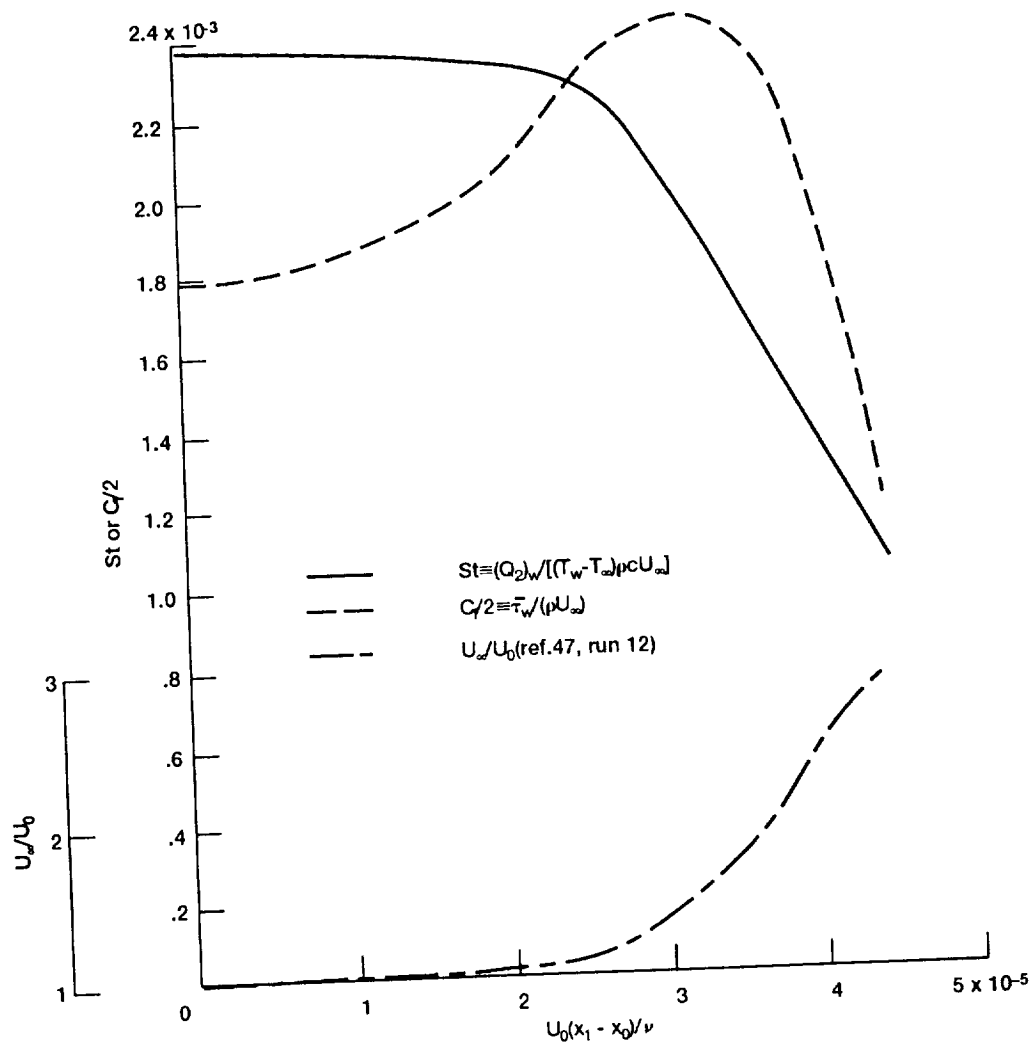


Figure 4-11.—Comparison of streamwise evolution of theoretical Stanton number  $St$  and skin-friction coefficient  $C_f$  in moderately short highly accelerated turbulent boundary layers.  $x_0$  is value of  $x_1$  at initial station.  $U_0$  is value of  $U_\infty$  at initial station.

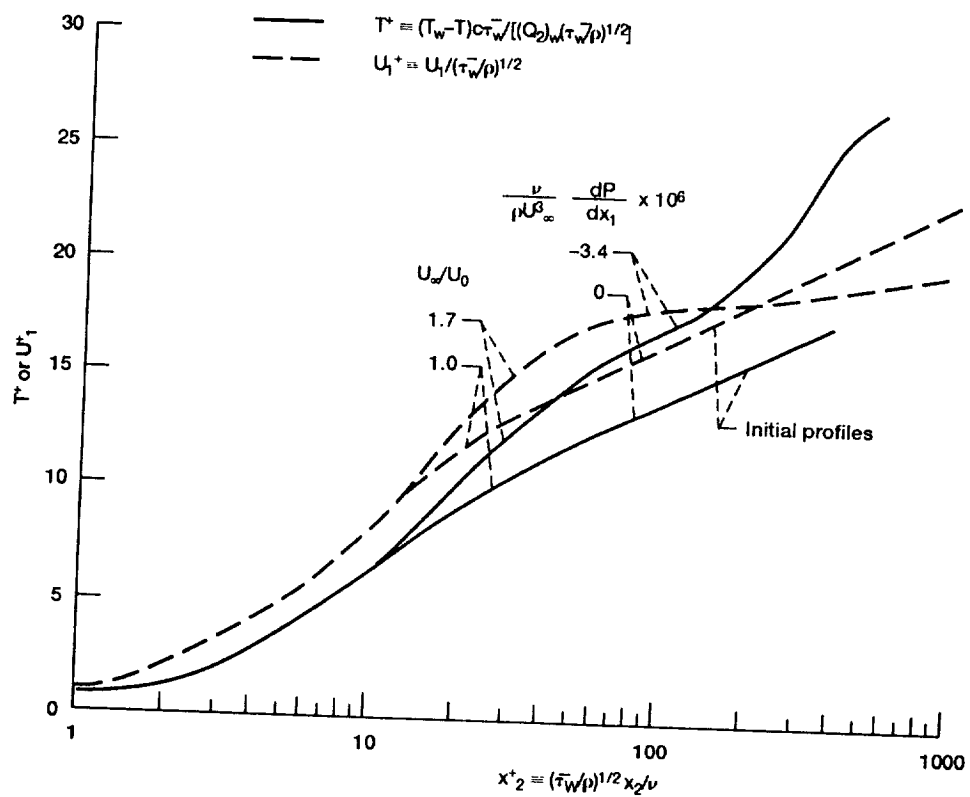


Figure 4-12.—Comparison of evolution of theoretical velocity and temperature distributions in moderately short highly accelerated turbulent boundary layers.

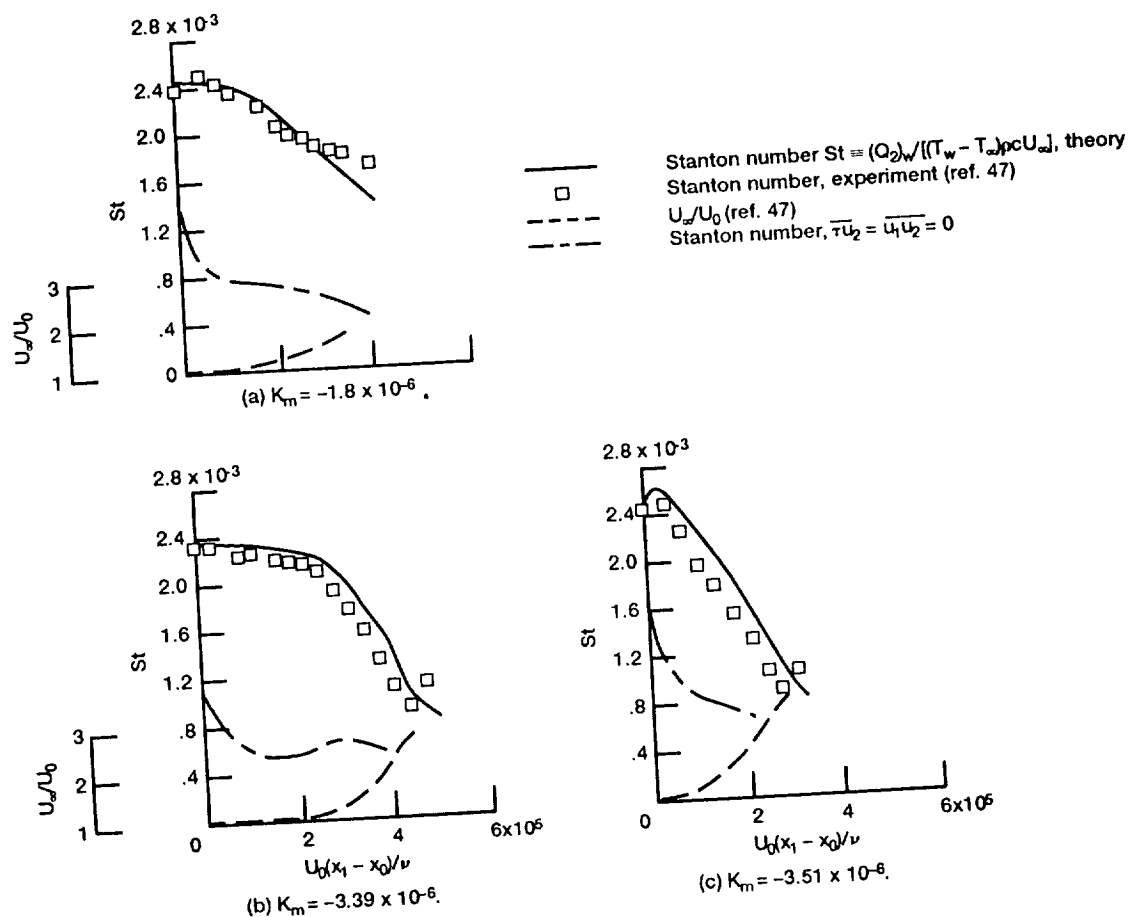


Figure 4-13.—Comparison of theory and experiment for streamwise evolution of Stanton number in moderately short highly accelerated turbulent boundary layers.  $x_0$  is value of  $x_1$  at initial station.  $K_m$  is maximum value of  $(\nu/\rho U_\infty^3) dP/dx_1$  for a particular run.

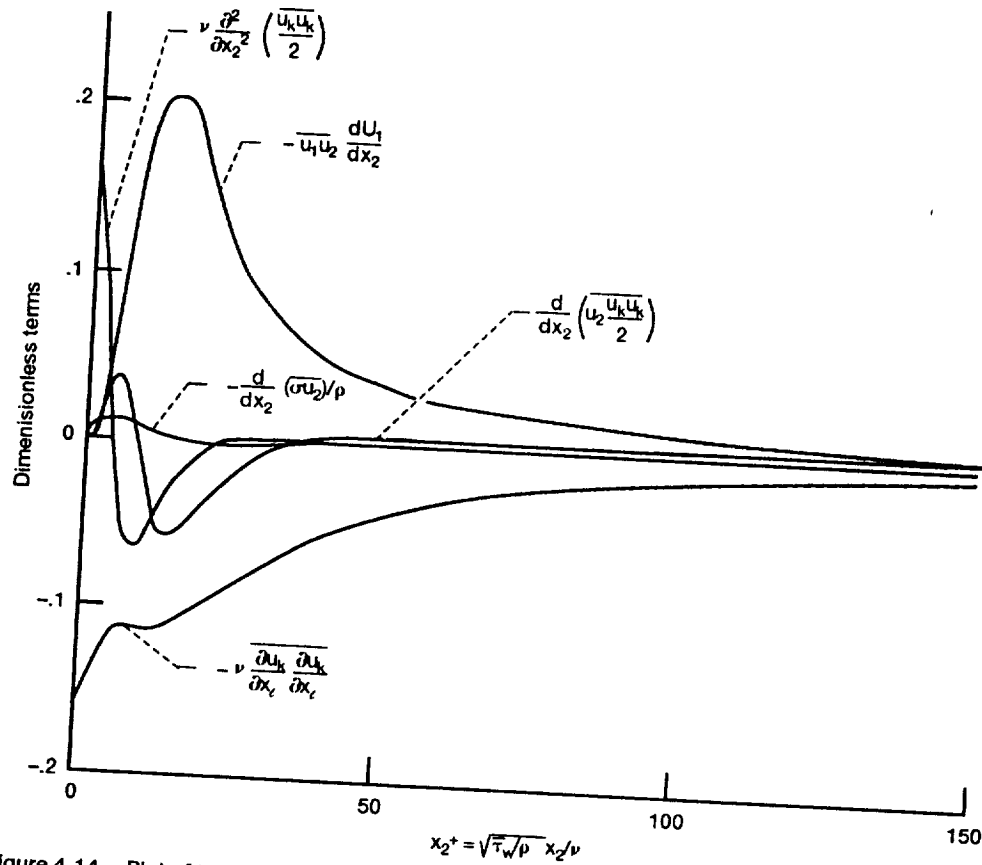


Figure 4-14.—Plot of terms in one-point equation for evolution of kinetic energy (eq. (4-144)) for fully developed channel flow. Results obtained by numerical solution of unaveraged Navier-Stokes equations (Mansour, Kim, and Moin ref. 49). Terms nondimensionalized by  $\sqrt{\tau_w/\rho}$  and  $\nu$ . Channel Reynolds number (based on centerline  $U_1$  and channel half-width) is 3200.



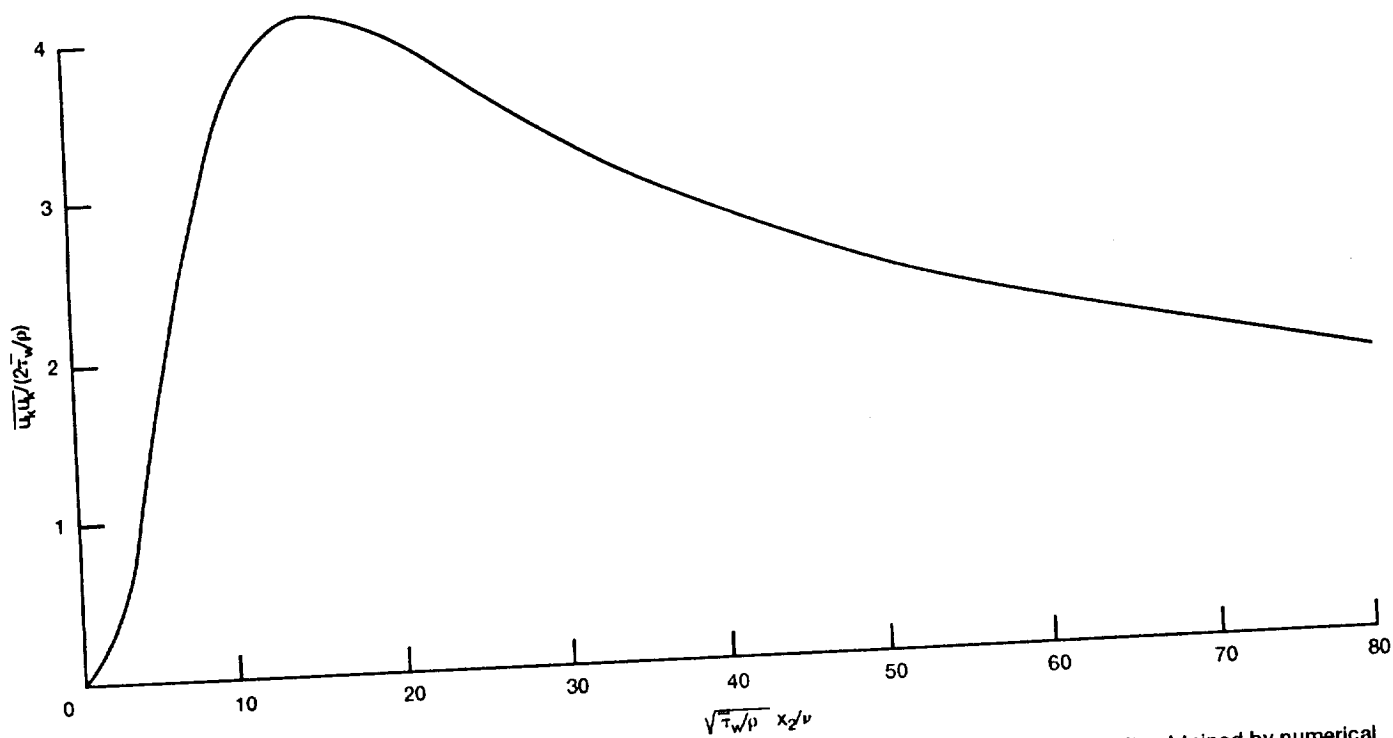


Figure 4-15.—Plot of turbulence kinetic energy for fully developed channel flow in figures 4-14 and 4-2. Results obtained by numerical solution of unaveraged Navier-Stokes equations (Kim, Moin, and Moser, ref. 17).

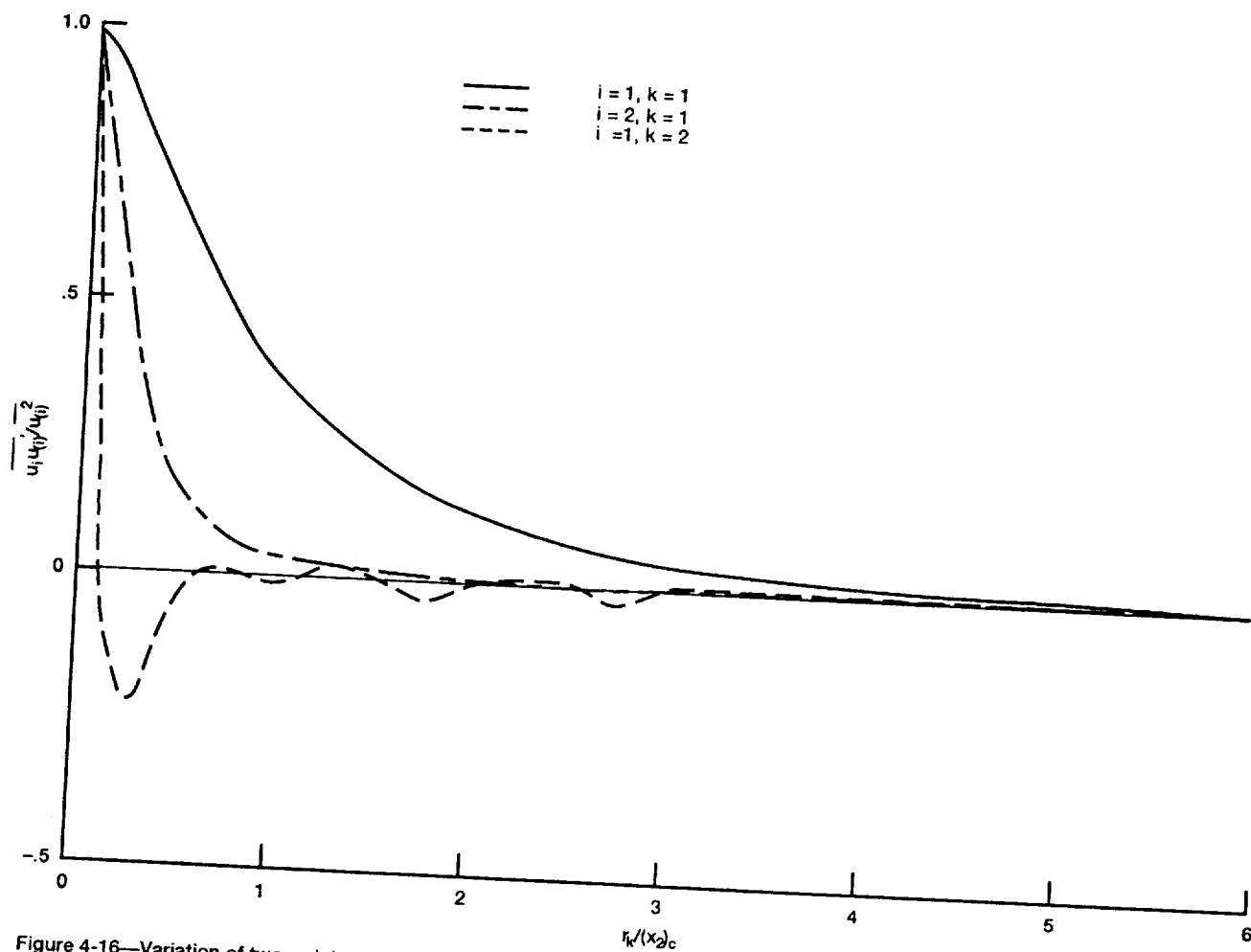


Figure 4-16—Variation of two-point correlation coefficients with point separation as obtained by Kim, Moin, and Moser (ref. 17) from a direct numerical simulation of unaveraged Navier-Stokes equations.  $x_2/(x_2)_c = 0.030$ ,  $x_2^+ = 5.39$ .

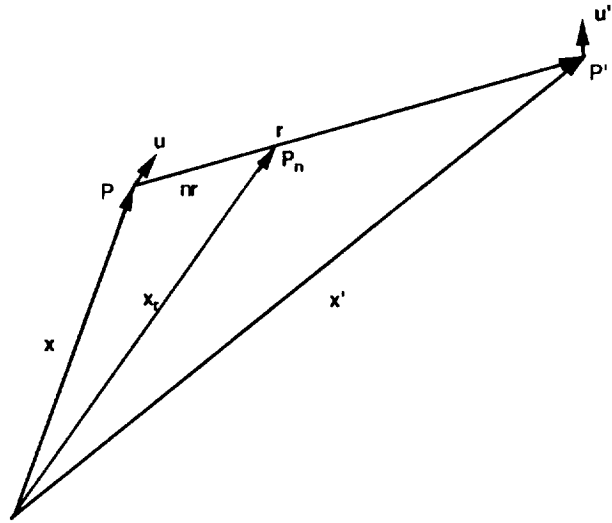


Figure 4-17.—Vector configuration for two-point correlation equations.

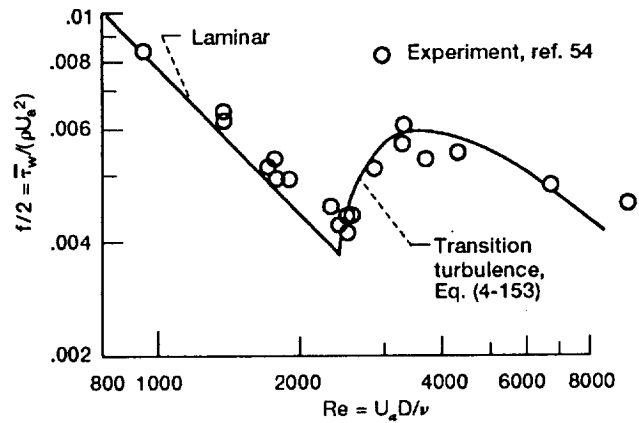


Figure 4-18.—Comparison of eq. (4-153) and solution for laminar flow, with pipe-flow data in turbulent transition and laminar regions.

**REPORT DOCUMENTATION PAGE**

Form Approved

OMB No. 0704-0188

Public reporting burden for this collection of information is estimated to average 1 hour per response, including the time for reviewing instructions, searching existing data sources, gathering and maintaining the data needed, and completing and reviewing the collection of information. Send comments regarding this burden estimate or any other aspect of this collection of information, including suggestions for reducing this burden, to Washington Headquarters Services, Directorate for Information Operations and Reports, 1215 Jefferson Davis Highway, Suite 1204, Arlington, VA 22202-4302, and to the Office of Management and Budget, Paperwork Reduction Project (0704-0188), Washington, DC 20503.

<b>1. AGENCY USE ONLY (Leave blank)</b>		<b>2. REPORT DATE</b> September 1992	<b>3. REPORT TYPE AND DATES COVERED</b> Technical Memorandum	
<b>4. TITLE AND SUBTITLE</b> Turbulent Fluid Motion IV-Averages, Reynolds Decomposition, and the Closure Problem			<b>5. FUNDING NUMBERS</b>  WU-505-90-53	
<b>6. AUTHOR(S)</b> Robert G. Deissler				
<b>7. PERFORMING ORGANIZATION NAME(S) AND ADDRESS(ES)</b> National Aeronautics and Space Administration Lewis Research Center Cleveland, Ohio 44135-3191			<b>8. PERFORMING ORGANIZATION REPORT NUMBER</b>  E-7253	
<b>9. SPONSORING/MONITORING AGENCY NAMES(S) AND ADDRESS(ES)</b> National Aeronautics and Space Administration Washington, D.C. 20546-0001			<b>10. SPONSORING/MONITORING AGENCY REPORT NUMBER</b>  NASA TM-105822	
<b>11. SUPPLEMENTARY NOTES</b> Responsible person, Robert G. Deissler, (216) 433-5823.				
<b>12a. DISTRIBUTION/AVAILABILITY STATEMENT</b>  Unclassified - Unlimited Subject Category 34			<b>12b. DISTRIBUTION CODE</b>	
<b>13. ABSTRACT (Maximum 200 words)</b> Ensemble, time, and space averages as applied to turbulent quantities are discussed, and pertinent properties of the averages are obtained. Those properties, together with Reynolds decomposition, are used to derive the averaged equations of motion and the one- and two-point moment or correlation equations. The terms in the various equations are interpreted. The closure problem of the averaged equations is discussed, and possible closure schemes are considered. Those schemes usually require an input of supplemental information unless the averaged equations are closed by calculating their terms by a numerical solution of the original unaveraged equations. The law of the wall for velocities and temperatures, the velocity- and temperature-defect laws, and the logarithmic laws for velocities and temperatures are derived. Various notions of randomness and their relation to turbulence are considered in the light of ergodic theory.				
<b>14. SUBJECT TERMS</b> Turbulence; Fluid motion; Averaging; Closure			<b>15. NUMBER OF PAGES</b> 66	
			<b>16. PRICE CODE</b> A04	
<b>17. SECURITY CLASSIFICATION OF REPORT</b> Unclassified	<b>18. SECURITY CLASSIFICATION OF THIS PAGE</b> Unclassified	<b>19. SECURITY CLASSIFICATION OF ABSTRACT</b> Unclassified	<b>20. LIMITATION OF ABSTRACT</b>	